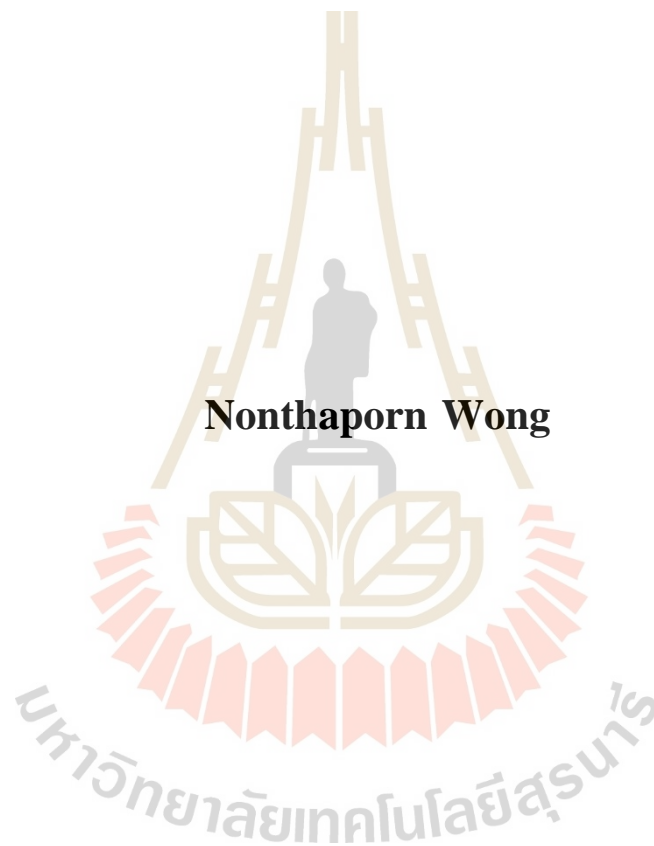


**METABOLIC ENGINEERING OF *Escherichia coli* TO
PRODUCE 1,3-PROPANEDIOL DEVOID OF A
PLASMID EXPRESSION SYSTEM**



**A Thesis Submitted in Partial Fulfillment of the Requirement for the
Degree of Doctor of Philosophy in Biotechnology
Suranaree University of Technology
Academic Year 2020**

วิศวกรรมเมทาบอสิกของเชื้อเอสเซอร์เรีย คอไล เพื่อการผลิต
1,3-โพรเพนไดออล โดยไม่ใช้ระบบการแสดงออก
ของยีนด้วยพลาสมิด

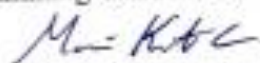


วิทยานิพนธ์นี้เป็นส่วนหนึ่งของการศึกษาตามหลักสูตรปริญญาวิทยาศาสตรดุษฎีบัณฑิต
สาขาวิชาเทคโนโลยีชีวภาพ
มหาวิทยาลัยเทคโนโลยีสุรนารี
ปีการศึกษา 2563

**METABOLIC ENGINEERING OF *Escherichia coli* TO PRODUCE
1,3-PROPANEDIOL DEVOID OF A PLASMID
EXPRESSION SYSTEM**

Suranaree University of Technology has approved this thesis submitted in partial fulfillment of the requirements for the Degree of Doctor of Philosophy.

Thesis Examining Committee



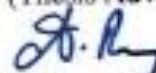
(Assoc. Prof. Dr. Mariena Ketudat-Cairns)

Chairperson



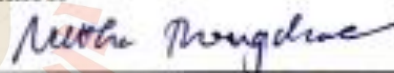
(Assoc. Prof. Dr. Kaemwich Jantama)

Member (Thesis Advisor)



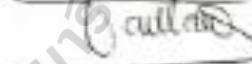
(Prof. Dr. Alissara Keungsang)

Member



(Assoc. Prof. Dr. Nuttha Thongchul)

Member



(Prof. Dr. Patricia Taillandier)

Member



(Asst. Prof. Dr. Claire Joannis-Cassan)

Member



(Prof. Dr. Neung Teaumroong)



(Assoc. Prof. Ft. Lt. Dr. Kantom Charniprasart)

Vice Rector for Academic Affairs
and Internationalization

Dean of Institute of Agricultural
Technology

นบพร ห่วง : วิศวกรรมเมทาบอติกของเชื้อเอสเชอริเชีย คอลิ เพื่อการผลิต
1,3-โพรเพนไดออล โดยไม่ใช้ระบบการแสดงออกของยีนด้วยพลาสมิด (METABOLIC
ENGINEERING OF *Escherichia coli* TO PRODUCE 1,3-PROPANEDIOL DEVOID OF
A PLASMID EXPRESSION SYSTEM) อาจารย์ที่ปรึกษา : รองศาสตราจารย์
ดร.ชนวิทย์ จันทร์มา, 138 หน้า

โอบีเพอรอนกลีเซอรอล ดีไฮดรอะต (gdrAB-dhaB123) จากเชื้อ *Klebsiella pneumoniae*
และยีน 1,3-โพรเพนไดออล ออกซิโครีดักเตส (yqhD) ที่ขึ้นกับ NADPH จาก *Escherichia coli* ถูก
แทรกบนโครโมโซมดีเอ็นเอของ *E. coli* และถูกแสดงออกภายใต้โปรโมเตอร์ *tdhA* และ *gfb* ของ
E. coli ตามลำดับ โดยเชื้อ *E. coli* NSK015 ($\Delta tdhA::gdrAB-dhaB123 \Delta ackA::FRT \Delta gfb::yqhD$
 $\Delta hndABCD::cat-sacB$) ที่ถูกพัฒนาขึ้นผลิต 1,3-โพรเพนไดออล (1,3-PDO) ได้ที่ความเข้มข้น 36.8
กรัมต่อลิตร และมีผลผลิตที่ 0.99 โมลต่อโมลของกลีเซอรอล การทดสอบผลการผลิตโดยใช้สารตั้ง
ต้นร่วมกันระหว่างกลีเซอรอลและแป้งมันสำปะหลังเพื่อผลิตสาร 1,3-โพรเพนไดออล พบว่าเชื้อนี้
สามารถผลิตสาร 1,3-โพรเพนไดออล ได้ที่ความเข้มข้น 31.9 กรัมต่อลิตรและมีผลการผลิตที่ 0.84
โมลต่อโมลของกลีเซอรอลตามลำดับ งานวิทยานิพนธ์นี้เป็นงานบุกเบิกที่แสดงการผลิต 1,3-โพร
เพนไดออล อย่างมีประสิทธิภาพโดยทำให้เกิดการแสดงออกของยีนจากสิ่งมีชีวิตอื่นบนจีโนมของ
E. coli โดยที่ไม่ได้ใช้ระบบพลาสมิดในการแสดงออกของยีน พลาสมิด ยาปฏิชีวนะ IPTG และ
สารอาหารที่ครบถ้วน ไม่ถูกนำมาใช้ในการผลิต 1,3-โพรเพนไดออล

เพื่อเพิ่มอัตราการผลิต การผลิต 1,3-โพรเพนไดออลภายใต้สภาวะที่เหมาะสมถูกศึกษาใน
E. coli NSK015 ซึ่งพบว่าสภาวะที่ดีที่สุดคือความเร็วในการกวน 300 รอบต่อนาทีและความเข้มข้น
ค่าของไดอะไนโตรเจน 12 ที่ 7.5 โมโคโรโมลาร์ โดยที่อัตราการผลิตเพิ่มขึ้นจาก 0.34 กรัมต่อลิตรต่อ
ชั่วโมง เป็นที่ 0.79 กรัมต่อลิตรต่อชั่วโมง ต่อมาเพื่อที่จะปรับปรุงความเข้มข้นของ 1,3-โพรเพนได
ออลให้สูงขึ้นจึงได้ทำการหมักแบบกึ่งกะ โดยที่มีการปรับเปลี่ยนรูปแบบการป้อนสารตั้งต้นร่วมของ
กลูโคสและกลีเซอรอล ผลการทดลองแสดงให้เห็นว่าการใช้รูปแบบการให้แบบแบ่งเป็นจังหวะ
อย่างค่อยเป็นค่อยไปมีประสิทธิภาพอย่างมากในการผลิต 1,3-โพรเพนไดออล ความเข้มข้นของ
1,3-โพรเพนไดออลเพิ่มขึ้นถึง 132.63 % จาก 38.1 กรัมต่อลิตร เป็น 88.6 กรัมต่อลิตรภายในเวลา
144 ชั่วโมง ด้วยอัตราการผลิตในการหมักแบบกึ่งกะที่อัตราการผลิต 0.62 กรัมต่อลิตรต่อชั่วโมง

สาขาวิชาเทคโนโลยีชีวภาพ
ปีการศึกษา 2563

ลายมือชื่อนักศึกษา นบพร ห่วง
ลายมือชื่ออาจารย์ที่ปรึกษา ดร.ชนวิทย์ จันทร์มา

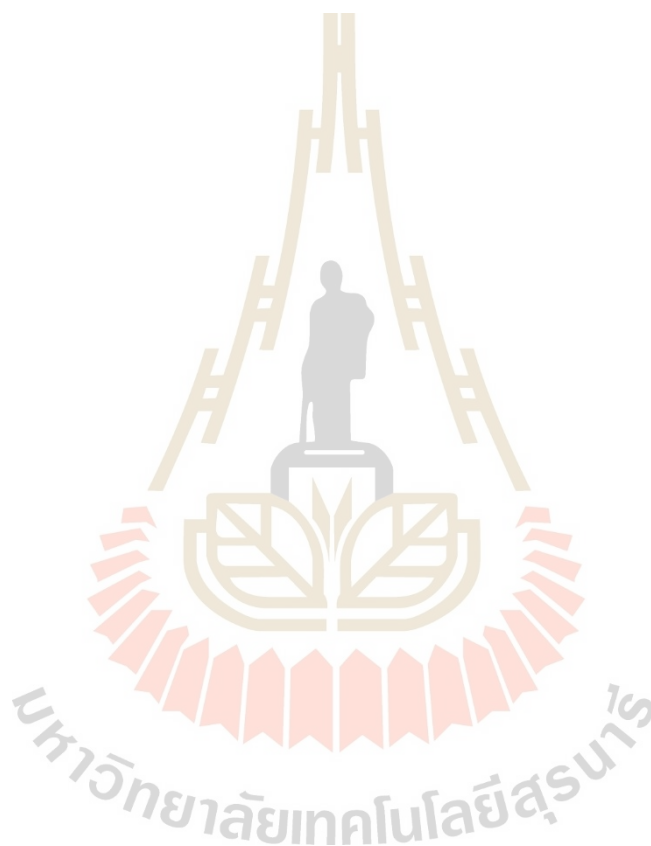
NONTHAPORN WONG : METABOLIC ENGINEERING OF
Escherichia coli TO PRODUCE 1,3-PROPANEDIOL DEVOID OF
A PLASMID EXPRESSION SYSTEM. THESIS ADVISOR : ASSOC. PROF.
KAEMWICH JANTAMA, Ph.D., 138 PP.

1,3-PROPANEDIOL/*E. COLI*/ *K. PNEUMONIAE*/GLYCEROL/CASSAVA

Glycerol dehydratase (*gdrAB-dhaB123*) operon from *Klebsiella pneumoniae* and *Escherichia coli* NADPH-dependent 1,3-propanediol oxidoreductase (*yqhD*) were stably integrated on the chromosomal DNA of *E. coli* and their overexpression was under the control of the native-host *ldhA* and *pflB* promoters, respectively. A developed *E. coli* NSK015 ($\Delta ldhA::gdrAB-dhaB123 \Delta ackA::FRT \Delta pflB::yqhD \Delta frdABCD::cat-sacB$) produced 1,3-propanediol (1,3-PDO) at the level of 36.8 g/L with a yield of 0.99 mol/mol glycerol. Co-substrate of glycerol and cassava starch was also utilized for 1,3-PDO production with the obtained concentration and yield of 31.9 g/L and 0.84 mol/mol glycerol respectively. This represents a pioneer work for efficient 1,3-PDO production in which the overexpression of heterologous genes on the *E. coli* host genome devoid of plasmid expression systems. Plasmids, antibiotics, IPTG, and rich nutrients were omitted during 1,3-PDO production.

To improve productivity, 1,3-PDO production by *E. coli* NSK015 was optimized. After performing optimization, the best condition for 1,3-PDO production was obtained at 300 rpm agitation with a low concentration of coenzyme B12 of 7.5 μ M. The 1,3-PDO productivity was enhanced from 0.34 g/L/h up to 0.79 g/L/h. To further improve 1,3-PDO production, the fed-batch fermentation mode was carried out

by varying different feeding modes of the co-substrate of glucose and glycerol. The results showed that the use of the continuous-pulsed mode was more powerful to produce 1,3-PDO. After 144 h incubation, 1,3-PDO concentration was improved from 38.1 g/L to 88.6 g/L, which is an 132.6 % with the 1,3-PDO productivity at 0.62 g/L/h.



School of Biotechnology

Student's Signature อนุพร พงษ์

Academic Year 2020

Advisor's Signature น. สันตมา

ACKNOWLEDGEMENTS

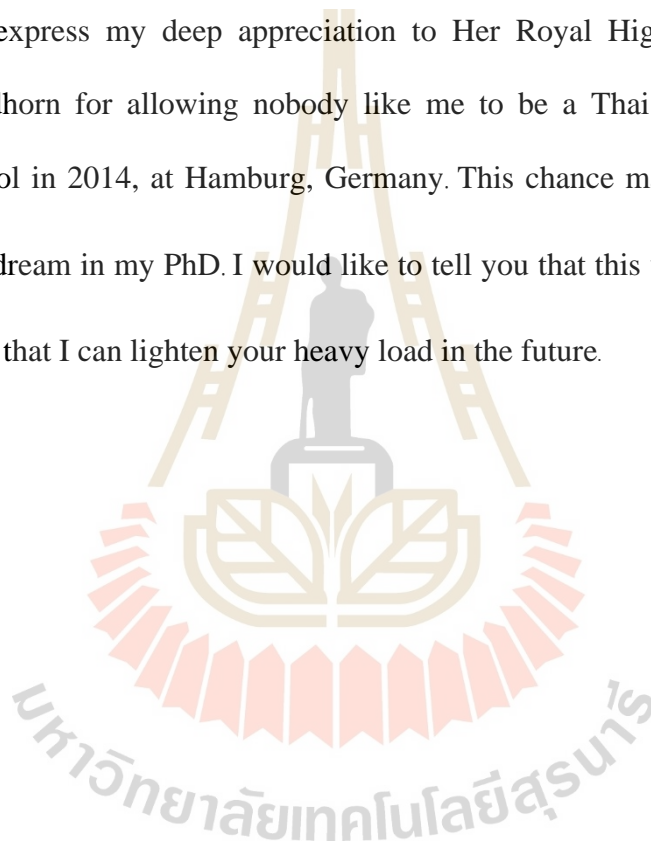
Along the Ph.D. journey for several years, I met a lot of incredible experiences, broadening my view and gaining new knowledge from several smart people. Importantly, this work cannot be possible without encouragement, and I would like to take this opportunity to express my gratitude to all who supported me as following. Firstly, I would like to express my utmost gratitude to my supervisor, Assoc. Prof. Dr. Kaemwich Jantama for giving me an enormous of opportunity and providing me with the Royal Golden Jubilee Ph.D. scholarship. Without your compassion and kindness, I do not have a chance to stand here. Your deep insight knowledge and intuition are different and always hidden from your appearance. But you taught me a lot indirectly how to be humble and good people. I would like to tell you that I am grateful to be a student under your encouragement and guidance. Thank you for your effort, patience, and forgiveness as if you are my second parent. This work cannot be accomplished without you. I would also like to extend the gratitude to French supervisors. Prof. Dr. Patricia Taillandier and Asst. Prof. Dr. Claire Joannis Cassan for taking care of me warmly throughout my work at the Institute National Polytechnique de Toulouse, France. Performing my work under your supervisions allowed me to see how professional scientists work. I was so lucky to be there and being one of your students. Your suggestion inspired me to follow how to be a great teacher and scientist to

manage everyone efficiently. I also would like to express my most appreciation to Asst. Prof. Dr. Thanet Urit from my heart to fulfil my dream and send me to the hand of Assoc. Prof. Dr. Kaemwich Jantama. I feel I am always indebted to you and I wish that one day it should be my turn to help you. As well, I would like to thank Assoc. Prof. Dr. Chonlada Dechakriatekrai and Asst. Prof. Dr. Teerayut Teantana for encouraging and believing in me to chase the dream in Ph.D. My special thanks also send to Dr. Apichai Sawaisit and Surawee Jampatesh for giving me a lot of basic techniques and idea in the lab and always discussing my experiment. I also would like to thank Dr. Pattra Charnchai for guiding me to meet the soul of being Buddhists. Many thanks also send beyond to my best friends, Amarrat Praiwgudrho and Waraporn Praiwgudrhao, for listening to me, breaking me when the bad thought struggling in my head and providing the laugh. and I also would like to send special thanks to Dr. Sandra, P'Mam, Igor, P'Dang, Natalie, and Maya during I stayed in Toulouse. Without your help to manage my accommodation, I could not handle the limited fund sufficiently in time. I would like to thank my most special teacher in high school, Suwannee Phromprasit who inspired me to study Science. Your passion and ideology make me keep the dream to be a scientist. I do not know what the future will be but I would like to tell you that my work is a partition of fulfilling your intention.

Of course, I must thank my scholarship, the Royal Golden Jubilee Ph.D. program for funding my work and supporting the incredible abroad experience. I learnt a lot of things because of this fund. I would like to send my heartfelt gratitude to my

most precious people; my mother, Siribhorn Boonlek and younger sister Vipabhorn Wong for standing by my side in every situation, encouraging me and cheering me. Whenever I almost gave up, I always smiled again at your words. I would also like to thank my aunt and uncle; Walaiporn and Winyoo Mektrirat to take care of my family. From now on, it must be my turn to take care of you all with love. Finally, I would like to sincerely express my deep appreciation to Her Royal Highness Princess Maha Chakri Sirindhorn for allowing nobody like me to be a Thai participant in DESY summer school in 2014, at Hamburg, Germany. This chance made me have the right and grab the dream in my PhD. I would like to tell you that this work also dedicates to you and hope that I can lighten your heavy load in the future.

Nonthaporn Wong



CONTENTS

	Page
ABSTRACT IN THAI.....	I
ABSTRACT IN ENGLISH	II
ACKNOWLEDGEMENT	IV
CONTENTS.....	VII
LIST OF TABLES	XII
LIST OF FIGURES	XIII
LIST OF ABBREVIATIONS.....	XVI
CHAPTER	
I INTRODUCTION	1
1.1 Background and scope of the study.....	1
1.2 Objectives.....	4
II LITERATURE REVIEWS	6
2.1 1,3-propanediol and its beneficial importance.....	6
2.2 Polytrimethylene terephthalate.....	9
2.3 Connection between glycerol and 1,3-propanediol	11
2.4 History of 1,3-propanediol.....	13
2.5 Native 1,3-propanediol producer	15
2.6 Pathway	18

CONTENTS (Continued)

	Page
2.7 The regulon encoding glycerol dehydratase in the different microorganisms ...	24
2.8 The modified microorganism for producing 1,3-propanediol	25
2.9 Glycerol dehydratase: mechanism, structure, and coenzyme	28
2.10 Process optimization of 1,3-propanediol production	31
III FUNCTIONAL EXPRESSION OF ARTIFICIALLY REARRANGED GLYCEROL DEHYDRATASE OPERON AND 1,3-PROPANEDIOL OXIDOREDUCTASE GENE DEVOID OF PLASMID EXPRESSION SYSTEMS IN <i>Escherichia coli</i> FOR THE HIGH YIELD OF 1,3- PROPANEDIOL	
3.1 Introduction	41
3.2 Materials and methods.....	43
3.2.1 Microbial strains, plasmid, media, primers and growth conditions...	43
3.2.2 Construction of an artificially expressing operon of glycerol dehydratase with its reactivating factors.....	43
3.2.3 Construction of an expressing cassette encoding the native <i>E. coli yqhD</i>	47
3.2.4 Deletions of <i>ldhA</i> , <i>ackA</i> and <i>frdABCD</i> genes, and chromosomal integrations of the artificial <i>gdrAB-dhaB123</i> operon and <i>yqhD</i> gene in <i>E. coli</i> C	50

CONTENTS (Continued)

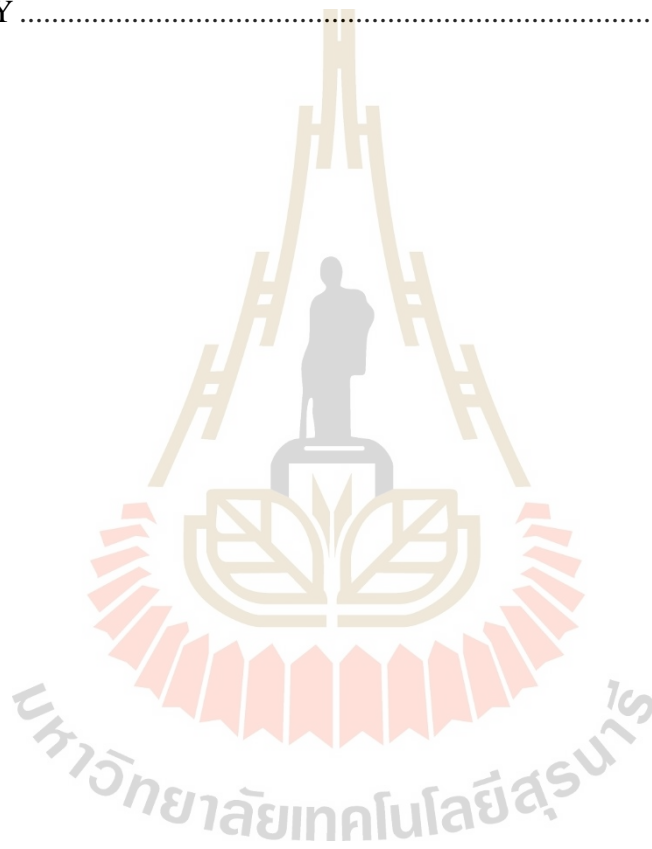
	Page
3.2.5 Enzymes assays	55
3.2.6 Fermentation experiment	55
3.2.7 Analytical method.....	56
3.3 Results and discussion.....	62
3.3.1 Functional expression of the <i>gdrAB-dhaAB123</i> operon for 1,3- propanediol pathway in <i>E.coli</i>	62
3.3.2 Improved 1,3-propanediol production caused by deletion of <i>pflB</i> but not the over-expression of <i>yqhD</i>	66
3.3.3 1,3-propanediol production is associated with a bicarbonate availability and succinate production in <i>E. coli</i> NSK strains	72
3.3.4 Improved 1,3-propanediol yield by the supplementation of Glucose but not yeast extract	75
3.3.5 1,3-propanediol production from co-substrate of glycerol and glucose or cassava starch in a 2 L fermenter by <i>E. coli</i> NSK015.....	78
3.4 Conclusions	81
IV OPTIMIZATION OF METABOLICALLY ENGINEERING <i>Escherichia coli</i> NSK015 FOR PROGRESSIVE IMPROVEMENT OF 1,3-PROPANEDIOL PRODUCTION.....	82

CONTENTS (Continued)

	Page
4.1 Introduction	82
4.2 Methods and materials.....	83
4.2.1 Microorganism.....	83
4.2.2 Medium and culture conditions.....	83
4.2.3 Batch fermentation.....	84
4.2.4 Fed-batch fermentation.....	85
4.2.5 Determination of k_{LA}	86
4.2.6 Analytical method.....	86
4.2.7 Statistic analysis.....	87
4.3 Results and discussion.....	88
4.3.1 Effect of vitaminB12 and coenzymeB12 on 1,3-propanediol production	88
4.3.2 Effect of k_{LA} and localization of impeller	93
4.3.3 Effect of concentration of coenzymeB12 with optimal k_{LA}	98
4.3.4 Improvement of 1,3-propanediol concentration by fed-batch fermentation	101
4.4 Conclusions	105
V GENERAL CONCLUSIONS AND RECOMMENDATIONS.....	107

CONTENTS (Continued)

	Page
REFERENCES	112
APPENDIX.....	135
BIOGRAPHY	138



LIST OF TABLES

Table	Page
2.1 Comparison of 1,3-propanediol fermentation by using the developed recombinant <i>E. coli</i> strains	36
3.1 Plasmids, strains and primers used for this study	57
3.2 Enzymatic activity of glycerol dehydratase and 1,3-propanediol oxidoreductase for different developed <i>E. coli</i> strains.....	67
4.1 Comparison of fermentation profile in type 1 of impeller localization with 200 rpm agitation and 1.0 vvm aeration	91
4.2 Comparison of fermentation profile in type 2 of impeller localization with different coenzymeB12	92
4.3 Detail of different modes of co-substrate feeding.....	100
4.4 Comparison of fermentation profiles at different feeding modes in type 2 fermenter.....	106

LIST OF FIGURES

Figure	Page
2.1 Applications of 1,3-propanediol.....	7
2.2 Chemical reactions of 1,3-propanediol synthesis.....	9
2.3 Synthesis of polytrimethylene terephthalate from 1,3-propanediol and terephthalic acid.....	10
2.4 The structure of different polyester; PET, PTT and PBT.....	11
2.5 Primary production of liquid biofuels.....	13
2.6 Co-substrate metabolism pathway of glycerol and glucose in <i>K.pneumoniae</i>	21
2.7 Organization of genes involving glycerol fermentation derived <i>K.pneumoniae</i> on plasmid pKM13.....	22
2.8 Organization of the partial <i>pdu</i> operon of <i>L. collinoides</i>	22
2.9 Glycerol metabolism under anaerobic conditions.....	23
2.10 Overview of B12-independent glycerol dehydratase in <i>C. butyricum</i>	25
2.11 Diol dehydratase-reactivating factor	31
3.1 Proposed metabolism for 1,3-propanediol production in a metabolically engineered <i>Escherichia coli</i> NSK015.....	42
3.2 Construction of artificially operon of <i>gdrAB-dhaB123</i> on pKJ1011	47
3.3 Construction of pKJ1014 for the replacement of <i>pflB</i> with <i>yqhD</i>	49

LIST OF FIGURES (Continued)

Figure	Page
3.4 An overview of molecular engineering for constructing recombinant <i>E. coli</i> NSK strains to produce 1,3-propanediol	54
3.5 Comparison of developed dark pink color on a modified aldehyde indicator plates containing glycerol between developed <i>E. coli</i> NSK strains and <i>K. pneumoniae</i> (positive control) and <i>E. coli</i> C as wildtype (negative control).....	63
3.6 Comparison of microbial growth (A) and maximum 1,3-propanediol production yield (B) of developed <i>E. coli</i> NSK strains in AM1 medium containing 20 g/L glycerol and 100 mM KHCO ₃ with or without glucose (Glu) and yeast extract (YE) in shaking flasks. Fermentation profiles of developed <i>E. coli</i> NSK strains in AM1 medium containing only 20 g/L glycerol and 100 mM KHCO ₃ in 250 mL shaking flasks (C).....	68
3.7 Fermentation profiles of 1,3-propanediol production by developed <i>E. coli</i> NSK strains from 20 g/L glycerol in AM1 medium without 100 mM KHCO ₃ in 500 mL shaking flasks	74
3.8 Fermentation profiles of developed <i>E. coli</i> NSK strains in AM1 medium containing only 20 g/L glycerol and 100 mM KHCO ₃ in 500 mL shaking flasks (A-F) and in AM1 containing 50 g/L co-substrate of glycerol and glucose (G) or cassava starch (H) in 2 L fermenter	77

LIST OF FIGURES (Continued)

Figure	Page
4.1 Schematics of the different impeller localization in 2 L fermenters.....	87
4.2 Effect of vitaminB12 and coenzymeB12 as a cofactor in the fermenter with type 1 of impeller localization for 1,3-propanediol production with 200 rpm agitation and 1.0 vvm aeration.....	90
4.3 Comparison of 1,3-propanediol production at different k_{La} in type 1 and type 2 of impeller localization at 200 rpm, 1 vvm.....	96
4.4 1,3-propanediol profiles under different k_{La} in type 2 of impeller localization..	97
4.5 Comparison of 1,3-propanediol production under different k_{La}	97
4.6 Comparison of different coenzymeB12 concentrations with optimal k_{La}	98
4.7 Fed-batch fermentation with the different co-substrate feedings	102
4.8 Fermentation profiles in the informal condition	104
5.1 Summary of optimized process for 1,3-propanediol production by <i>E. coli</i> NSK015.....	107
A.1 Graph plotting between OD500 against cell dry weight.....	137

LIST OF ABBREVIATIONS

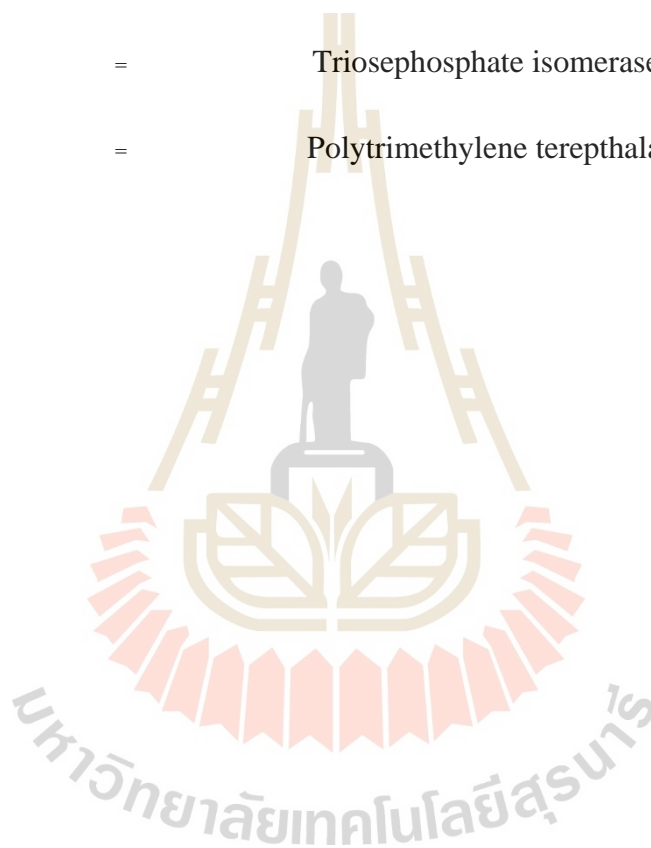
<i>ackA</i>	=	Acetate kinase gene
<i>adhE</i>	=	Alcohol dehydrogenase gene
<i>budA</i>	=	α -acetolactate synthase gene
<i>budB</i>	=	α -acetolactate decarboxylase gene
<i>C. beijerinckii</i>	=	<i>Clostridium beijerinckii</i>
<i>C. butyricum</i>	=	<i>Clostridium butyricum</i>
<i>C. diolis</i>	=	<i>Clostridium diolis</i>
DHAK	=	Dihydroxyacetone kinase
DHAT	=	NADH-dependent 1,3-propanediol oxidoreductase gene
<i>dhaKLM</i>	=	Dihydroxyacetone kinase genes
<i>dhaD</i>	=	Glycerol dehydrogenase gene
<i>dhaR</i>	=	Transcriptional regulator gene
<i>dhaT</i>	=	NADH-dependent 1,3-propanediol oxidoreductase gene
<i>dhaB</i>	=	Glycerol dehydratase gene (large subunit)
<i>dhaC</i>	=	Glycerol dehydratase gene (medium subunit)

LIST OF ABBREVIATIONS (Continued)

<i>dhaE</i>	=	Glycerol dehydratase gene (small subunit)
<i>frdABCD</i>	=	Fumarate reductase genes
<i>gldA</i>	=	Glycerol dehydrogenase gene
<i>glpK</i>	=	Glycerol kinase gene
GDHt	=	Glycerol dehydratase
3-HPA	=	3-Hydroxypropionaldehyde
3-HP	=	3-Hydroxypropionic acid
HOR	=	Hypothetical oxidoreductase
<i>K. pneumoniae</i>	=	<i>Klebsiella pneumoniae</i>
<i>K. oxytoca</i>	=	<i>Klebsiella oxytoca</i>
<i>ldhA</i>	=	Lactate dehydrogenase gene
<i>L. collinoides</i>	=	<i>Lactobacillus collinoides</i>
<i>orfX</i>	=	Reactivating factor or <i>gdrB</i> (Small unit)
<i>orfZ</i>	=	Reactivating factor or <i>gdrA</i> (Large unit)
<i>orfW</i>	=	Putative gene
1,3-PDO	=	1,3-Propanediol
<i>pdu</i>	=	Gene relevant to diol dehydratase or propanediol utilization pathway
<i>pflB</i>	=	Pyruvate formate lyase

LIST OF ABBREVIATIONS (Continued)

<i>pta</i>	=	Phosphotransacetylase gene
<i>ptsG</i>	=	glucose-specific PTS enzyme IIBC components
<i>poxB</i>	=	pyruvate oxidase
<i>tpi</i>	=	Triosephosphate isomerase gene
PTT	=	Polytrimethylene terephthalate



CHAPTER I

INTRODUCTION

1.1 Background and scope of the study

Oil and natural gas products are also essential parts of living life and affect the economic growth throughout the world unavoidably. It is responsible for being a core energy source used in several types of transportation, including the generation of electricity. Furthermore, petroleum is also transformed into a wide range of chemicals, which are an initial raw material for a tremendous quantity of household products, for example, toothpaste, shampoo, clothes, cosmetics, pharmaceutical products, tools in the kitchen, electric appliances, laptop, cell phone, plastic bags, pipe, shoes, construction materials, and medical materials. Thus, all these petroleum products touch us everywhere. Its intervention does not make us only comfortable and easy, but also contribute the infinity global development.

As our planet encounters global warming due to the greenhouse effect released from a variety of industries, particularly petrochemical plant. Releasing an enormous amount of CO₂ and CH₄ directly influences the ozone atmosphere as mentioned above, leading to numerous problems, such as an increase in temperature, and climate change. Nevertheless, the fossil fuel resource is not renewable. As it is used, it is going to run out and cannot be replenished. Eventually, it causes the fluctuation of crude oil prices

worldwide and impacts other petrochemical sections in a chain reaction. All of these become major factors to drive the scientist to concern and develop the sustainable greenway for replacing the non-renewable resource. Therefore, renewable energy, for example, wind power, waterpower, solar power, geothermal power, biomass fuel, is gaining attractiveness and widely used in many trial places and vehicles.

Biodiesel is one of renewable energy and is employed in vehicles for the replacement of petroleum diesel. It is capable of production from vegetable oils or animal fats by the reaction of transesterification. In this process, 10% w/v glycerol is always generated as the main byproduct (Kaur et al., 2012). In 2015, the global biodiesel production is approximately produced 30.1 billion liters (REN21, 2016). Thus, three-hundred million liters of glycerol are generally generated each year according to the increasing biodiesel demand. However, glycerol has diverse benefits and used as an ingredient in many related products, such as cosmetics, pharmaceuticals, food, and chemical synthesizing process (Hájek and Skopal, 2010). Importantly, it also serves as a carbon substrate for conversion to the other value-added chemicals and 1,3-PDO is one of those chemicals.

1,3-propanediol or 1,3-PDO used as a monomer for producing polytrimethylene terephthalate or PTT, which is one of polyester that further used in the industries of apparel and carpet mostly. Conventionally, 1,3-PDO is predominantly synthesized from the petrochemical industry. As the increasing greenhouse effects from the fuel combustion in plants, and the usage expedition of alternative white energy, these factors support the target chemical production through the renewably biological process by

using raw material from nature, agricultural residuals, and industrial wastes. As a result, a large amount of glycerol derived from rising biodiesel demand is gaining more attractive for adding value to glycerol, especially crude glycerol. Therefore, the utilization of crude glycerol is worthwhile for investment and can reduce the cost of biodiesel production, including addressing the surplus of by-product properly (Della Pina et al., 2011; Werpy and Petersen, 2004).

Although most of the 1,3-PDO biological production has been commercialized by DuPont and well known that they use a best developed recombinant *E. coli* for producing 1,3-PDO, it seemed recently that the new companies of bio-based 1,3-PDO production have been continuously established in France and China with the company of METabolic EXplorer S.A (METAX) and Zhangjiagang Glory Biomaterial, respectively. This indicates that 1,3-PDO is attracted from many scientists so far by using both native producers and non-native producers. For example, co-cultivation of two *E. coli* strains containing *dhaB12* and *dhaT* produced 1,3-PDO at 41.65 g/L in a 10 L fermenter (Yun et al., 2021). Lee et al. (2018) also constructed the *E. coli* BL21(DE3) for producing 1,3-PDO from glucose by deleting genes involving conversion of glycerol to dihydroxyacetone phosphate (DHAP) (*glpABCD*, *glpK*) and overexpressed the genes related to the conversion of DHAP to glycerol (*gpd1*, *gpp2*). The final yield was obtained from glucose at 0.33 mol/mol. However, the result of 1,3-PDO concentration was still low at around 2-3 g/L. Recently, *K. pneumonia* J2B was metabolically engineered with 33 genetic modifications to produce 1,3-PDO from glucose. The strain could

produce 62 g/L 1,3-PDO with a yield of 1.2 mol/mol under the fed-batch fermentation. (Lama et al., 2020). This study disclosed the method clearly how to engineer *K. pneumoniae* for producing 1,3-PDO from glucose. This strain takes advantages of using glucose that presents in a huge amount of agricultural resource. However, *K. pneumoniae* is capable of pathogenicity that may bring risks to the environment and health when it is used in industrial scales. Unlike *E. coli*, most of the works tried overexpressing heterologous genes on plasmids. The concentration of 1,3-PDO was lower and fluctuated in the industry scale because of the plasmid instability.

1.2 Objectives

E. coli C was selected and engineered to produce 1,3-PDO from glycerol under aerobic conditions. Genes *ldhA*, *ackA*, *pflB* and *frdABCD* encoding lactate dehydrogenase, acetate kinase, pyruvate formate lyase, and fumarate reductase, respectively, were interrupted to eliminate by-products. Genes, *dhaB1*, *dhaB2*, *dhaB3*, *grdA* and *gdrB* originated from *K. pneumoniae* were rearranged in one operon and integrated in front of the *ldhA* host promoter. *E. coli* expressing the functional glycerol dehydratase under the native promoter was then initially evaluated the aldehyde production on the modified indicator plate. The *yqhD* gene was also integrated in frame with the *pflB* promoter to enhance the conversion of 3-hydroxypropionaldehyde (3-HPA) to 1,3-PDO. Finally, 1,3-PDO production by the last developed *E. coli* strain

NSK015 was optimized to find the best parameters that enhanced 1,3-PDO production efficacy from co-substrate of glucose and glycerol.



CHAPTER II

LITERATURE REVIEWS

2.1 1,3-propanediol and its beneficial importance

Although, alcohol has been well known for several thousand years, 1,3-propanediol (1,3-PDO) is one of the chemical products generated from fermentation and known for several centuries. Generally, 1,3-PDO is a colorless viscous liquid, having specific gravity at 1.054 g/cm^3 and lower than that of glycerol at 1.26 g/cm^3 . It can be used as a component in several products in the market such as cosmetics, lubricant, antifreeze, adhesives, detergents (Kaur et al., 2012). In the past, 1,3-PDO was characterized only in the group of a niche market, but recently 1,3-PDO was identified as a commodity interesting chemical. By considered the global market of 1,3-PDO, it has been forecasted to reach the market price of USD 691 million by 2025. (1,3-Propanediol (PDO) Market, 2020).

Increasing demand of 1,3-PDO in the chemical trade is the result of the final end-product. Especially, polytrimethylene terephthalate (PTT), which has outstanding properties in polyester. This polymer has attracted the attention of many scientists. The major characteristics are derived from elasticity, tolerance, strength, stiffness, and stain resistance, which take advantage of PBT (Polybutylene terephthalate) or PET

(Polyethylene terephthalate). These features make PTT become several types of target products and can practically be applied in many fields of industries either materials used for medical product, cloth or thermoplastic (Liu et al., 2010).

Besides, 1,3-PDO is also used as a component for producing a wide range of commodities such as solvent, fragrance, sanitary product, cosmetic, fiber, laminate, and so on (Fig. 2.1). In some cases, 1,3-PDO is used as an ingredient to produce the biocide for example, 2-Bromo-2-nitro-1,3-PDO. This chemical is used for preventing the accumulation of microorganism in the circulating water system (Saxena et al., 2009). 1,3-PDO is thus attracted several scientists to develop its microbial production process for replacing petroleum-based production. However, DuPont is still nowadays a main predominant company that produces 1,3-PDO by using engineered *E. coli* and glucose as a raw material in the manufacture of 1,3-PDO.

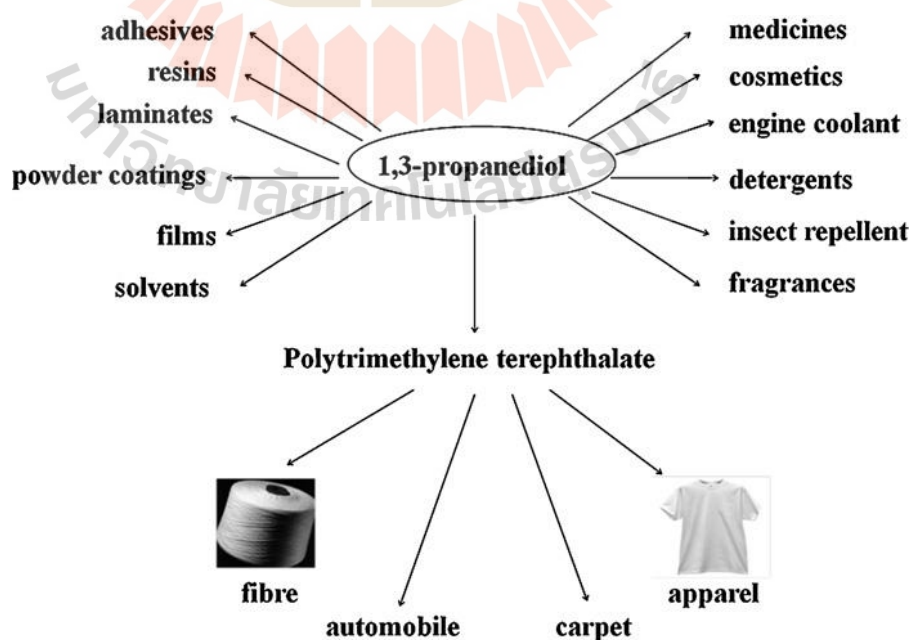


Figure 2.1 Applications of 1,3-propanediol (Kaur et al., 2012).

Typically, 1,3-PDO was traditionally produced via chemical processes (Fig. 2.2). In the first reaction, acrolein is hydrated to 3-hydroxypropionaldehyde (3-HPA) under catalyzation solution using the acid catalyst. 3-HPA is then hydrogenated by the expensive catalyst (Fig. 2.2A) such as nickel and transformed to 1,3-PDO at high temperature up to 180°C (Arntz et al., 1994; Lawrence and Sullivan, 1972). For the second chemical synthesis (Fig. 2.2B), ethylene oxide, serves as the substrate, for converting to 1,3-PDO by the reactions of hydroformylation and hydrogenation, respectively (Brown et al., 2000). However, these pathways of 1,3-PDO synthesis are required high temperature, expensive catalyst, or high pressure during the hydroformylation and hydrogenation processes. Importantly, the toxic from both processes is necessary to be eliminated. Thus, they are not suitable and sustainable for an environment. However, the chemical process is decreasing when DuPont developed their recombinant microbial strain for producing 1,3-PDO and using corn sugar as a feedstock. This breakthrough discovery opened the green way of 1,3-PDO production. The production of PTT is then grown gradually and expanding the production base.

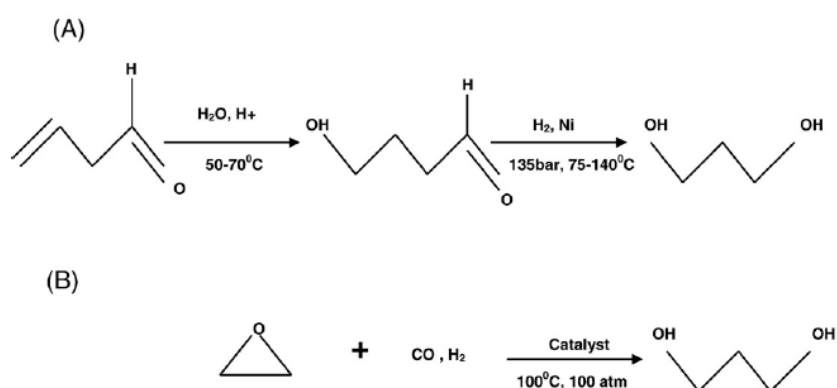


Figure 2.2 Chemical reactions of 1,3-propanediol synthesis: (A) Degussa method and (B) Shell method (Saxena et al., 2009).

2.2 Polytrimethylene terephthalate

Polytrimethylene terephthalate or PTT is a novel interesting polyester. It is synthesized from polycondensation between terephthalic acid and 1,3-PDO (Fig. 2.3). After the discovery of how to synthesize PTT in 1941, this polymer is attracted by many scientists because of its potential properties. By considering the structure of this polymer, three methylene groups result in PTT possesses the zigzag structure, composing the outstanding properties that blend between nylon, PET, and PBT (Fig. 2.4). Therefore, PTT can substitute other polyesters to some extents. The properties of PTT are shown as the uniqueness such as good endurance, strength, high elastic recovery. However, at the beginning of producing PPT, it was not possible for commercialization because the cost of 1,3-PDO production was still high. Until Shell developed the chemical synthesis of 1,3-PDO for further producing PTT. PTT was thus first entered into the market by Shell under the trade name of CORTERRA. PTT is applied in many products. Either yarn, fiber, monofilament, or engineering thermoplastics. All PTT-transformed objects can be used as raw materials for other industries such as medical equipment, electronic parts, film, packaging, and glass, particularly, in the group of carpet, textile, and apparel.

With the special characteristics of the chemical structure of PTT, these make the clothes from PTT have high elasticity, stain resistance but still give the fresh color

from intrinsic polymer, cleaning and drying faster, printable, no requirement of coating on polymer. This polymer is therefore quite suitable for producing sport clothes and can be replaced with nylon. Moreover, when 1,3-PDO can be produced based on bioprocess fermentation from the recombinant *E. coli*. This led both markets of 1,3-PDO and PTT to enlarge rapidly. To synthesize PTT, 1,3-PDO is condensed with terephthalic acid or dimethyl terephthalate, catalyzing to PTT (Fig. 2.3) (Houck et al., 2001; Liu et al., 2010).

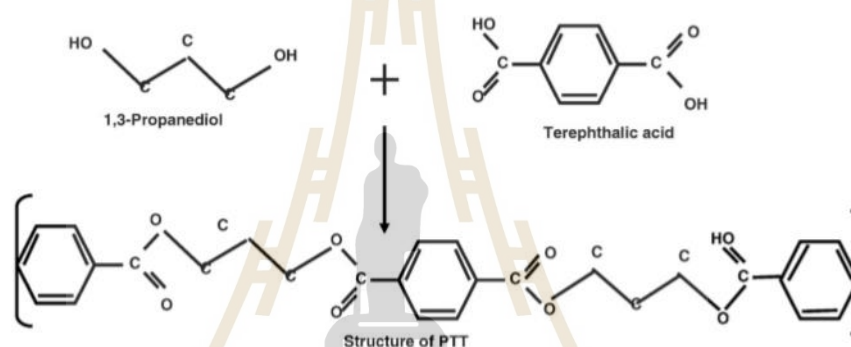


Figure 2.3 Synthesis of poly(trimethylene terephthalate) from 1,3-propanediol and terephthalic acid (Saxena et al., 2009).

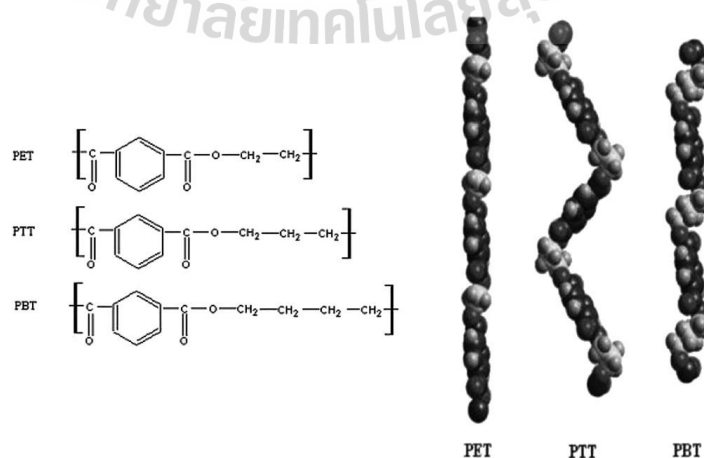


Figure 2.4 The structure of different polyester ; PET, PTT and PBT (Liu et al., 2010).

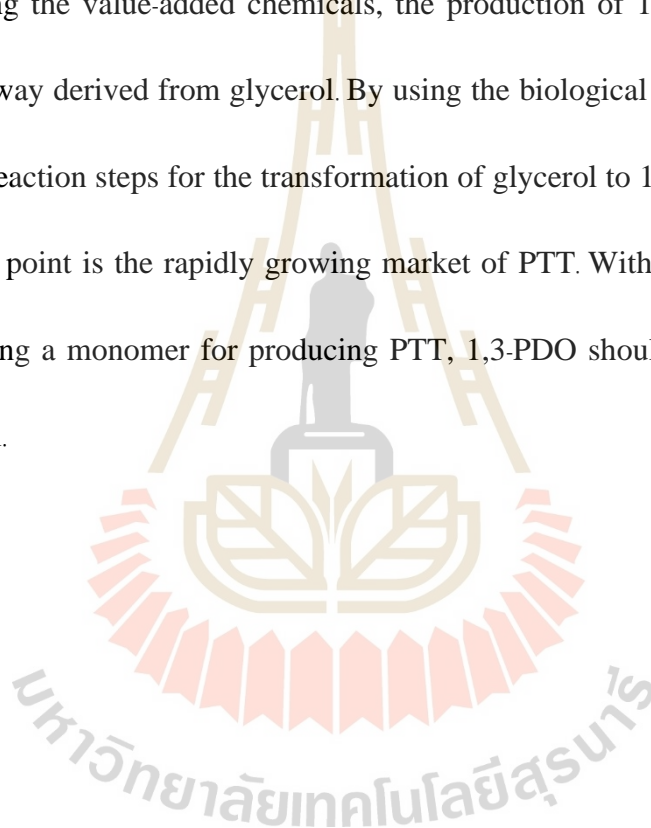
2.3 Connection between glycerol and 1,3-propanediol

Petroleum is a predominant resource, behind energy and many products that have been used for a long time. Among them, Diesel, gasoline, jet fuel and natural gas are the energy derived from petroleum that employed in transportations. In the European region, around 47.5% of the oil was consumed in the road transportation section (Eurostat statistics Explained, 2020). Compared to Thailand, fuel was consumed in transportation by 39.2%. The remaining sectors were divided into the group of industry, household, commerce, and agriculture, accounting for 36.4, 13.0, 8.0, and 3.4 %, respectively (Department of Alternatives Energy Development and Efficiency, 2019).

The phenomena of climate change in recent years have a large impact on the earth. A long drought, flood, dust pollution, monsoon including pandemic or even moving the settlement of animals are more serious problems and intensify. To reduce fossil fuel, alternative energies are required. Among sustainable fuel, biodiesel is one of them and increasingly taken to substitute the fossil-derived diesel as shown in Fig 2.5. Several plant oils and animals fat or even cooking oil such as palm oil, soybeans, rapeseed, jatropha can be used as feedstock resource of biodiesel production via transesterification (da Silva et al., 2009; Ogunkunle and Ahmed, 2019). By using choices, the emission of greenhouse gas can be possibly reduced. However, in the process of transesterification reaction, a 10% surplus of glycerol is usually generated from the process. This leads the price of glycerol in the market to fall accordingly. Nevertheless, the cost of glycerol removal is also required. These result in the

uneconomical production and a risk to environmental contamination. To manage the waste to become zero and increase the driving force of the utilization of sustainable source concomitantly, glycerol should be changed to other products that have high value such as ethanol, succinic acid, and even 1,3-PDO (Dharmadi et al., 2006; Saxena et al., 2009).

Among the value-added chemicals, the production of 1,3-PDO seemed to be the simplest way derived from glycerol. By using the biological pathway, it composes of only two reaction steps for the transformation of glycerol to 1,3-PDO. Significantly, the attractive point is the rapidly growing market of PTT. With the properties of 1,3-PDO and being a monomer for producing PTT, 1,3-PDO should be tried to produce from glycerol.



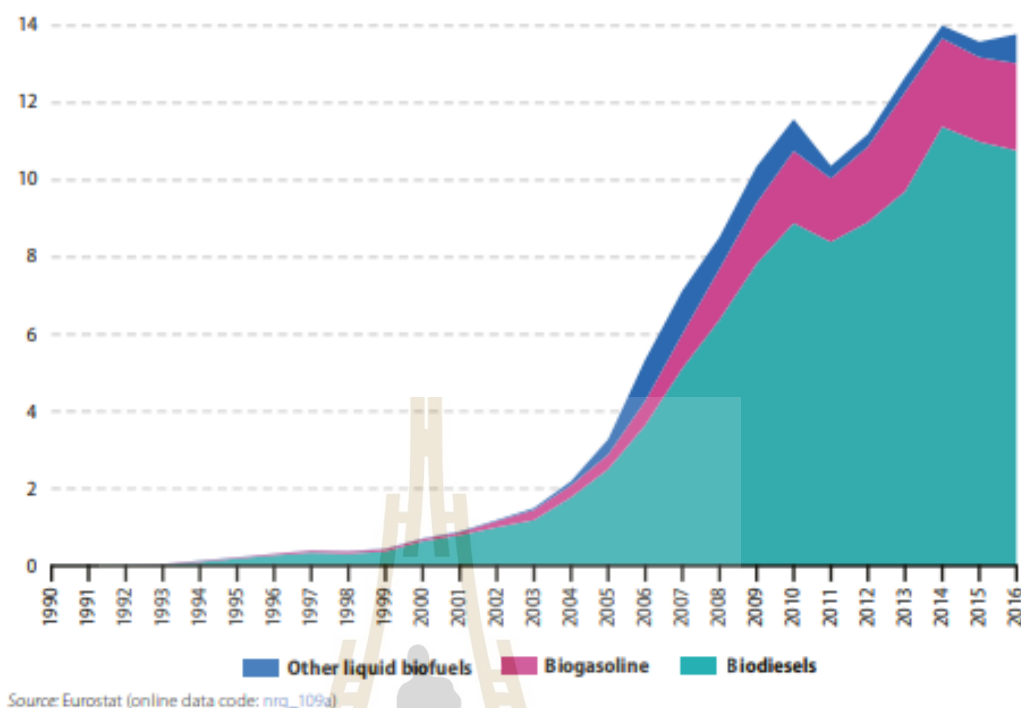


Figure 2.5 Primary production of liquid biofuels, EU-28, 1990-2016 (Eurostat, 2018)

2.4 History of 1,3-propanediol

The journey of 1,3-PDO was back into around the late 18th century, when August Freund (1881) found 1,3-PDO from his spontaneous fermentation of soap lyes by *Clostridium pasterianum* (Przystałowska et al., 2015a). Even he tried to remove butyl-alcohol, but the new product still existed with different specific gravity to glycerol. 1,3-PDO in that time was reported in name of trimethylene glycol. Later in 1928, Braak further identified *Bacterium freundii* which is the microorganism that can produce 1,3-PDO. This led to works that isolated more microorganisms capable of producing 1,3-PDO from various animal manures. It found that those microorganisms preferred citrate as a carbon source. These microorganisms were first characterized in a

group of *Citrobacter* sp. including *Citrobacter glycoligenes*, *C. album*, *C. intermedium*, *C. decolorans*, *C. diversum*, *C. anindolicum* (Werkman and Gillen, 1932).

In the same period, microorganisms related to 1,3-PDO production were also studied indirectly from several reports and found in the spoiled wine by Pasteur (1866). Voisenet (1918) discovered the connection between bitterness character and acrolein from the presence of *Bacillus amaracrylus* in the wine spoilage. He indicated that the acrolein is generated from glycerol and always presents in the wine thus having a bitter character. In that wine, he also found the formation of 3-HPA and 1,3-PDO (Engels et al., 2016; Serjak et al., 1954; Vollenweider and Lacroix, 2004). This glycerol formation results from the attempt of yeast for preventing the osmotic stress, redox balancing, and maintaining phosphate level during the alcoholic fermentation (Scanes et al., 1998). This makes wine also have glycerol as a by-product. Other contaminating microbial strains besides *S. cerevisiae* can grow and use glycerol as substrate. Small amounts of other by-products were thus generated and found in the spoiled wine. Besides wine, acrolein was also found in cider, brandy, and pear juice by the contamination of *Clostridium perfringens* (Warcollier et al., 1932; 1934). The presence of acrolein in cider or beer also affected the character of alcoholic fermentation to be the lachrymatory or called Pepper. However, the bitterness flavor could be summarized that it was the result of the reaction between polyphenol compounds especially tannins and acrolein (Rentschler and Tanner, 1951). These discoveries led to other numerous investigations either the

production pathway of 1,3-PDO and 3-hydroxypropionic acid (3-HP), the enzyme encoding intermediate chemicals or even microorganisms.

2.5 Native 1,3-propanediol producer

Besides microorganisms abovementioned, five main native producers that can produce 1,3-PDO from glycerol have also been usually reported including *Klebsiella* spp., *Clostridia* spp., *Citrobacter* spp., *Bacillus* spp., and *Lactobacilli* spp. (Ju et al., 2020, Forsberg et al., 1987, Sun et al., 2018). After 1,3-PDO-producing microorganisms have known in the field of alcoholic fermentation, this leads to the isolation and development of microbial strains for producing the essential monomer of PTT extensively by using native producers. For example, Vivek et al. (2016) selected *Lactobacillus brevis* N1E9.3.3 from the soil contaminated with crude glycerol. Concentration, productivity, and yield obtained from their strain were at 18.6 g/L, 0.78 g/Lh, and 0.89 gg glycerol, respectively. Ju et al., (2020) used the isolated *Lactobacillus reuteri* CH3 for 1,3-PDO fermentation. Under the fed-batch fermentation and corn steep liquor as nitrogen source, 1,3-PDO can be derived at 68.32 g/L. Whereas, Maervoet et al. (2016) selected *C. werkmanii* and performed the additional deletion of *dhaD*, *ldhA*, *adhE* genes. This strain can produce 1,3-PDO with a maximum theoretical yield of 1 mol/mol glycerol in shake flask and 1, 3-PDO was achieved at the concentration of 422.01 mM (~32.11 g/L) by using co-substrate of glycerol and glucose. *K. oxytoca* was also reported with the by-product gene deletions ($\Delta budA$,

$\Delta budB$, $\Delta adhE$, $\Delta ackA$, Δpta , $\Delta poxB$, $\Delta frdA$) in which 1,3-PDO was obtained at 76.2 g/L with the remained by-product of D-lactate at 111.9 g/L (Xin et al., 2017). With the deletion of *ldhA* in *K. oxytoca*, 1,3-PDO was improved up to 83.56 g/L accordingly, but 60.11 g/L 2,3-butanediol was also simultaneously produced (Yang et al., 2007). This indicates that even some by-product genes are removed, other by-products are still generated for balancing redox in the metabolic pathway.

As mentioned previously, *K. pneumoniae* and *C. butyricum* are mostly well known that are the major players in the field of 1,3-PDO production. Because they are tolerant to glycerol and 1,3-PDO concentration, and always selected as natural producers that are suitable for 1,3-PDO production in term of both productivity and concentration. Numerous studies reported 1,3-PDO production in high concentration from these microorganisms with and without molecular modifications. For example, the native *K. pneumoniae* (Mu et al., 2006) can produce 1,3-PDO to 51.3 g/L in fed-batch fermentation by using crude glycerol. Cheng et al. (2004) optimized the aeration level to observe the suitable conditions for producing 1,3-PDO by *K. pneumoniae*. 1,3-PDO was achieved at 70 g/L in the mix mode of anaerobic and microaerobic conditions. Besides the typical *K. pneumoniae*, gene manipulations are also moderately applied in this microorganism to improve concentration, productivity, and yield. For example, gene deletions of *poxB*, *pta*, and *ackA* (Lin et al., 2016) in *K. pneumoniae* were performed. Under the fed-batch condition, 1,3-PDO was derived at 76.8 g/L with a yield of 0.66 mol/mol by the strain. This concentration was improved by 15% compared to the

parental strain ($\Delta ldhA$). In addition to the removal of by-product genes for eliminating the competitive routes in *K. pneumoniae*, the expression of *dhaL* was also studied. This strain could produce 1,3-PDO of 20.59 g/L with a yield of 0.76 mol/mol in batch fermentation by using co-substrate of glycerol and mannitol (Lee et al., 2018). Recently, the new strain of *K. pneumoniae* J2B, was published with 33 gene modifications after developed this strain for several years. In this strain, *ccr*, *ptsG* and *ptsH* genes involving glucose transport system were removed. The diverse by-product genes such as *ldhA*, *adhE*, *frdA*, *pflB*, *mgsA*, *poxB*, *budA*, *budB*, and *budC*, were eliminated to direct carbon flow through 1,3-PDO as much as possible. The *nuoA* and *ndh* were also deleted to enhance reoxidation. Importantly, genes relevant to conversion of glucose to glycerol *gpdI* and *gpp2* were expressed. By using this strain, *K. pneumoniae* J2B produced 1,3-PDO from glucose up to 62 g/L. This was the successful report of employing glucose as a substrate in *K. pneumoniae* (Lama et al., 2020).

For *Clostridium* spp., this microorganism relies on the strictly anaerobic conditions and hard to control the operation on the industrial scale, there were many reports about this microorganism. For example, *C. butyricum* AKR102a could produce 1,3-PDO from pure glycerol up to 93.7 g/L with a productivity of 3.3 g/L/h. When this strain was upscaled to 200 L, concentration and productivity were reduced to 61.5 g/L and 2.1 g/L/h, respectively. However, the concentration and productivity were still high and satisfactory (Wilkens et al., 2012). Furthermore, *C. butyricum* was also taken to fermentation in kind of immobilization. Productivity derived from this study was quite

high compared to the free cell (Dolejš et al., 2019). On the other hand, Wischral et al. (2016) overexpressed *gldA* and *dhaKLM* in *C. beijerinckii* DSM791 to increase the supply of NADH in the second reaction during 1,3-PDO production. The result confirmed that the overexpression of these genes supported the glycerol utilization, leading to a high concentration of 1,3-PDO (26.1 g/L) compared to the wild type strain (~20 g/L).

However, the constraint for *K. pneumoniae* is still characterized as an opportunistic pathogen that risks the industrial operator (Gonzalez-Pajuelo et al., 2006). Whereas *Clostridium* spp. is dependent on strictly anaerobic conditions that are difficult to control the parameter in the industry. This indicates that they seem not suitable for use as a host to produce 1,3-PDO in the industrial scale until some limitations are addressed.

2.6 Pathway

Among native producers, 1,3-PDO production pathway in *K. pneumoniae* was studied apparently. It is used as a model for 1,3-PDO production under anaerobic conditions. However, *K. pneumoniae* is a facultative anaerobe. Formation of 1,3-PDO under aerobic or microaerobic conditions can be possible (Liu et al., 2007). The characteristics of oxygen requirement for 1,3-PDO-producing microorganisms in the other genus such as *Citrobacter* sp. and *Lactobacilli* sp. were also reported (Maervoet

et al., 2016; Vivek et al., 2016) except *Clostridium* sp. that is strictly sensitive to oxygen (Raynaud et al., 2003).

For the well-known pathway in *K. pneumoniae*, glycerol is initially entered into the cell by a glycerol facilitator (GlpF) which is strongly over expressed under aerobic conditions (Huang et al., 2002). Glycerol is then separated into two coupled ways, oxidative and reductive pathways. On the oxidative route, glycerol is directed to the glycolytic pathway. After glycerol come into the cell, it is initially converted to dihydroxyacetone (DHA) by glycerol dehydrogenase (DhaA or DhaD), releasing reducing power NADH. Dihydroxyacetone kinase (DhaKLM) then catalyzes on DHA by taking phosphate from phosphoenolpyruvate or ATP to DHA and adding phosphate to DHA before transformed to dihydroxyacetone phosphate (DHAP). DHAP is further converted to glyceraldehyde-3 phosphate before directing to glycolysis pathway and reduced to several by-products that subsequently re-generated reducing power to the formation of 1,3-PDO in the reductive route (Lin et al., 2016) (Fig. 2.6). In a similar way, this route also presents in other microorganism groups, but by-production formations are different distinctly, depending on microorganisms. For example, 2,3-butanediol is specially derived from *K. pneumoniae* and *C. freundii*, butanol is obtained from *Clostridium pasteurianum*, butyrate and acetate are mainly generated from *C. acetobutyricum*. Whereas, ethanol, lactate, acetate, are typically found in *Klebsiella*, *Citrobacter freundii*, *Lactobacillus* sp. and *E. coli*. (Homann et al., 1990; Luers et al., 1997; Magdouli et al., 2016; Sun et al., 2018; Vivek et al., 2016).

On the other hand, in the reductive branch, the entering glycerol is also changed to 3-HPA by coenzymeB12-dependent glycerol dehydratase (DhaB). 3-HPA is then reduced to 1,3-PDO by the NADH-dependent 1,3-PDO oxidoreductase (DhaT) or hypothetical oxidoreductase (HOR). In the second step of the reductive pathway, reducing power, especially NADH from the oxidative pathway is required to reduce 3-HPA to 1,3-PDO. As a result, glycerol metabolism usually couples with oxidative and reductive pathways. Furthermore, in the second reaction of a reductive pathway of *K. pneumoniae*, 3-HPA can be oxidized to 3-HP by aldehyde dehydrogenase in which 3-HP is one of another valuable building block biochemicals (Oh et al., 2018; Sun et al., 2018). It is also an interesting chemical due to the much more benefit of 3-HP with a broad range of applications.

In case of providing another source of carbon, such as glucose or xylose, glucose is directed to the oxidative route compared to use only glycerol. Besides, glucose is used as the source providing energy and intermediate in the metabolism and also serves as a source for generating ATP and reducing power (Sun et al., 2018). The glucose-glycerol co-utilization pathway presenting in *K. pneumoniae* is also similar in *L. brevis*. However, the operon encoding coenzyme B12-dependent glycerol dehydratase is the *pdu* operon instead of the *dhaB* operon for *K. pneumoniae* (Vivek et al., 2016).

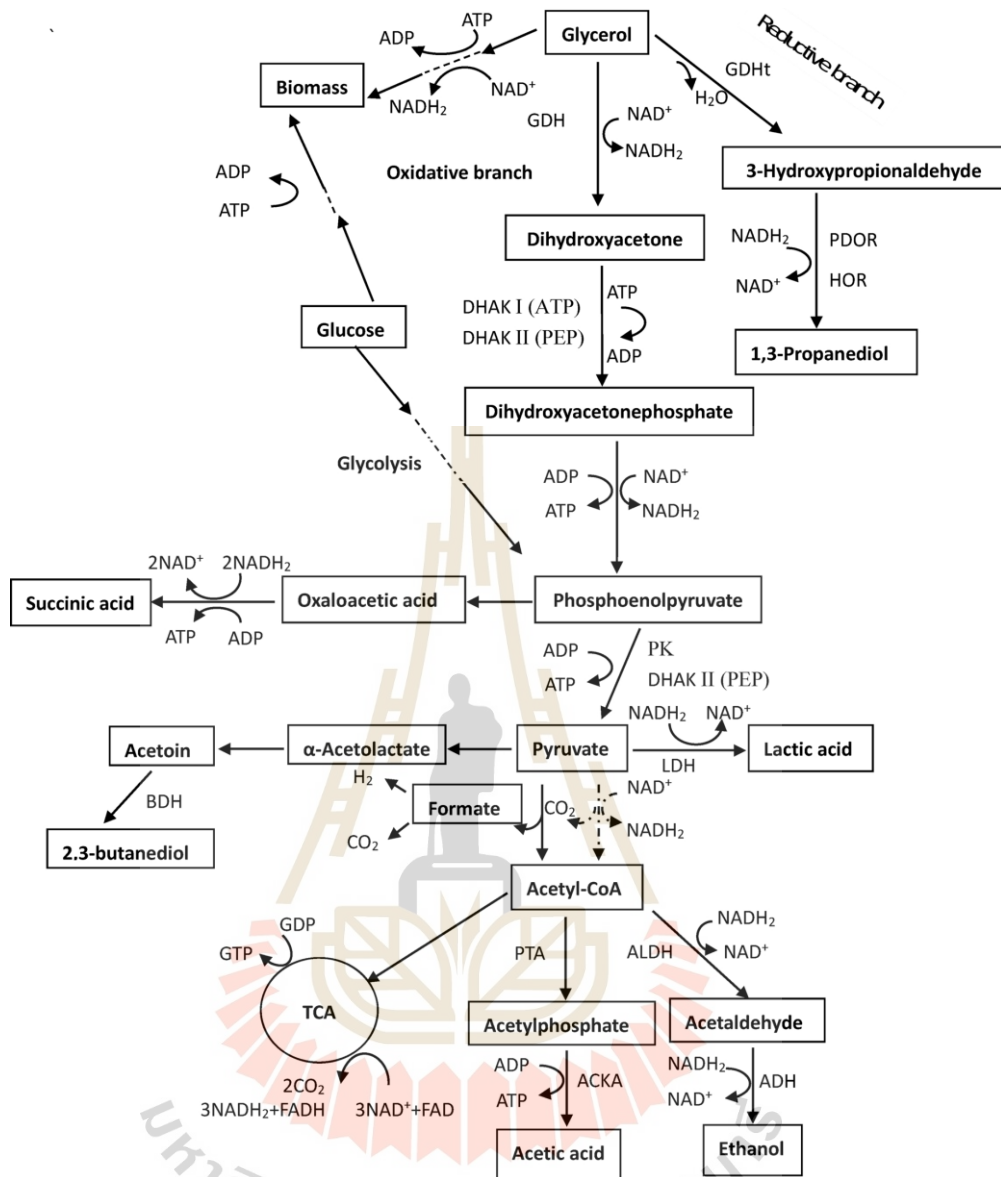


Figure 2.6 Co-substrate metabolism pathway of glycerol and glucose in *K.*

pneumoniae (Sun et al., 2018)

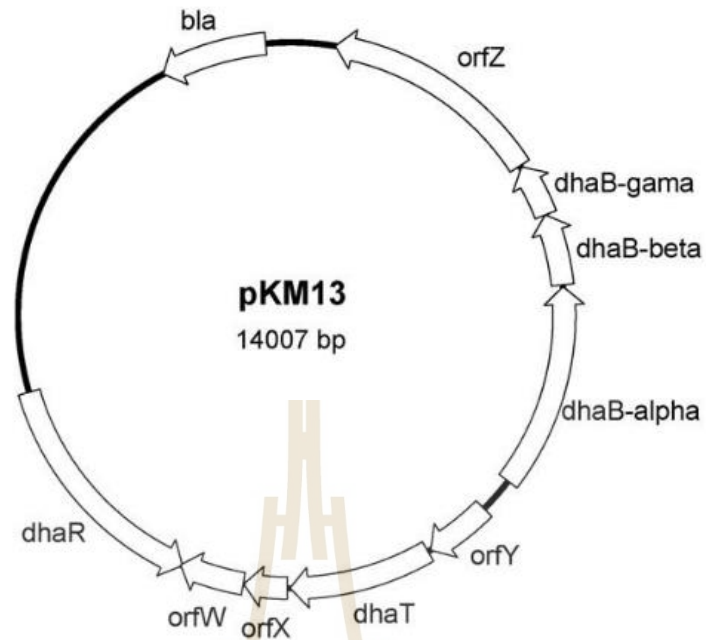


Figure 2.7 Organization of genes involving glycerol fermentation derived *K. pneumoniae* on plasmid pKM13 (Zheng et al., 2006).

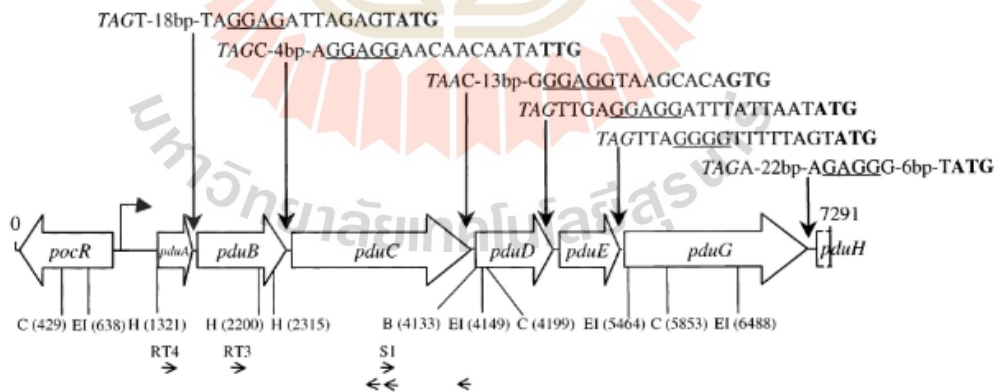


Figure 2.8 Organization of the partial *pdu* operon of *L. collinoides* (Sauvageot et al., 2002)

(A) Pathway of glycerol fermentation by enteric bacteria

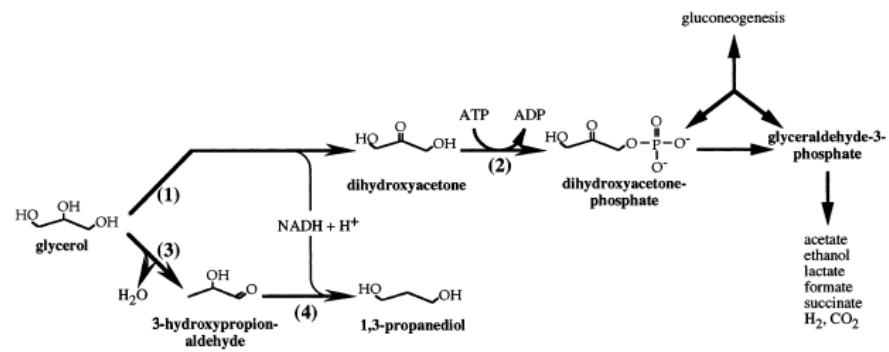
(B) Genetic organization in *C. freundii*(C) Genetic organization in *Cl. pasteurianum*

Figure 2.9 Glycerol metabolism under anaerobic conditions (A) Typical glycerol pathway for enteric bacteria (B) regulon of glycerol utilization for *Citrobacter freundii* (C) operon of glycerol utilization for *Clostridium pasteurianum*; *dhaD*, glycerol dehydrogenase, *dhaK*, dihydroxyacetone kinase, *dhaB*, *dhaC*, and *dhaE* are the subunits of glycerol dehydratase, *dhaT*, 1,3-propanediol dehydrogenase, *dhaR*, regulatory protein, *orfW*, *orfX*, *orfY*, and *orfZ* are the open reading frames with unknown function. (Daniel et al., 1998).

2.7 The regulon encoding glycerol dehydratase in the different microorganisms

Although *K. pneumoniae*, *K. oxytoca*, *Lactobacilli* spp., and *Citrobacter* spp. have the same enzyme for catalyzing glycerol into 1,3-PDO which is coenzymeB12-dependent glycerol dehydratase (Raynaud et al., 2003). Gene clusters involving regulation of glycerol catabolism in these microorganisms are aligned with three mainly different patterns. In *K. pneumoniae* and *C. freundii*, *dha* regulon is responsible for the same glycerol utilization. Considering the gene orientation as shown in Fig.2.7 and 2.9, genes involving glycerol fermentation are positioned in the opposite direction. Most genes of glycerol dehydratase which composed of *dhaBCDE* and *orfZ* (or *dhaB123*, *gdrA*) are oriented and grouped, whereas *orfX* (*gdrB*) encoding small reactivating factor of glycerol dehydratase is on another side and corresponds to the *dhaT* gene encoding of 1,3-PDO oxidoreductase. Compared to *C. pasteurianum*, genes related to the glycerol dehydratase and 1,3-PDO oxidoreductase are aligned in the same direction (Fig.2.9C). On the other hand, the *pdu* operon which is in turn responsible for 1,3-PDO pathway was found in the *L. collinoides*, and these genes are transcribed in the one direction as same as the operon of *dhaB* in *C. butyricum* (Fig. 2.8 and 2.10). However, every operon or regulon as stated previously can convert glycerol to 1,3-PDO.

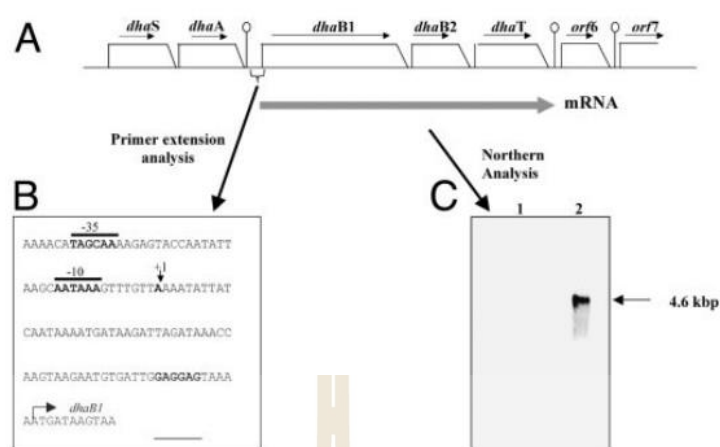


Figure 2.10 Overview of B12-independent glycerol dehydratase in *C. butyricum*. A. represents the arrangement of genes involving 1,3-production pathway. B represents the sequence in the promoter region. C. represents the result of northern blot analysis (Raynaud et al., 2003).

2.8 The modified microorganism for producing 1,3-propanediol

K. pneumoniae and *Clostridium* spp. are considered as the powerful player in the field of 1,3-PDO production even though the regard of the safety of authority is also important. Therefore, the use of microorganisms that is free of risk compared to those of *K. pneumoniae* as a host for 1,3-PDO production is a suitable way in the industry. *E. coli* is one of choice practically employed in the industry, especially DuPont. Several genes were modified in the metabolic pathway and can use glucose effectively instead of glycerol. This substrate takes a high advantage over glycerol in term of price and being a preferred carbon source for *E. coli*. Although, there were several genes were

modified in DuPont's strain to produce 1,3-PDO from glucose, only some relevant major genes were disclosed.

In DuPont's strain, essential genes derived from *K. pneumoniae*, *dhaB123* and *gdrAB* were introduced to the pathway in a non-native producer. Then other genes were modified to force the most of carbon from glucose direct to 1,3-PDO as much as possible as following. Genes relevant to converting DHAP to glycerol, which composed of glycerol 3-phosphate phosphatase (GPP2) and glycerol 3-phosphate dehydrogenase (DAR1) derived from *Saccharomyces cerevisiae* were introduced in the pathway. By overexpression of these two genes, DHAP is converted to glycerol-3-phosphate. Furthermore, to prevent the glycerol reversibly catalyzed to DHAP via glycerol-3-phosphate and DHA, respectively, the *glpK* and *gldA* were thus removed. The *tpiA* was eliminated to ensure the conversion of DHAP to glyceraldehyde 3-phosphate (GAP). Besides, *tpiA* and *gapA* genes were also downregulated for alleviating the conversion GAP to other intermediates in the central glycolysis pathway. On the other hand, gene responsible for glucose transportation was replaced with *galP* and *glk* (Nakamura and Whited, 2003).

In other studies, especially in *E. coli*, most of the works put the effort into *E. coli* by overexpression of coenzyme B12-dependent glycerol dehydratase operon derived from *K. pneumoniae* or *Citrobacter freundii* on plasmid as shown in Table 2.1. However, Yun et al. (2021) recently used B12-independent glycerol dehydratase from *Clostridium butyricum*, which has the advantage in term of no requirement of

coenzyme B12 for catalyzation. This study indicates the one advanced step, due to the possible reduction of industrial cost. However, this study used the two strains of *E. coli* for expressing different enzymes. This is relatively complicated and may allow the instability of plasmids to happen on an industrial scale. The NADH+H⁺ or NADPH+H⁺ dependent 1,3-PDO oxidoreductase gene (*dhaT* and *yqhD*) that convert 3-HPA to 1,3-PDO was also combined in *E. coli*. No apparent difference of 1,3-PDO concentration between the utilization of *dhaT* and *yqhD* was observed (Table 2.1). Emptage et al. (2003) clearly showed that *yqhD* is more preferable than *dhaT* in *E. coli* to produce 1,3-PDO.

Numerous studies tried to create the recombinant *E. coli* like DuPont by expression of glycerol dehydratase, deletion of by-product, and overexpression of genes relevant to convert glucose to glycerol. For example, Lee et al., 2018 expressed the essential gene for producing 1,3-PDO and eliminated genes relevant to the possible competitive pathways such as *glpK*, *glpABC*, *glpD* for preventing glycerol conversion to DHAP and removing *pta-ackA* genes for reducing acetate, respectively. The disruption of *glpR* and *eda-edd* were also carried out to increase glycerol assimilation rate and protect the carbon flow to the unproductive pathway. However, the yield was still lower than the theoretical yield at 1.0 mol/mol while obtained only 0.47 mol/mol with a concentration around 30 mM (2.22 g/L) in the shake flask. Yang et al. (2018) also performed similarly but attempted to improve the 1,3-PDO concentration by overexpression of *gapN* (glyceraldehyde-3-phosphate dehydrogenase) to increase the

reducing power source. In this strain, 1,3-PDO was produced at 13.47 g/L with a yield of 0.64 mol/mol.

The problems for most of the works found are the shortage of reducing power and the deficiency of cell viability when deletes *ptsG* in *E. coli* (Lee et al., 2018; Yang et al., 2018). In some studies, they usually used only glycerol as a substrate and evaluated the efficiency of strain in only shaking flask scale. Glucose and glycerol were not provided appropriately or in the same ratio as Tong and Cameron (1992) suggested that the theoretical yield (1 mol/mol) can be possible when combining 2 mol glycerol and 1 mol glucose. Importantly, the conditions used to produce 1,3-PDO become limited in kind of micro or anaerobic conditions. These obstacles make us do not exactly determine the maximum possible concentration and yield in *E. coli*. For example, Yun et al., (2021) added 80 g glycerol with 10 g glucose to produce 1,3-PDO. The yield of 1,3-PDO was reached 0.67 mol/mol. Przystałowska et al. (2015b) also used their recombinant *E. coli* strain to produce 1,3-PDO with two-stage conditions. The first stage of conditions was set for producing the high cell density, following the typical mode of batch fermentation at 0.4 vvm and 60 rpm. These limitations should be addressed and optimized conditions to find the best condition for producing 1,3-PDO.

2.9 Glycerol dehydratase: mechanism, structure, and coenzyme

As we know that glycerol dehydratase is an important enzyme for the formation of 1,3-PDO and not exist naturally in *E. coli*. To design *E. coli* to produce 1,3-PDO, we

need to provide genes from native producers to catalyze glycerol to 3-HPA. In contrast to other enzymes, glycerol dehydratase requires the coenzyme B12 or adenosyl cobalamin (AdoCbl) as a cofactor. Moreover, there is no genes function to produce vitamin B12 like *K. pneumoniae* or *K. oxytoca* in *E. coli*. This point is accounting as a challenging task for a scientist when we select the non-native producer as a host because genes for synthesizing vitaminB12 are complex and maybe another step for developing strain in the future. CoenzymeB12 or vitaminB12 are thus supplemented to culture for making glycerol dehydratase function properly.

Glycerol dehydratase is an enzyme depending on coenzymeB12. It normally tends to function anaerobically for utilization of glycerol in the native producer. Among the coenzymeB12-dependent enzyme, glycerol dehydratase was characterized in group II which functions to rearrangement of a substrate by elimination of hydroxyl group and involves in the reduction of coenzymeB12. In the presence of the glycerol and coenzymeB12, the mechanism of the chemical reaction is going to activate immediately. Glycerol dehydratase is thus catalyzed promptly but also inactivated rapidly. Because binding to substrate results in the conformational change of enzyme, triggering the homolytic cleavage on Co-C bond of coenzymeB12 and leading the covalent bond to break irreversibly. CoenzymeB12 is then becoming the dissociated form, resulting in unknown cobalamin (II) species (or slowly transformed to OH-Cbl) and adenosyl radical (Toraya and Mori, 1999). The adenosyl radical formed serves as an oxidizing agent and requires hydrogen from a substrate, forming 5'-deoxyadenosine. A

substrate is then rearranging into a product. The hydroxyl group from C-2 is transferred to C-1. Then, the product radical obtained by the transfer of hydrogen back from 5'-deoxyadenosine and the hydroxyl group is removed, becoming the aldehyde and H₂O (Daniel et al., 1998; Toraya, 2000).

After the aldehyde product is generated, the enzyme becomes substrate-free form, remaining only the biologically inactive coenzymeB12 or cobalamin species that interacted to enzyme tightly. Glycerol dehydratase is thus irreversibly inactive rapidly from homolytic cleavage of Co-C of coenzymeB12. Importantly, cobalamin species holding in glycerol dehydratase cannot function like at the beginning of a chemical reaction. The reaction is then stop and cannot be continued because of the suicide inactivation of glycerol dehydratase. However, the native producer always has reactivating factors to support glycerol dehydratase to reactivate and function again (Toraya et al., 2016). Based on the assumption of Shibata et al. (2005), the reactivating factors reactivate by the exchange of ATP and ADP. The ADP-containing reactivating factors initially binds to the inactivated glycerol dehydratase, releasing adenine residue and cobalamin (I). ADP on reactivating factors was then replaced with ATP, before finally becomes to ADP-binding reactivating factors to reactivate the inactivate glycerol dehydratase again.

On the other hand, after 5'-deoxyadenosine residue was released from the coenzyme B12 during catalysis, Cob(II)alamin or coenzyme B12 has become an inactive form. To regenerate the active form of coenzyme B12, adenosyl transferase is catalyzed

on the inactive coenzyme B12 by bringing the adenosyl residue from ATP to add on an inactive form of coenzyme B12.

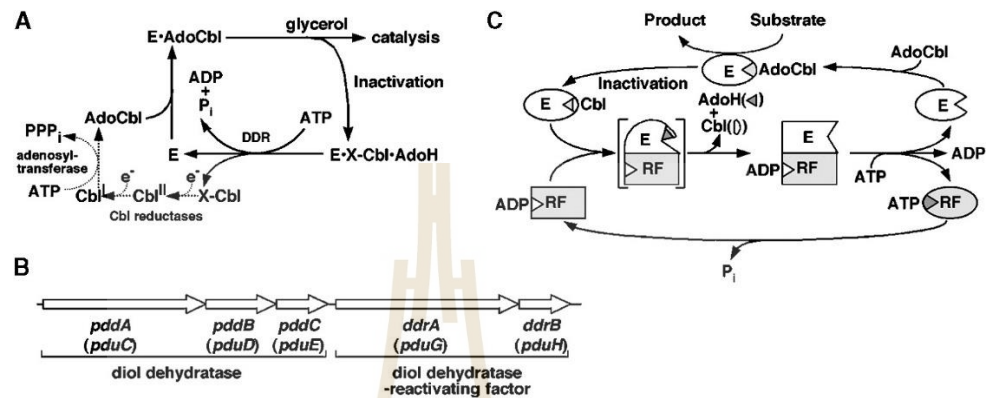


Figure. 2.11 Diol dehydratase-reactivating factor (Shibata et al., 2005). (A) Reactivation of inactivated hololDD by exchange of a damaged cofactor for intact coenzyme. AdoH, 5'-deoxyadenosine; Cbl^{II}, cob(II),cob(II)alamin; Cbl^I, cob(I)alamin; X-Cbl, a damaged cofactor, Dotted lines indicated the reactions outside of DD. (B) Organization of the genes for DD and DDR in the *pdu* operon. (C). Postulated mechanism of reactivation of inactivated hololDD by DDR. E, apoDD; RF, DDR; AdoH, 5'-deoxyadenosine; Cbl, cobalamin.

2.10 Process optimization of 1,3-propanediol production

2.10.1 Mode of operations: anaerobic, microaerobic, and aerobic conditions

Although glycerol dehydratase was believed to function effectively under anaerobic conditions, it is not always true. Liu et al. (2007) performed fed-batch

fermentation by using *K. pneumoniae* to ferment under anaerobic and microaerobic conditions. They found that the result of 1,3-PDO concentrations was not distinctly different under both conditions either concentration (75 g/L and 72 g/L), productivity (2.2 and 2.1 g/L/h), or even yield (0.61 and 0.57 mol/mol). However, this study did not indicate the detail of conditions clearly about how to set anaerobic and microaerobic conditions. Oh et al. (2012) also determined the mode of operations by setting the different aeration level against 1,3-PDO production in *K. pneumoniae* deficient *ldhA* in the range of 0.5-3.5 vvm. They found the aeration of 2.0 vvm, 1,3-PDO can be achieved satisfactorily at 94.3 g/L, that was higher than those of the low aeration at 0.5 vvm (80.8 g/L). Whereas Ji et al. (2009) employed microaerobic conditions in the first five hours by a combination of between 0.1 vvm and 200 rpm, 1,3-PDO can be derived at 70 g/L. Noticeably that not only *K. pneumoniae* is a facultative anaerobe, but it is also a natural producer for 1,3-PDO. Hence it tends to efficiently generate 1,3-PDO in both conditions.

Compared to *E. coli*, conditions that applied for the cultivation of microorganism under microaerobic conditions or aerobic conditions were not applied clearly and not fully disclosed. Normally, several studies on *E. coli* used mild conditions. For example, Przystalowska et al. (2015) employed low speed at 60 rpm for generating 1,3-PDO at 10.6 g/L. Whereas, Zhang et al., (2006) varied the concentrations of components in 1,3-PDO fermentation with fixed parameters at 180 rpm and 0.8 vvm. The 1,3-PDO concentration was at 43.1 g/L from 61.8 g/L of glycerol, 6.2 g/L of yeast

extract, and 49 mg/L of vitamin B12. On the other hand, for a native producer like *L. reuteri* CH53, the generation of 1,3-PDO was achieved efficiently under mild anaerobic conditions (no-aerated conditions) (Ju et al., 2020). 1,3-PDO from this strain under aerobic conditions was obviously such a low level at 1.51 g/L. Compared to anaerobic or unaerated conditions, 1,3-PDO were presented at a higher level of 11.88 or 11.57 g/L, respectively. In contrast to these aforementioned microorganisms, *Clostridium* spp. is different from other 1,3-PDO-producing bacteria because it requires anaerobic conditions for microbial growth (Szymanowska-Powalowska and Bialas, 2014). As a result, aeration or speed is one of the most important parameters to optimize 1,3-PDO production. 1,3-PDO is thus varied considerably according to the different microorganisms and conditions.

2.10.2 pH

As well as other conditions most of the works focused only *K. pneumoniae*, by varying the pH in the short range. For example, Oh et al. (2018) determined the effect of pH in the range of 6-7 (6, 6.5, and 7) upon 1,3-PDO production in *K. pneumoniae*. The result showed that a pH of 6.5 is suitable for glycerol utilization. The 1,3-PDO concentration was around 53.5-57.7 g/L that was higher than those of pH 6 and 7 (47.4-49.9 and 44.6-49.8 g/L, respectively). On the other hand, Sattayasamitsathit et al. (2011) also studied the effect of pH at 6.5, 7.0, and 7.5, respectively. The lowest pH at 6.5 provided the highest 1,3-PDO concentration at 7.8 g/L compared to the pH at 7 and 7.5 (18.51 and 16.18 g/L). In contrast, the cell growth was high at pH 7.5 with a

specific growth rate of 0.31 h^{-1} . As a result, they combined two pHs in their fermentation by building biomass in the first 6 h at pH 7.5 and following with pH 6.5 until the end of fed-batch fermentation.

2.10.3 Co-substrate

Glycerol is the true substrate for 1,3-PDO production. To produce 1,3-PDO, the theoretical yield from glycerol is only 0.72 mole/mole. However, most of the research cannot make 1,3-PDO reaching that theoretical yield either natural or non-natural producers, this is due to naturally metabolic limitation. To make the redox balance, some by-products are thus generated, leading to reduce the maximum theoretical yield. However, if the system is supported by the source of reducing equivalent, the practical yield can be achieved close to theoretical yield at 1 mol/mol. By using co-substrate and several types of 1,3-PDO producing microorganisms, 1,3-PDO concentration can be improved evidently and always close to 1 mol/mol. Ju et al. (2020) used *L. reuteri* CH53 for producing 1,3-PDO by using glycerol and glucose, yield of 1,3-PDO can be obtained at 0.80 g 1,3-PDO/g glycerol (0.96 mol/mol). Likewise, Xin et al (2016) employed *C. diolis* for producing 1,3-PDO from a combination of glucose and glycerol. They found that yield was improved by 22%, accounting for 0.86 mol/mol.

2.10.4 Biomass and waste

The resource of glycerol does not come from only the industry of purified glycerol. The utilization of crude glycerol derived from biodiesel is one of the interesting choices for adding the value of waste. The powerful final target of applying

several native producers is always a demonstration of crude glycerol consumption. Furthermore, agricultural residue like corn steep liquor sometimes is combined with crude glycerol, serving as nitrogen source instead of yeast extract or beef extract in 1,3-PDO production (Oh et al., 2018). For example, Dolejš et al. (2019) determined 1,3-PDO production from crude glycerol using *C. butyricum*. 1,3-PDO was generated at 12.6 g/L from 40.2 g/L of crude glycerol, accounting for the yield of 0.35 g/g. Whereas, Laura et al., (2020) also selected *K. pneumoniae* as a host for producing 1,3-PDO from crude glycerol. These studies indicate that 1,3-PDO-producing microorganisms are powerful and possible for developing on an industrial scale. Importantly, by using crude glycerol, the purification process is not required. However, caution for using crude glycerol should take considered. The certain microorganism may not tolerate methanol or ash which is a residual component from the biodiesel process. For example, Laura et al., (2020) used crude glycerol as a substrate, 1,3-PDO was reduced to 51% compared to pure glycerol.

Table 2.1 Comparison of 1,3-propanediol fermentations by using the developed recombinant *E. coli* strains.

Microorganism	Aeration	Main Carbon Source	Cultivation Condition	Concentration (g/L) Yield [mol/mol]	Productivity (g/L/h)	Sources
<i>E. coli</i> AG1 overexpressing <i>dha</i> operon (<i>K. pneumoniae</i>) on pTC1	Anaerobic (ND)	Gly	Modified ST medium + YE	0.7 [0.46 mol/mol glycerol]	0.02	Tong et al. (1991)
	Anaerobic (ND)	Gly/Glu	Modified ST medium + YE	1.2 [0.63 mol/mol glycerol]	0.04	Tong and Cameron. (1992)
	Anaerobic (ND)	Gly/Glu	Minimal medium + YE	6.3 [0.82 mol/mol glycerol]	0.20	Skraly et al. (1998)
<i>E. coli</i> BL21 overexpressing <i>dha</i> operon (<i>K. pneumoniae</i>) on pACYCDuet- <i>dhaBT</i>	Aerobic conditions, Shake flask, 150 rpm	Gly	Minimal medium + YE	11.3 [0.34 mol/mol glycerol]	0.38	Ma et al. (2009)
<i>E. coli</i> K-12 overexpressing <i>dhaB12</i> derived from <i>C. butyricum</i> and <i>yqhD</i> derived from <i>E. coli</i> on pDY220	2 step fermentation. First: aerobic conditions at 2 vvm, 400 rpm	Gly/Glu	Minimal medium + YE	104.4 [1.09 mol/mol glycerol]	2.61	Tang et al. (2009)

ND = Not determined, YE = Yeast extract, Gly = Glycerol, Glu = Glucose

Table 2.1 Comparison of 1,3-propanediol fermentations by using the developed recombinant *E. coli* strains (Continued).

Microorganism	Aeration	Main Carbon Source	Cultivation Condition	Concentration (g/L) Yield [mol/mol]	Productivity (g/L/h)	Sources
	Second: anaerobic conditions					
Co-culture of <i>E. coli</i> Rosetta-<i>dhaB12</i> derived from <i>C. butyricum</i> on pANY with <i>E. coli</i> BL21 overexpressing <i>dhaT</i> from <i>C. butyricum</i> on pET-30a(+)	Anaerobic conditions, Shake flask (200 rpm)	Gly/Glu	Minimal medium + YE	41.6 [0.67 mol/mol glycerol]	0.69	Yun et al. (2021)
<i>E. coli</i> DH5α overexpressing <i>dha</i> operon (<i>K. pneumoniae</i>) and <i>gpd1-gpp 2</i> (<i>S. cerevisiae</i>) on pQKG and the stress-induced region (SIR) on pSCD	Micro-aerobic conditions, Shake flask (200 rpm)	Glu	Minimal medium (M9) + YE	12.1 [0.47 mol/mol glucose]	0.2	Liang et al. (2011)

ND = Not determined, YE = Yeast extract, Gly = Glycerol, Glu = Glucose

Table 2.1 Comparison of 1,3-propanediol fermentations by using the developed recombinant *E. coli* strains (Continued).

Microorganism	Aeration	Main Carbon Source	Cultivation Condition	Concentration (g/L) Yield [mol/mol]	Productivity (g/L/h)	Sources
<i>E. coli</i> BL21 overexpressing <i>dha</i> operon from <i>C. freundii</i> and <i>dhaT</i> from <i>K. pneumoniae</i> on pCF1 and pKP2	Micro-aerobic conditions, Fermenter (0.4 vvm, 60 rpm)	Gly	Minimal medium + YE	10.6 [0.4 mol/mol glycerol]	0.06	Przystalowska et al. (2015)
<i>E. coli</i> JM-30BY15AB overexpressing <i>dha</i> operon (<i>K. pneumoniae</i>) and <i>yqhD</i> (<i>E. coli</i>) on dual vector pQE30 and pQE15A	Aerobic conditions, Fermenter (- vvm, 400 rpm)	Gly	LB medium	13.1 [0.59 mol/mol glycerol]	ND	Hong et al. (2015)

ND = Not determined, YE = Yeast extract, Gly = Glycerol, Glu = Glucose

<i>E. coli</i> EB13-1	Micro-aerobic	Glu	Minimal	ND	ND	Lee et al. (2018)
-----------------------	---------------	-----	---------	----	----	-------------------

Table 2.1 Comparison of 1,3-propanediol fermentations by using the developed recombinant *E. coli* strains (Continued).

Microorganism	Aeration	Main Carbon Source	Cultivation Condition	Concentration (g/L) Yield [mol/mol]	Productivity (g/L/h)	Sources
<p>(<i>ΔglpK</i> <i>ΔglpABC</i> <i>ΔglpD</i>, <i>ΔglpR</i> <i>Δedd-eda</i> <i>Δpta-ackA</i>) overexpressing <i>dhaB</i>, <i>gdrAB</i>, and <i>dhaT</i> (<i>K. pneumoniae</i>) and <i>gpd1-gpp2</i> (<i>S. cerevisiae</i>) on pABG and pDPT</p>	<p>conditions, Shake flask 50 mL/100 rpm)</p>		<p>medium (M9)+ YE</p>	<p>[0.47 mol/mol glucose]</p>		

ND = Not determined, YE = Yeast extract, Gly = Glycerol, Glu = Glucose

Table 2.1 Comparison of 1,3-propanediol fermentations by using the developed recombinant *E. coli* strains (Continued).

Microorganism	Aeration	Main Carbon Source	Cultivation Condition	Concentration (g/L) Yield [mol/mol]	Productivity (g/L/h)	Sources
<i>E. coli</i> JA11 overexpressing <i>gdrAB-dhaB123-yqhD</i> on pTrc02 and employing optimizing UTR combined with overexpressing <i>gapN</i> and <i>galP-glK</i> on pACYC09	Micro-aerobic conditions, Shake flask 80 mL/220 rpm)	Gly/Glu	Minimal medium + YE	13.5 [0.64 mol/mol glycerol]	0.22	Yang et al. (2018)
<i>E. coli</i> NSK015 (Δ <i>ldhA::gdrAB-dhaB123</i> Δ <i>ackA::FRT</i> Δ <i>pflB::yqhD</i> Δ <i>frd::cat-sacB</i>)	Aerobic conditions (1 vvm, 400 rpm)	Gly/Glu	Minimal medium (AM1)	36.8 [0.99 mol/mol glycerol]	0.34	This study
	(1 vvm, 400 rpm)	Gly/Cassava starch	Minimal medium (AM1)	31.9 [0.84 mol/mol glycerol]	0.29	This study
ND = Not determined,		YE = Yeast extract,		Gly = Glycerol,		Glu = Glucose

CHAPTER III

**FUNCTIONAL EXPRESSION OF ARTIFICIALLY
REARRANGED GLYCEROL DEHYDRATASE OPERON
AND 1,3-PROPANEDIOL OXIDOREDUCTASE GENE
DEVOID OF PLASMID EXPRESSION SYSTEMS IN
Escherichia coli FOR THE HIGH YIELD OF
1,3-PROPANEDIOL**

3.1 Introduction

As stated in previous chapter, 1,3-Propanediol (1,3-PDO) has been known for a long time to have the diverse benefits and can be applied in different products such as cosmetics, laminates, coating, lubricant, antifreeze, etc. Importantly, 1,3-PDO is also essential component to produce polytrimethylene terephthalate (PTT) which further transformed to use in the fiber and apparel industries. 1,3-PDO is thus still attracted from several scientists to produce via biological process for replacing the conventionally chemical method, although DuPont is a forefront company to produce the bio-based 1,3-PDO with the breakthrough methods. Numerous studies are still focus to observe the alternative way.

To present the new aspect of 1,3-PDO production via biological process in this study, our metabolically engineered *E. coli* NSK015 for producing 1,3-PDO was developed and disclosed in this chapter by introducing the *gdrAB-dhaB123* derived from *Klebsiella pneumoniae* and overexpressing *yqhD* under the control of *E. coli ldhA* and *pflB* promoters, respectively. The positive clones were then verified the expression of heterologous genes on the modified aldehyde indicator plates before further eliminating the major by-products genes. The different developed 1,3-PDO-producing *E. coli* was subsequently determined the efficiency of 1,3-PDO in the shake flask. The details can be found in this chapter.

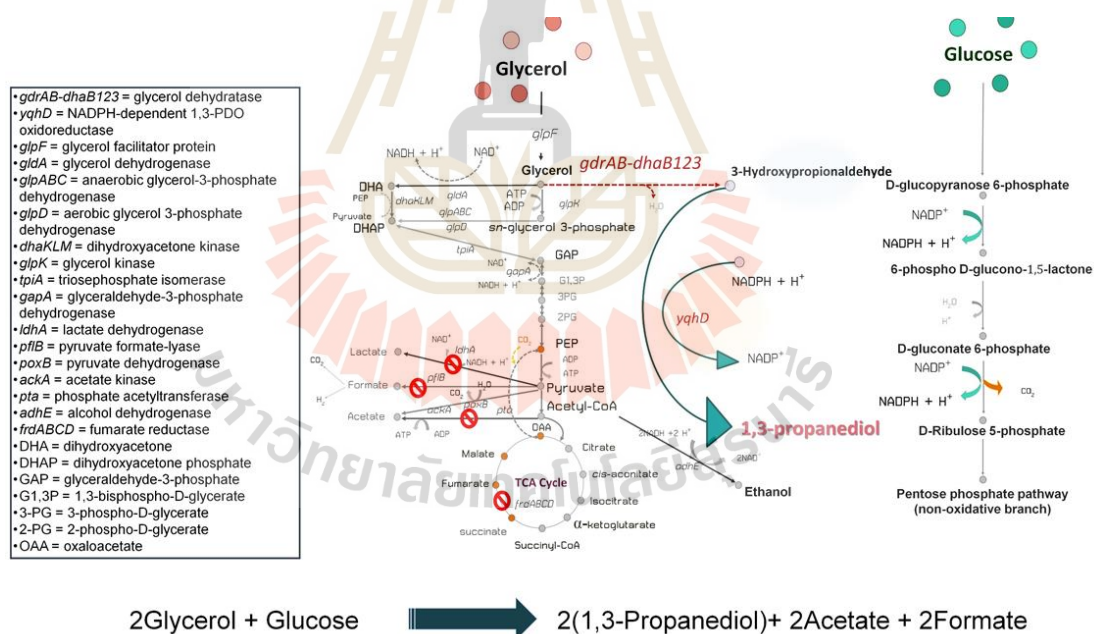


Figure.3.1 Proposed metabolism for 1,3-propanediol production in a metabolically engineered *E. coli* NSK015. Genes involving in the pathway are summarized in the box. Red cross signs represent the gene deletion. Genes *gdrAB-dhaB123* and *yqhD* were expressed under the control of native *ldhA* and *pflB* promoters.

3.2 Materials and methods

3.2.1 Microbial strains, plasmid, media, primers, and growth conditions

Table 3.1 shows plasmids, primers and microbial strains used in this study. *E. coli* C was used as a parental strain for engineering its metabolic pathway. *E. coli* TOP 10 was used to maintain constructed plasmids. Microbial strains were cultivated and maintained in LB broth or agar, at 37°C Apramycin (Apra), Chloramphenicol (Cm), Ampicillin (Amp), and Kanamycin (Km) antibiotics were supplemented into media as appropriated. An LB aldehyde indicator plate containing 3% (w/v) glycerol, 0.5% (w/v) sodium bisulfite and 0.05% (w/v) pararosaniline in ethanol was modified from the report of Conway et al. (1987) and used to identify the expression of glycerol dehydratase operon under the native *ldhA* promoter. Coenzyme-B12 was also provided at the concentration of 15 μ M during 1,3-PDO production. The low salt AM1 production medium (Martinez et al., 2007) was used throughout this study. Yeast extract (5 g/L) was also provided in AM1 as appropriate to determine its effect over fermentation.

3.2.2 Construction of an artificially expressing operon of glycerol dehydratase with its reactivating factors

Genes encoding glycerol dehydratase operon (*dhaB1*, *dhaB2*, and *dhaB3*) and its re-activating proteins (*gdrA* and *gdrB*) were derived from *K. pneumoniae* subsp. *pneumoniae* TISTR1867. Since *gdrB* gene is naturally oriented in the opposite

direction to other genes in *dhaB* operon and *gdrA*, the expressing cassette for glycerol dehydratase operon and its reactivating factors was then artificially constructed by the re-arrangement of the *gdrB* orientation to be identical to other genes in the operon. This artificial cassette was then expressed under the control of an intact *E. coli ldhA* promoter. The detail for construction of the artificial cassette is shown in Fig. 3.2. In step 1, *gdrB* gene and its surrounding sequences were amplified using Comp-gdrA(down)-gdrB-R (forward) and DH-ldhAp-gdrAB-dhaB123-F (reverse) primers. The forward primer contained sequences corresponding to the downstream region of *gdrA* (dash underlined letters) with space sequences between *gdrA* and *gdrB* genes (bold letters), and the upstream region of *gdrB* gene (underlined letters) at 5' and 3' ends respectively. The reverse primer contained sequences corresponding to the downstream region of the *ldhA* gene of *E. coli* host cell (bold) and to the termini of *gdrB* gene (underlined letters) at 5' and 3' ends respectively. The amplified PCR fragment (*gdrB* fragment) was cloned into pCR2.1-TOPO (Step 2), and the plasmid containing *gdrB* sequences lying in the same orientation of *dhaB* operon was selected and designated to be pKJ1010 (Step 3). On the other hand, *dhaB123* and *gdrA* genes and their surrounding sequences were also amplified using Comp-gdrB(up)-gdrA-F (forward) and DH-ldhAp-gdrAB-dhaB123-R (reverse) primers. The forward primer contained sequences corresponding to the upstream region of *gdrB* (dash underlined letters) with space sequences between *gdrA* and *gdrB* genes (bold letters), and the downstream region of *gdrA* gene (underlined letters) at 5' and 3' ends respectively. The reverse primer contained sequences corresponding

to the upstream region of the *ldhA* promoter of *E. coli* host cell (bold letters) and to the start codon of *dhaB1* gene (underlined letters) at 5' and 3' ends respectively. The resulting PCR fragment contained 5'-*gdrA-dhaB123*-3' sequences lying in the same orientation of *gdrB* gene on the plasmid pKJ1010 (Step 4).

The plasmid pKJ1010 was further used as the template for PCR amplification in an inside-out direction using *dhaB1*-M13-R/F (forward) and Comp-*gdrA*(down)-*gdrB*-R (reverse) primers. The forward primer contained sequences complementary to the upstream region of *dhaB1* gene (bold letters) and corresponding to M13 region on the plasmid (dash underlined letters) at 5' and 3' ends, respectively. This resulting PCR fragment was then treated with *DpnI* restriction enzyme and purified. The PCR fragment was a linearized pKJ1010 plasmid missing surrounding sequences of *gdrB* gene (Step 5). To facilitate the ligation of the linearized plasmid with an insert cassette (*gdrA-dhaB123*) in the next step, the linearized *DpnI*-treated pKJ1010 plasmid was used as the template to generate sticky ends at both sides using either *dhaB1*-M13-R/F or Comp-*gdrA*(down)-*gdrB*-R primers in separated PCR reactions (Step 6). Both amplified single-stranded PCR fragments were combined. The re-combined double-stranded PCR product was therefore treated with calf intestinal phosphatase (CIP) and purified. The resulting double-stranded CIP-treated PCR product contained sequences derived from the linearized pKJ1010 plasmid with sticky ends at both sides (Step 7). Consequently, the amplified PCR product in Step 4 was also used as a template in separate PCR reactions using either Comp-*gdrB*(up)-*gdrA*-F and M13-*dhaB1*-R

primers (Step 8). The M13-dhaB1-R primer contained sequences corresponding to M13 region on the plasmid and the upstream neighbouring region of *gdrA* (underlined letters). Both amplified single-stranded PCR fragments were combined, followed by the annealing reaction between two single-stranded PCR fragments performed in the same manner as previously mentioned. The resulting double-stranded PCR fragment contained sequences derived from the *gdrA-dhaB123* with sticky ends at both sides. The double-stranded PCR fragment was further treated with T4 polynucleotide kinase (T4-PNK) in Step 9. Finally, the CIP-treated linearized pKJ1010 plasmid was ligated with the T4-PNK treated *gdrA-dhaB123* insert cassette facilitated by the complementary sequences at overhangs on their both ends. The ligated plasmid contained the artificially expressing cassette *gdrAB-dhaB123* and was designated to pKJ1011 (Step 10).

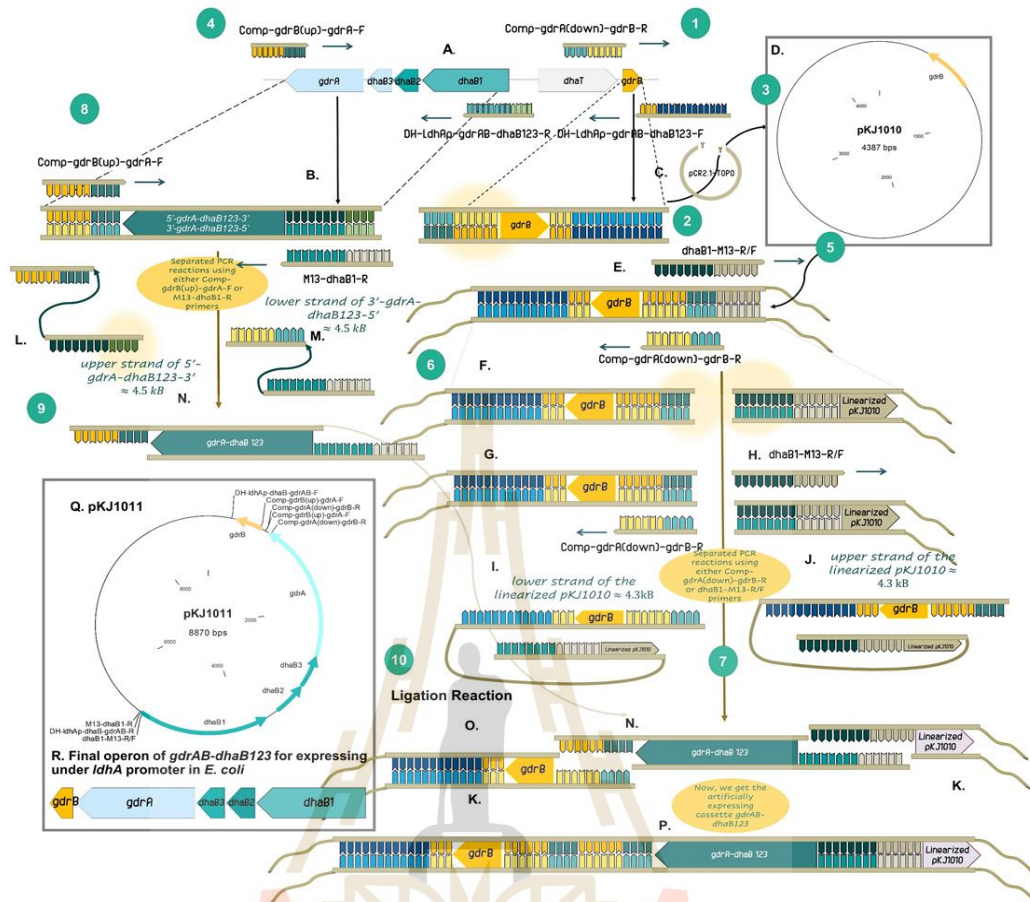


Figure 3.2 Construction of artificially operon of *gdrAB-dhaB123* on pKJ1011.

3.2.3 Construction of an expressing cassette encoding the native *E. coli* *yqhD*

E. coli yqhD gene was also cloned, integrated, and overexpressed under the control of the *E. coli pflB* promoter. This strategy was performed by the replacement of the *pflB* gene with the expressing cassette, thus simultaneously preventing the accumulation of acetyl-CoA, a precursor for acetate, but facilitating a higher re-oxidation rate of NADPH (Fig. 3.1). The detail for construction of the expressing cassette

is shown in Fig. 3.3. The upstream of *pflB* was first amplified by *yqhD*-*pflB*-F (forward) and *upfocA*-R (reverse) primers (Step 1). The forward primer contained sequences corresponding to the upstream regions of *yqhD* gene (bold letters) and *pflB* gene (underlined letters) at 5' and 3' ends, respectively. The resulting PCR fragment contained *yqhD*'-*pflB*-*focA*' sequences (Table 3.1).

The *yqhD* gene including its own promoter was further amplified by *pflB*-*yqhD*-F and *pflB*-*yqhD*-R (Step 2) while the downstream of *pflB* gene was amplified by *pflA*-F and *yqhD*-*pflB*-R primers (Step 3). The *yqhD*-*pflB*-R primer contained sequences corresponding to the downstream regions of *yqhD* gene (bold letters) and *pflB* gene (underlined letters) at 5' and 3' ends respectively (Table 3.1). After individual fragments were generated, the downstream of the *pflB* fragment was initially joined to *yqhD* fragment. Briefly, both PCR fragments were combined as a molar ratio of 1:1 and added in the PCR reaction containing Phusion polymerase (Invitrogen, USA) without primers using a slow annealing procedure at a decreasing rate of 0.1 °C/min for 15 cycles (Step 4). The gradual annealing step was facilitated by the overlap regions derived from *yqhD*-*pflB*-R and *pflB*-*yqhD*-F primers. The resulting fragment contained *yqhD*'-*yqhD*-*pflB*'-*pflA*' sequences. The fragment was further amplified using *pflA*-F and *pflB*-*yqhD*-R primers (Step 5). The amplified fragment was then joined to the upstream fragment of *pflB* as aforementioned (*yqhD*-*pflB*-*focA*) from Step 1 in PCR reaction containing Phusion polymerase without primers using a slow annealing procedure at a decreasing rate of 0.1 °C/min for 15 cycles (Step 6). The annealed fragment was used as

a template for the amplification of the shorter fragment containing *focA*-*yqhD*-*pflB* sequences using *pflA*-F and *focA*-R primers (Step 7). The *focA*-*yqhD*-*pflB* is thus cloned into pCR2.1-TOPO (Step 8), generating the plasmid pKJ1014.

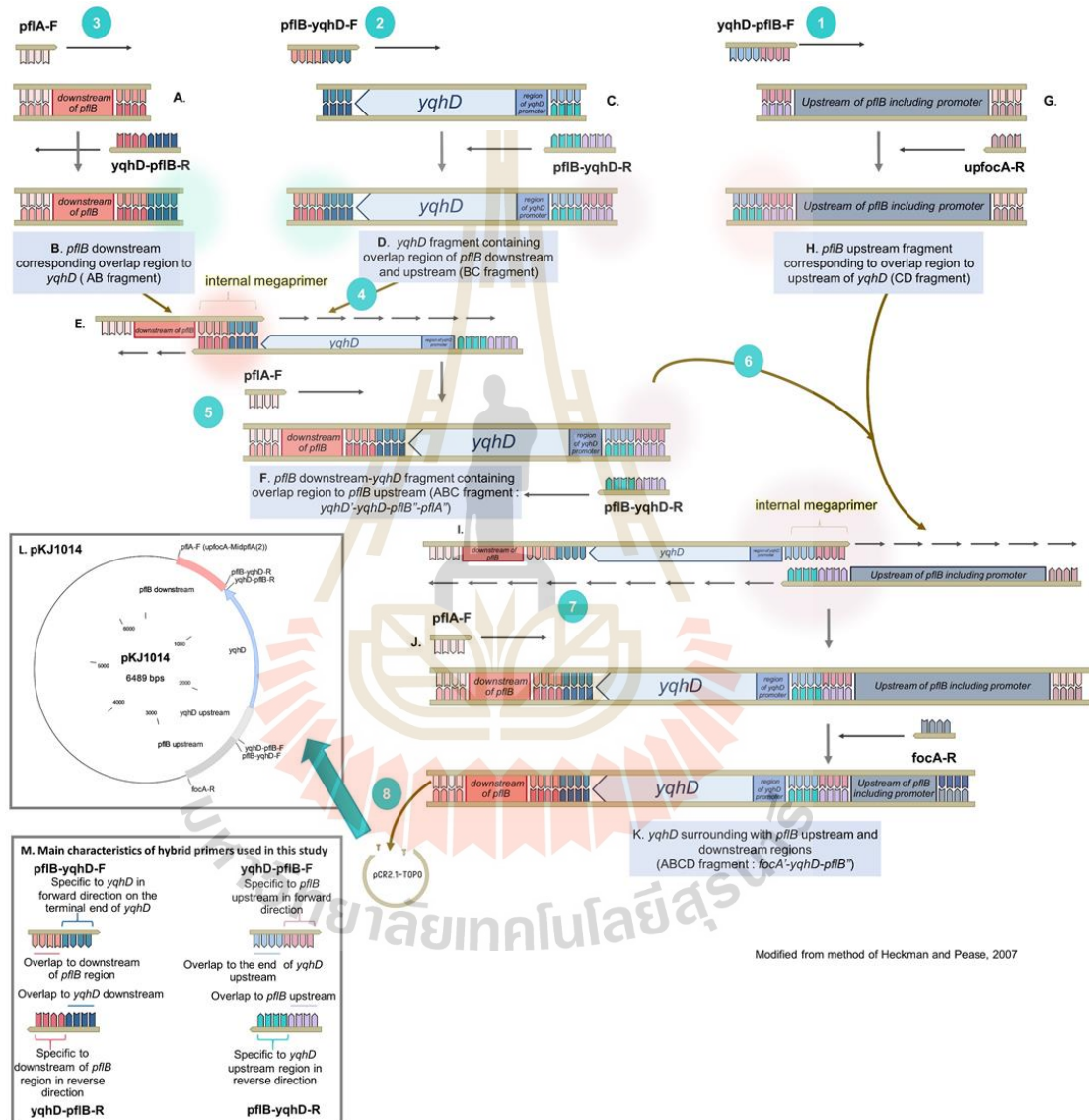


Figure 3.3 Construction of pKJ1014 for the replacement of *pflB* with *yqhD*.

3.2.4 Deletions of *ldhA*, *ackA* and *frdABCD* genes, and chromosomal integrations of the artificial *gdrAB-dhaB123* operon and *yqhD* gene in *E. coli* C

Gene encoding lactate dehydrogenase (*ldhA*) was initially deleted in *E. coli* C wild type. Briefly, the *cat-sacB* (chloramphenicol acetyltransferase-levan sucrose) cassette was amplified by PCR using the genomic DNA of *K. oxytoca* KMS005 (Jantama et al., 2015) as a template. The forward primer (DH-*ldhA*p-*cat-sacB*-F) contained hybrid sequences homologous to the downstream regions of *E. coli ldhA* gene and the *cat-sacB* cassette (bold letters) at 5' and 3' ends respectively, while the reverse primer (DH-*ldhA*p-*cat-sacB*-R) contained hybrid sequences homologous to upstream regions of *E. coli ldhA* gene and the *cat-sacB* cassette (bold letters) at 5' and 3' ends respectively. The amplified PCR fragment (*ldhA'*-*cat-sacB*-*ldhA''*) was then transformed into *E. coli* C carrying the plasmid pLOI3420. The homologous recombination of the fragment on the chromosomal *ldhA* region of *E. coli* C wildtype was confirmed using the colony PCR technique. The verified clone was renamed as *E. coli* NSK001 (Δ *ldhA*::*cat-sacB*).

Gene encoding acetate kinase (*ackA*) was also interrupted using techniques previously developed by Datsenko and Wanner (2000). Briefly, the PCR fragments containing kanamycin resistant gene flanked by parts of upstream and downstream sequences encoding *ackA* genes, were amplified by PCR reaction using the pKD4 plasmid as a template. The forward (*ackA*-pKD4-F) and reverse (*ackA*-pKD4-R) primers contained hybrid sequences homologous to upstream and downstream

regions of *E. coli ackA* gene at both 5' ends, respectively, followed by upstream and downstream regions of aminoglycoside phosphotransferase (*km*) gene on pKD4 plasmid at both 3' ends (bold letters) respectively. The resulting PCR fragments (*ackA'*-FRT-*km*-FRT-*ackA''*) were transformed into *E. coli* NSK001 carrying the plasmid pLOI3420. The integration of the fragment on the chromosomal *ackA* region of *E. coli* NSK001 was also confirmed using the colony PCR technique using *ackA*-F and JMackA-R primers. The verified clone was renamed as *E. coli* NSK002 ($\Delta ldhA::cat-sacB \Delta ackA::FRT-km-FRT$).

E. coli NSK002 strain further replaced the *cat-sacB* cassette on its chromosomal DNA by the artificially expressing cassette *gdrAB-dhaB123*. Briefly, *E. coli* NSK002 strain carrying pLOI3420 was transformed with the fragment of *gdrAB-dhaB123* cassette derived from pKJ1011 by electroporation. A specific integration of the artificially expressing *gdrAB-dhaB123* cassette at *E. coli ldhA* region occurred via a double homologous re-combination event facilitated by homologous sequences between upstream and downstream regions on chromosomal DNA and flanked regions on the cassette. The *gdrAB-dhaB123* cassette was designed to integrate in frame with the start codon at the *ldhA* promoter. The cassette therefore was expressed under the control of the host *ldhA* promoter. Colonies that exhibited loss of apramycin, and chloramphenicol resistances and viability on sucrose medium subsequently verified the integration of the cassette at the *ldhA* promoter by the PCR technique. The confirmed clone was designated *E. coli* NSK003 ($\Delta ldhA::gdrAB-dhaB123\Delta ackA::FRT-km-FRT$). To

remove the *km* gene, a plasmid pFT-A expressing a recombinase was transformed into *E. coli* NSK003. *E. coli* NSK003 strain carrying pFT-A was further cultured in LB medium containing chlortetracycline (20 µg/mL) at 30°C for 8 h to allow self-recombining between FRT sites facilitated by the recombinase. Then single colonies were obtained on LB agar on incubating plates at 45°C for 24 h. Clones that did not confer antibiotic resistances were picked and confirmed for the loss of antibiotic resistant genes by the colony PCR technique using *ackA*-F and *JMackA*-R primers. The verified clone was renamed as *E. coli* NSK012 ($\Delta ldhA::gdrAB-dhaB123\Delta ackA::FRT$).

Gene encoding pyruvate formate lyase (*pflB*) was further deleted in *E. coli* NSK012 following the same strategy for deletion of *ldhA* gene as previously mentioned. The forward (WMpflBA-F) and reverse (WMpflBA-R) primers contained hybrid sequences homologous to downstream and upstream regions of *pflB* gene at both 5' ends (underlined) respectively, followed by downstream and upstream regions of *cat-sacB* cassette on genomic DNA of *K. oxytoca* KMS005 at both 3' ends (bold letters) respectively. The amplified PCR fragment (*pflB*'-*cat-sacB*-*pflB*") was then transformed into *E. coli* NSK012 carrying the plasmid pLOI3420. The integration of the *pflB*'-*cat-sacB*-*pflB*" fragment on the chromosomal *pflB* region of *E. coli* NSK012 was further confirmed using the colony PCR technique. The verified clone was re-named as *E. coli* NSK013 ($\Delta ldhA::gdrAB-dhaB123\Delta ackA::FRT\Delta pflB::cat-sacB$). *E. coli* NSK013 strain carrying pLOI3420 was further transformed with the fragment of *focA*'-*yqhD*-*pflB*" derived from pKJ1014. Colonies were screened on replica plates including LB agar

supplemented with sucrose, apramycin, and chloramphenicol. Colonies that exhibited loss of apramycin, and chloramphenicol resistances and viability on sucrose medium subsequently verified the integration of the cassette at the *pflB* promoter by PCR technique. The confirmed clone was designated *E. coli* NSK014 ($\Delta dhAB::gdrAB-dhaB123\Delta ackA::FRT\Delta pflB::yqhD$).

Gene encoding fumarate reductase (*frdABCD*) was further deleted in *E. coli* NSK014 following the same strategy of inside-out technique (Jantama et al., 2008), the *frdABCD* fragments were amplified by *frdABCD*-F and *frdABCD*-R primers and cloned into pCR2.1-TOPO. The cloned plasmid was used as the template in the inside-out PCR reaction by IO*frd*-F and IO*frd*-R primers. The inside-out resulting PCR product contained sequences derived from pCR2.1-TOPO with the flanking regions of *frdABCD* gene thus missing its central sequences. The *cat-sacB* cassette was then amplified from *K. oxytoca* KMS005 by *catfrd*-F and *catfrd*-R primers using the PCR reaction and ligated into the inside-out resulting plasmid, generating pKJ1012. The amplified PCR fragment (*frd'*-*cat-sacB*-*frd''*) derived from pKJ1012 was then transformed into *E. coli* NSK014 carrying the plasmid pLOI3420. The integration of the *frd'*-*cat-sacB*-*frd''* fragment on the chromosomal *frd* region of *E. coli* NSK014 was also confirmed using the colony PCR technique. The verified clone was re-named *E. coli* NSK015 ($\Delta dhA::gdrAB-dhaB123\Delta ackA::FRT\Delta pflB::yqhD\Delta frdABCD::cat-sacB$).

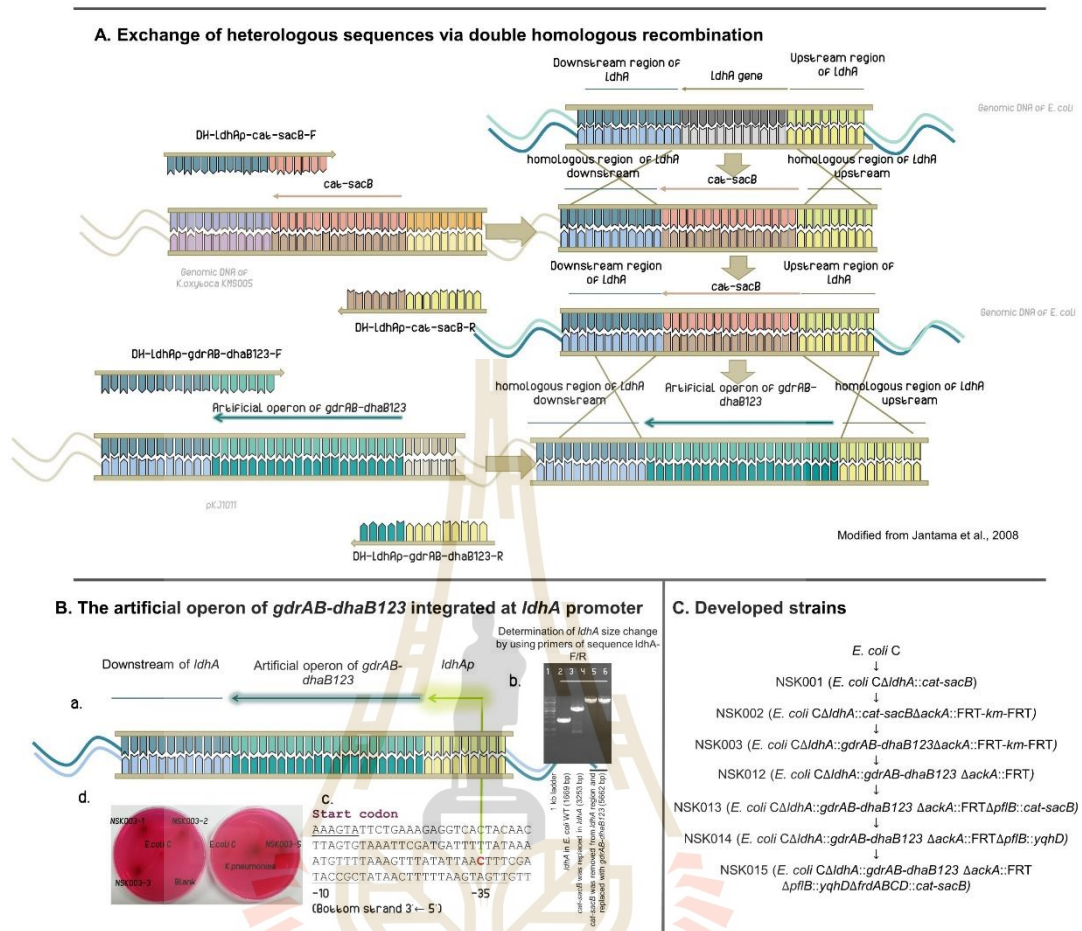


Figure 3.4 An overview of molecular engineering for constructing recombinant *E. coli* NSK strains to produce 1,3-propanediol. (A) Genome replacement between the artificial operon of *gdrAB-dhaB123* and *ldhA* genes by double homologous recombination in *E. coli* C (B) Schematic model of the integrated artificial operon of *gdrAB-dhaB123* under the control of *E. coli* *ldhA* promoter. (C) Sequential development of *E. coli* NSK strains for 1,3-PDO production.

3.2.5 Enzyme assay

Cells at the late-log phase cultures were harvested by centrifugation of 4000 *g* at 4°C for 10 min. The pellets were washed using 0.05 M PBS buffer (pH 8.0) twice then re-suspended with a final volume of 2 mL. The cell was further disrupted by an ultrasonic disintegrator at 40 kHz with alternate pulses of sonication for 10 min. The cell debris in the crude lysate were separated. The supernatant was used to determine the total protein concentration by the Bradford's method (Bradford, 1976) and its enzymatic activities.

To determine the activity of glycerol dehydratase, the method of Knietsch et al. (2003) was applied. The apparent molar extinction coefficient derived from 3-hydroxypropionaldehyde(3-HPA) used for the calculation of the specific enzyme activity of glycerol dehydratase was $5.23 \times 10^3 \text{ M}^{-1}\text{cm}^{-1}$. The specific glycerol dehydratase activity was reported as amounts of aldehydes formed per mg total protein. To determine the 1,3-PDO oxidoreductase activity, the enzymatic compositions in the reaction were the same as in those of the glycerol dehydratase activity according to the method of Knietsch et al. (2003). However, 1,3-PDO was used as substrate instead of glycerol. The specific 1,3-PDO oxidoreductase activity was reported as amounts of aldehydes formed per mg total protein.

3.2.6 Fermentation experiment

In shake flask experiments, the seed cultures were inoculated in 100 mL AM1 medium containing 20 g/L glycerol with or without either glucose or yeast extract

at an initial OD₅₅₀ of 0.1 in 500 mL in an Erlenmeyer flask at 37°C, 200 rpm for 72 h. Samples were intermittently taken every 12 h for analyses.

E. coli NSK015 strain was grown in 100 mL LB supplemented with 2% (w/v) glucose in a 250 mL shaking flask at 37°C, 200 rpm for 12 hours. The inoculum was transferred into 1 L AM1 medium containing substrates with the initial OD₅₅₀ of 0.1 in a 2L fermenter. The solution of 3M KOH was automatically added into the broth to maintain pH of cultures at 7.0. The aeration rate of 1 vvm and agitation of 200 rpm were provided. One mL of sample was taken every 12 hours for analyses for 108 h.

The mixed cassava starch (60 g/L) and glycerol (50 g/L) in AM1 medium containing coenzyme B12 were used as substrates for studying 1,3-PDO production in a 2L fermenter. After sterilization, the solution mixture was cooled down to 60°C. Amylase (Amy) and amylo-glucosidase (AMG) at concentrations of 100 U and 600 U per gram cassava starch respectively to hydrolyse the cassava starch. The cassava hydrolysis was allowed for 4 h at 50°C for 2 h. After hydrolysis, the seed of *E. coli* NSK015 strain was inoculated into the medium with the initial OD₅₅₀ of 0.1 and temperature was maintained at 37°C during fermentation.

3.2.7 Analytical method

Fermentation broth was collected and separated by centrifugating at 15,000 rpm for 5 min. The supernatant was analysed with HPLC while cell pellet was mixed with 1 mL DI water and determined the cell biomass. The biomass concentration was determined ($3 \text{ OD}_{550} = 1 \text{ g/L}$ cell dry weight; Khunnonkwao et al. (2018)). HPLC

analysis coupled with an anion exclusion column (Bio-RAD, Aminex, HPX-87H, USA) was used to analyse sugars and fermentative products. The column was controlled at the temperature of 45°C. The solution of 4 mM H₂SO₄ was used as a mobile phase with a flow rate of 0.4 mL/min. The experiments were performed in triplicate. Average values with the standard deviation were reported. Duncan's multiple-ranges test (DMRT) was used to determine differences among mean values at 95% significance level (P<0.05).

Table 3.1 Plasmids, strains and primers used for this study.

Strains	Relevant Characteristic	Source
<i>Plasmid</i>		
pLOI3420	<i>acc γ β exo</i> (Red recombinase), sensitive replicon of temperature	Wood et al. (2005)
pKD4	<i>bla</i> ;FRT- <i>kan</i> -FRT cassette	Datsenko and Wanner (2000)
pFT-A	<i>bla flp</i> low-copy vector containing recombinase and temperature-conditional pSC101 replicon	Datsenko and Wanner (2000)
pCR2.1-TOPO	<i>bla</i> , <i>kan</i> TOPO TA cloning vector	Invitrogen
pKJ1010	pCR2.1-TOPO- <i>gdrB</i>	This study
pKJ1011	pCR2.1-TOPO- <i>gdrAB-dhaB123</i>	This study
pKJ1012	pCR2.1-TOPO- <i>frd'</i> - <i>cat-sacB-frd''</i>	This study
pKJ1013	pCR2.1-TOPO- <i>yqhD</i>	This study

Table 3.1 Plasmids, strains and primers used for this study (Continued).

Strains	Relevant Characteristic	Source
pKJ1014	pCR2.1-TOPO- <i>focA</i> · <i>yqhD</i> - <i>pflB</i> ''	This study
<i>E. coli</i> TOP10		Invitrogen
<i>E. coli</i> C	Wild type	ATCC
KMS005	<i>K. oxytoca</i> Δ <i>adhE</i> Δ <i>ackA</i> - <i>pta</i> Δ <i>ldhA</i> :: <i>cat</i> - <i>sacB</i>	Jantama et al. (2015)
NSK001	<i>E. coli</i> C Δ <i>ldhA</i> :: <i>cat</i> - <i>sacB</i>	This study
NSK002	<i>E. coli</i> C Δ <i>ldhA</i> :: <i>cat</i> - <i>sacB</i> Δ <i>ackA</i> ::FRT- <i>km</i> -FRT	This study
NSK003	<i>E. coli</i> C Δ <i>ldhA</i> :: <i>gdrAB</i> - <i>dhaB123</i> Δ <i>ackA</i> ::FRT- <i>km</i> -FRT	This study
NSK012	<i>E. coli</i> C Δ <i>ldhA</i> :: <i>gdrAB</i> - <i>dhaB123</i> Δ <i>ackA</i> ::FRT	This study
NSK013	<i>E. coli</i> C Δ <i>ldhA</i> :: <i>gdrAB</i> - <i>dhaB123</i> Δ <i>ackA</i> ::FRT Δ <i>pflB</i> :: <i>cat</i> - <i>sacB</i>	This study
NSK014	<i>E. coli</i> C Δ <i>ldhA</i> :: <i>gdrAB</i> - <i>dhaB123</i> Δ <i>ackA</i> ::FRT Δ <i>pflB</i> :: <i>yqhD</i>	This study
NSK015	<i>E. coli</i> C Δ <i>ldhA</i> :: <i>gdrAB</i> - <i>dhaB123</i> Δ <i>ackA</i> ::FRT Δ <i>pflB</i> :: <i>yqhD</i> Δ <i>frdABCD</i> :: <i>cat</i> - <i>sacB</i>	This study
Primers		
Comp-	5' <u>CGGGCTGCTACTGGCCGGTCAGGCGAATTAA</u>	This study
<i>gdrA</i> (down)-	AGTGTTAACGAGGGGACCGTC <u>ATGTCGCTTTC</u>	
<i>gdrB</i> -R	<u>ACCGCCA</u> 3'	

Table 3.1 Plasmids, strains and primers used for this study (Continued).

Strains	Relevant Characteristic	Source
<i>Primers</i>		
DH-ldhAp-	5·ATTGGGGATTATCTGAATCAGCTCCCCT	This study
gdrAB-	GGAATGCAGGGGAGCGGCAAGA	
dhaB123-F	<u>TCAGTTTCTCTCACTTAACG3</u> ·	
Comp-	5· <u>GCGTACGCCTGGCGGTGAAAGCGACAT</u>	This study
gdrB(up)-gdrA-	GACGGTCCCCTCGTTAACACTTTAATTCG	
F	<u>CCTGACCGGCCAGT3</u> ·	
DH-ldhAp-	5·AAATATTTTTAGTAGCTTAAATGTGATT	This study
gdrAB-	CAACATCACTGGAGAAAGTCTTATGAAA	
dhaB123-R	<u>AGATCAAAACGATT3</u> ·	
dhaB1-M13-	5·CCAGTACTGCAAATCGTTTTGATCTTTT	This study
R/F	<u>CATCACTGGCCGTCGTTTTAC3</u> ·	
M13-dhaB1-R	5·GTAAAACGACGGCCAGTGATGAAAAGA	This study
	<u>TCAAAACGATTTGCAGTACTGG3</u> ·	
DH-ldhAp-cat-	5·ATTGGGGATTATCTGAATCAGCTCCCCT	This study
sacB-F	GGAATGCAGGGGAGCGGCAAGAACACTG	
	CTTCCGGTAGTCAA3·	

Table 3.1 Plasmids, strains and primers used for this study (Continued).

Strains	Relevant Characteristic	Source
<i>Primers</i>		
DH-ldhA _{p-cat}	5'AAATATTTTTAGTAGCTTAAATGTGATTC	This study
sacB-R	AACATCACTGGAGAAAGTCTTCGGCACGT AAGAGGTTCCAA3'	
ackA-pKD4-F	5'CTATGGCTCCCTGACGTTTTTTTAGCCAC GTATCAATTATAGGTA CTTC CGTGTAGGCT GGAGCTGCTTC3'	This study
ackA-pKD4-R	5'TCAGGCAGTCAGGCGGCTCGCGTCTTGC GCGATAACCAGTTCCTCCATATGAATATCC TCCTTAG3'	This study
ackA-F	5-CACCTCAACTTCACATATAAAG3'	This study
JMackA-R	5GCACGATAGTCGTAGTCTGA3'	This study
yqhD-pflB-F	5-CTTTCGCACGTACACCGGTGGTAACACCT ACCTTCTTAAG3'	This study
yqhD-pflB-R	5'GTATATACGAAGCCGCCCCTAATAGAT TTGACTGAAATCGT3'	This study
pflB-yqhD-F	5'ACGATTCAGTCAAATCTATTAGCGGGC GGCTTCGTATATAC3'	This study

Table 3.1 Plasmids, strains and primers used for this study (Continued).

Strains	Relevant Characteristic	Source
<i>Primers</i>		
pflA-F	5·AACCGTTGGTGTCCAGACAG3·	Jantama et al., 2008
upfocA-R	5·AGATCGCCAGCCGCTGCAAT3·	Jantama et al., 2008
focA-R	5·ACCTGGTCGGCGCACTGCTG3·	This study
WMpflBA -F	5·TTACATAGATTGAGTGAAGGTACGAGTA ATAACGTCCTGCTGCTGTTCTACACTGCTT CCGGTAGTCAA3·	Jantama et al., 2008
frdABCD-F	5·TTAGATTGTAACGACACCAATCAG3·	This study
frdABCD-R	5·GTTTCGCAGACCGTAACTTT3·	This study
IOfrd-F	5·TTGGAACCTCTTACGTGCCGTCGCCACCC GCTACTGTATC 3·	This study
IOfrd-R	5·TTGACTACCGGAAGCAGTGTCGCGCAGA GCTTCATTGGTC 3·	This study
catfrd-F	5·GACCAATGAAGCTCTGCGCGACACTGCT TCCGGTAGTCAA 3·	This study

Table 3.1 Plasmids, strains and primers used for this study (Continued).

Strains	Relevant Characteristic	Source
<i>Primers</i>		
catfrd-R	5'GATACAGTAGCGGGTGGCGACGGCACG TAAGAGGTTCCAA 3'	This study
sequence-ldhA-F	5'CACATGCTGCCGGAATCATC3'	This study
sequence-ldhA-R	5'ACGCGTAATGCGTGGGCTTTC3'	This study

3.3. Results and discussion

3.3.1 Functional expression of the *gdrAB-dhaB123* operon for 1,3-propanediol pathway in *E. coli*

K. pneumoniae, naturally utilizes glycerol to produce 1,3-PDO, it is though considered as a potential pathogen and may not be safe for operators in an industrial scale of production. Over the two past decades, all previous studies made efforts in *E. coli* as an alternative host to produce 1,3-PDO by the over-expression of heterologous genes involved in the glycerol utilization (Table 2.1). However, a plasmid instability in developed *E. coli* strains may cause a low production rate and yield of 1,3-PDO during cultivation of them on an industrial scale (Friehs, 2004). Additionally, antibiotics and IPTG are required for the maintenance of plasmids and the induction of gene expressions for 1,3-PDO production, resulting in ever-increasing production cost.

To resolve these obstacles, genes involved in glycerol metabolism through 1,3-PDO producing pathway should be designed to be integrated into the *E. coli* genome and expressed under the control of one of the host constitutive promoters.

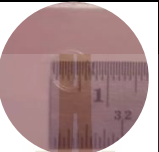
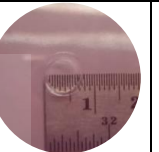
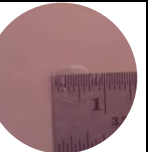
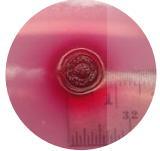
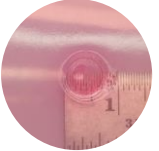
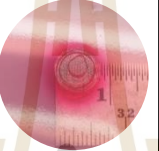
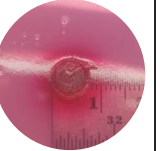
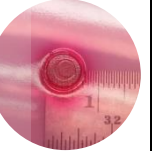
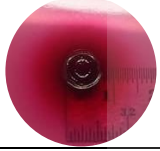
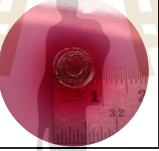
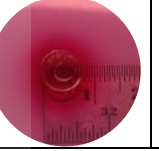
Time (h)	<i>K. pneumoniae</i>	<i>E. coli</i> C (wildtype)	NSK012	NSK013	NSK014	NSK015
0						
10						
16						

Figure. 3.5 Comparison of developed dark pink color on a modified aldehyde indicator plates containing glycerol between developed *E. coli* NSK strains and *K. pneumoniae* (positive control) and *E. coli* C as wildtype (negative control).

In this study, the glycerol dehydratase operon (*dhaB123* genes) from *K. pneumoniae* subsp. *pneumoniae* TISTR1867 was simultaneously expressed with its reactivating factors (*gdrAB*) in *E. coli* NSK002. Glycerol dehydratase requires reactivating factors for glycerol conversion to 3-HPA. Since *dhaB123* and *gdrA* genes in *K. pneumoniae* are arranged in the opposite direction to *gdrB* gene (Rathnasingh et al.,

2009), the re-arranged *gdrAB-dhaB123* cassette was used as a one operon (pKJ1011; Fig. 3.2). The structural *ldhA* gene of *E. coli* NSK002 was simultaneously deleted and replaced by the artificially constructed *gdrAB-dhaB123* operon (Fig. 3.1). The operon was then stably integrated in frame with the *E. coli* *ldhA* promoter. The automated sequencing analysis confirmed that no mutations at the *ldhA* promoter region and *gdrAB-dhaB123* gene were found (Fig. 3.4a-c) on the genome of recombinant clones. All positive clones (*E. coli* NSK003 strains) showed the dark pink colonies on the aldehyde indicator plate, thus resemble to that of *K. pneumoniae* while *E. coli* C wild type did not (Fig. 3.4d; Fig. 3.5). This result indicated that the artificially constructed *gdrAB-dhaB123* operon was successfully expressed and functioned in the *E. coli* NSK003 clones under the control of *ldhA* promoter and the clones accumulated 3-HPA from glycerol. This also confirmed that the strategy for the expression of the *gdrAB-dhaB123* operon under the native *ldhA* promoter was sufficient to allow a glycerol conversion to 3-HPA.

Previous studies suggested that an imbalance expression and an instability of glycerol dehydratase enzyme caused the accumulation of 3-HPA thus exhibiting cell growths and the production of 1,3-PDO (Chen et al., 2011; Kim et al., 2014). Then glycerol dehydratase was expressed on low-copy number plasmids (Rathnasingh et al., 2009) or its codon optimization was performed (Lim et al., 2016) to ensure that the glycerol conversion to 3-HPA was not too rapid by the high activity of the enzyme, while 3-HPA did not accumulate such an inhibitory level of inside cells. Based on this study's result, it is likely that the *ldhA* promoter is suitable for the

employment of a constitutive expression of the *gdrAB-dhaB123* operon without the growth retardation (Fig. 3.6A) in *E. coli* NSK012 (a derivative of *E. coli* NSK003) in the shake flask experiment. It is well known that lactate dehydrogenase (LDH) is substantially present under both aerobic and anaerobic conditions with a basal level but is activated when *E. coli* grew on a variety of sugars under at acidic pH (Bunch et al., 1997). Additionally, *E. coli* NSK012 possessed the significantly higher activity of glycerol dehydratase at the level of 0.38 ± 0.07 U/mg protein compared with that of its parental *E. coli* NSK002 strain (0.26 ± 0.05 U/mg protein). However, the background of the enzyme activity may be a result from the presence of another iso-functional diol dehydratases usually found in *E. coli* and *Klebsiella* species. Surprisingly, the specific activity of 1,3-PDO oxidoreductase catalysing 3-HPA to 1,3-PDO was significantly increased in *E. coli* NSK012 (0.25 ± 0.02 U/mg protein) compared to that of *E. coli* NSK002 (0.17 ± 0.01 U/mg protein) (Table 3.2) even though it was not overexpressed in the strain. This result suggested that the over-expression of glycerol dehydratase may up-regulate an enzymatic activity of 1,3-PDO oxidoreductase to catalyse the accumulated 3-HPA and to prevent its negative effects in *E. coli* NSK012. *E. coli* NSK012 produced 1,3-PDO from glycerol at the level of 4.5 g/L within 72 h incubation in a shaking flask while no 1,3-PDO production was observed by *E. coli* NSK002 (Fig. 3.6B and C). Acetate and succinate were major by-products. This study's success in the demonstration of the functional expression of the *gdrAB-dhaB123* operon by the *ldhA* promoter to produce 1,3-PDO in *E. coli* NSK012 resembles the work of Zhang et al.

(2007) in which they successfully utilized the host *ldhA* promoter for driving the expression of alanine dehydrogenase (*alaD*) to produce L-alanine. The engineered *E. coli* strain produced L-alanine at its high production yield.

3.3.2 Improved 1,3-propanediol production caused by deletion of *pflB* but not the over-expression of *yqhD*

Acetate up to 2.0 g/L with a few formate was accumulated during 1,3-PDO production by *E. coli* NSK002 and *E. coli* NSK012 strains even though both strains possessed the deletion of *ackA* (encoding acetate kinase enzyme) (Fig. 3.6C). In et al. (2020) demonstrated that the elimination of *pflB* gene in *K. oxytoca* KIS004-91T led the strain lacking the ability to produce acetyl-CoA and formic acid from pyruvate in the central metabolism, thus significantly lowering the acetate production during productions of succinic acid and lactic acid, respectively, under anaerobic conditions. After the deletion of *pflB*, *E. coli* NSK013 drastically increased the level of 1,3-PDO up to 5.8 g/L (Fig. 3.6C), which was about a 26.1% increase, compared to that of *E. coli* NSK012 (4.6 g/L).

Additionally, acetate production significantly declined by three folds in *E. coli* NSK013 (0.8 g/L), compared to that of *E. coli* NSK012 (2.4 g/L). The 1,3-PDO production yield by *E. coli* NSK013 was significantly improved to be 0.38 mol/mol glycerol used in the shaking flask conditions (Fig. 3.6B). This suggested that the deletion of *pflB* conserved the carbon flux and diverted it through 1,3-PDO pathway. The result also demonstrated that the activation of the *pflB* transcription may be relieved from an

induction of FNR and ArcAB regulatory proteins under aerobic conditions (shaking flasks in our study), even though Hasona et al. (2004) have revealed that PflB catalyses the non-oxidative cleavage of pyruvate to acetyl-CoA and formic acid under anaerobic conditions. This study's results also showed that *E. coli* NSK012 accumulated acetyl-CoA, a precursor of acetate, at a higher level than that of *E. coli* NSK013 regardless of oxygen deprivation. Wagner et al. (2001) and Zhu et al. (2007) revealed that YfiD protein, a pyruvate formate-lyase activase enzyme, activated PflB by acting as the glycy radical domains to reconstitute the catalytic center of oxygen-fragmented PflB, and to rapidly recover PflB activity, thus generating ATP in the presence of oxygen even or under oxidative stress in *E. coli*. These researchers also suggested that *E. coli* utilized both PflB and pyruvate dehydrogenase to supplement the acetyl-CoA pool under aerobic or micro-aerobic conditions.

Table 3.2 Enzymatic activity of glycerol dehydratase and 1,3-propanediol oxidoreductase for different developed *E. coli* strains

Enzyme	Enzymatic activity (U/mg protein)						
	Strain	<i>K. pneumoniae</i>	NSK002	NSK012	NSK013	NSK014	NSK015
Glycerol dehydratase		0.64±0.11 ^a	0.26±0.05 ^b	0.38±0.07 ^c	0.44±0.04 ^c	0.42±0.04 ^c	0.27±0.06 ^b
1,3-PDO oxidoreductase		1.11±0.13 ^a	0.17±0.01 ^b	0.25±0.02 ^c	0.47±0.03 ^d	0.50±0.07 ^d	0.24±0.07 ^{b,c}

- The superscript letters represent the significant difference of values between columns in the same row.

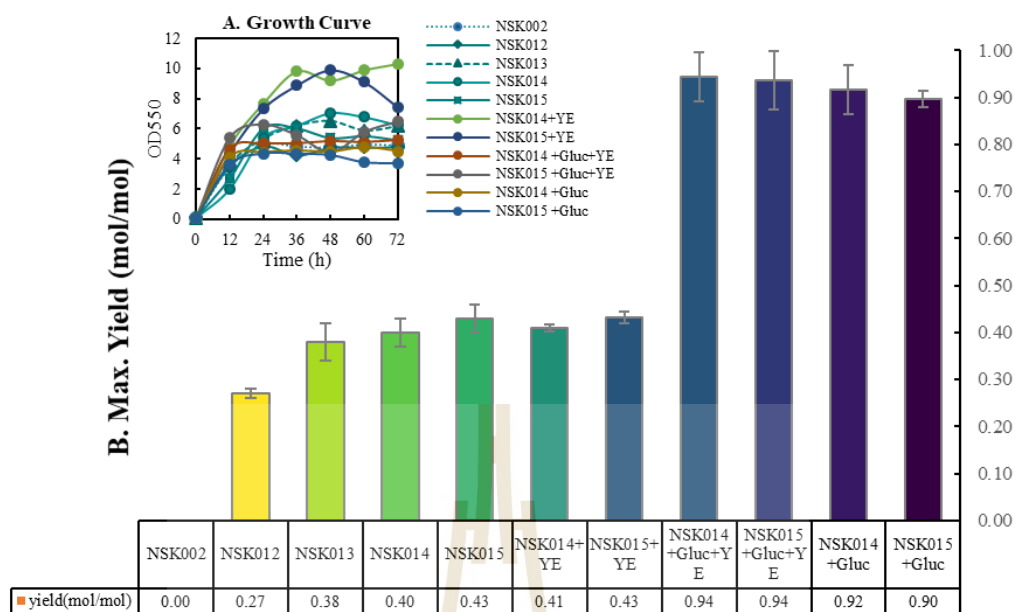


Figure 3.6 Comparison of microbial growth (A) and maximum 1,3-propanediol production yield (B) of developed *E. coli* NSK strains in AM1 medium containing 20 g/L glycerol and 100 mM KHCO_3 with or without glucose (Glu) and yeast extract (YE) in shaking flasks. Fermentation profiles of developed *E. coli* NSK strains in AM1 medium containing only 20 g/L glycerol and 100 mM KHCO_3 in 250 mL shaking flasks (C).

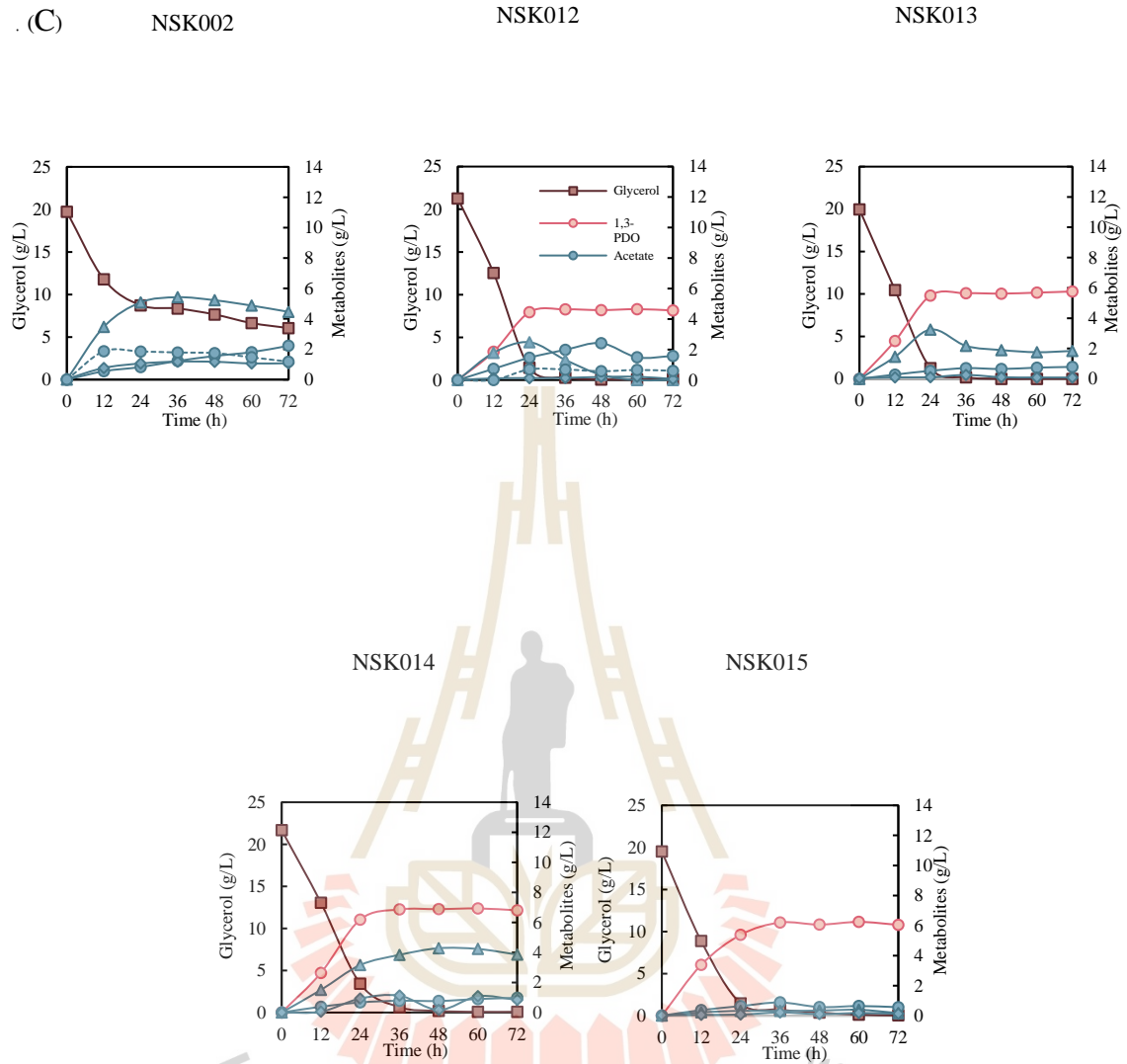


Figure 3.6 (Continued).

To further increase 1,3-PDO production, *pflB* gene was simultaneously replaced by the native *E. coli yqhD* gene and the 1,3-PDO oxidoreductase (YqhD or PDOR) was simultaneously overexpressed. Surprisingly, the over-expression of *yqhD* gene did not result in an increase in 1,3-PDO titre and yield in *E. coli* NSK014 compared to those of *E. coli* NSK013 (Fig. 3.6B and C). The results of the enzymatic activity analysis also revealed that both *E. coli* NSK013 and *E. coli* NSK014 strains showed comparable levels of glycerol dehydratase activity (0.44 ± 0.04 and 0.42 ± 0.04 U/mg protein, respectively) compared to that of *E. coli* NSK012 (0.38 ± 0.07 U/mg protein). However, *E. coli* NSK013 (0.47 ± 0.03 U/mg protein) possessed the YqhD activity at a significantly higher level (2 folds increase) than that of *E. coli* NSK012 (0.25 ± 0.02 U/mg protein) but at an equivalent level compared to that of *E. coli* NSK014 (0.50 ± 0.07 U/mg protein) (Table 3.2). These results indicated that the over-expression of glycerol dehydratase and the accumulation of 3-HPA in *E. coli* NSK013 were able to enhance its intact YqhD activity to detoxify 3-HPA and to sufficiently complete the 1,3-PDO pathway. This was confirmed by that the *yqhD* was overexpressed in *E. coli* NSK014 though the YqhD activity was still comparable to that of *E. coli* NSK013 (Table 3.2). No further increase in 1,3-PDO yield (Fig. 3.6B and C) was thus observed in *E. coli* NSK014. Our results were in an accordance with the study of Emptage et al. (2003) in which they also demonstrated that *E. coli* strain was more preferable to utilize its intact YqhD to efficiently converted 3-HPA to 1,3-PDO. The further overexpression of a dual 1,3-PDO

dehydrogenase/oxidoreductase (encoded by *dhaT*) or similar dehydrogenases from *Klebsiella* species did not substantially enhance the 1,3-PDO yield.

The conversion of 3-HPA by the activity of PDOR may be considered as a rate-limiting step in the 1,3-PDO biosynthesis (Jiang et al., 2015). The availability of reducing powers, NADH or NADPH, during the reduction of 3-HPA by PDOR activity, may additionally govern the reaction. Yun et al. (2018) investigated the biotransformation of 3-HPA derived from the whole cell *C. butyricum* YJH-09 that co-cultured with *E. coli* BL21 overexpressing *dhaT*. The 1,3-PDO concentration and yield at levels of 20.8 g/L and 0.51 mol/mol glycerol were obtained, respectively, while *C. butyricum* YJH-09 alone produced 1,3-PDO at the concentration and yield of only 11.7 g/L and 0.28 mol/mol, respectively. However, the supplement of exogenous NADH to the co-culture enhanced the metabolic shift toward reduction of 1,3-PDO oxidoreductase and improved 1,3-PDO yield from the mixture of glycerol and glucose. The concentration and yield of 1,3-PDO were increased up to 25.9 and 0.65 mol/mol glycerol, respectively. Yang et al. (2018) also overexpressed the NADP⁺-dependent glyceroldehyse-3-phosphate dehydrogenase to increase NADPH pool in *E. coli* JA11. The strain synthesized 13.5 g/L 1,3-PDO and could enhance two folds of 1,3-PDO yield (0.64 mol/mol) from glycerol/glucose mixture compared to its parental strain. Not only enhancing the activity of PDOR but also the increasing NAD(P⁺)H/NAD ratio must be employed to detoxify 3-HPA through 1,3-PDO biosynthesis pathway.

3.3.3 1,3-propanediol production is associated with a bicarbonate availability and succinate production in *E. coli* NSK strains

Surprisingly, growth and glycerol assimilation of all engineered strains used in this study were impaired in AM1 medium without supplementation of 100 mM bicarbonate (Fig. 3.7). The glycerol was rarely consumed by all strains compared to those cultivated with AM1 medium containing bicarbonate (source of CO₂). This implied that bicarbonate was essential for the growth and utilization of glycerol during 1,3-PDO production for the strains. This speculation was supported by the better growth of *E. coli* NSK012 than those of *E. coli* NSK derivatives that possessed the *pflB* deletion (Fig. 3.7). Dharmadi et al. (2006) revealed that glycerol fermentation was associated with an availability of CO₂ (produced by pyruvate by the activity of PflB) via the oxidation of formic acid by the formate-hydrogen lyase enzyme under acidic conditions in *E. coli* regardless of oxygen availability. The produced CO₂ derived from formate was usually utilized by the reductive branch of TCA cycle via carboxylation of PEP for succinate. The researchers also demonstrated that the consumed glycerol by *E. coli* was generally converted to ethanol and succinate due to its highly reduced nature of glycerol. Though, succinate was rarely formed in aerobic conditions but was efficiently produced under anaerobic conditions (Jantama et al., 2008). They also demonstrated that *E. coli* KJ122, a derivative of *E. coli* C, efficiently produced succinate when KHCO₃ was supplemented into the fermentation medium under both aerobic and anaerobic conditions. This confirmed that CO₂ had a key role for PEP carboxylation to generate

OAA in the reductive branch of TCA cycle. McClosky et al. (2018) also indicated that the production of succinate was relatively high in *E. coli* C wild type compared to other *E. coli* wild type strains regardless of level of oxygen. This may also support that *E. coli* NSK014 as a *E. coli* C derivative diverted glycerol through the succinate-producing pathway. Based on this study's results in Fig. 3.6C, *E. coli* NSK014 produced up to 4.3 g/L succinate as a major by-product, which accounted for about 20.7% of the carbon recovery during fermentation. It was likely that 1,3-PDO biosynthesis by developed strains was also the CO₂ dependent process that concomitantly produced succinate via the reductive branch of TCA cycle to maintain the overall redox balance. This was reflected by a co-production of reduced compounds including 1,3-PDO and succinate during glycerol fermentation.

To further conserve more carbon flux and NADH through 1,3-PDO route, the *frdABCD* genes were therefore deleted from *E. coli* NSK014. The resulting strain, *E. coli* NSK015, did not exhibit an impaired growth. However, the 1,3-PDO yield of 0.43 mol/mol was improved compared to that of *E. coli* NSK014 (Fig. 3.6B). Additionally, succinate was also dramatically abolished in *E. coli* NSK015 (Fig. 3.6C). The results suggested that *E. coli* NSK015 possessed 1,3-PDO pathway as a major route for NADH or NADPH reoxidation. Even though *E. coli* NSK015 lacking FRD activity, the glycerol utilization by the strain in the medium required the supplementation of bicarbonate (Fig. 3.5). Dharmadi et al. (2006) suggested that bicarbonate or CO₂ was essentially required when glycerol was metabolized during the growth of *E. coli* for the

biosynthesis of macromolecules for anabolism. Lacoursiere et al. (1986) and Repaske and Clayton (1978) also found that *E. coli* grew without a lag period under anaerobic or microaerobic conditions if CO₂ was provided at the suitable level. The metabolic analysis in *E. coli* by Cintolesi et al. (2012) also disclosed that activities of glycerol dehydrogenase and dihydroxyacetone kinase increased under aerobic conditions when using glycerol as substrate with the CO₂ availability resulting in increasing rates of glycolytic flux and glycerol utilization.

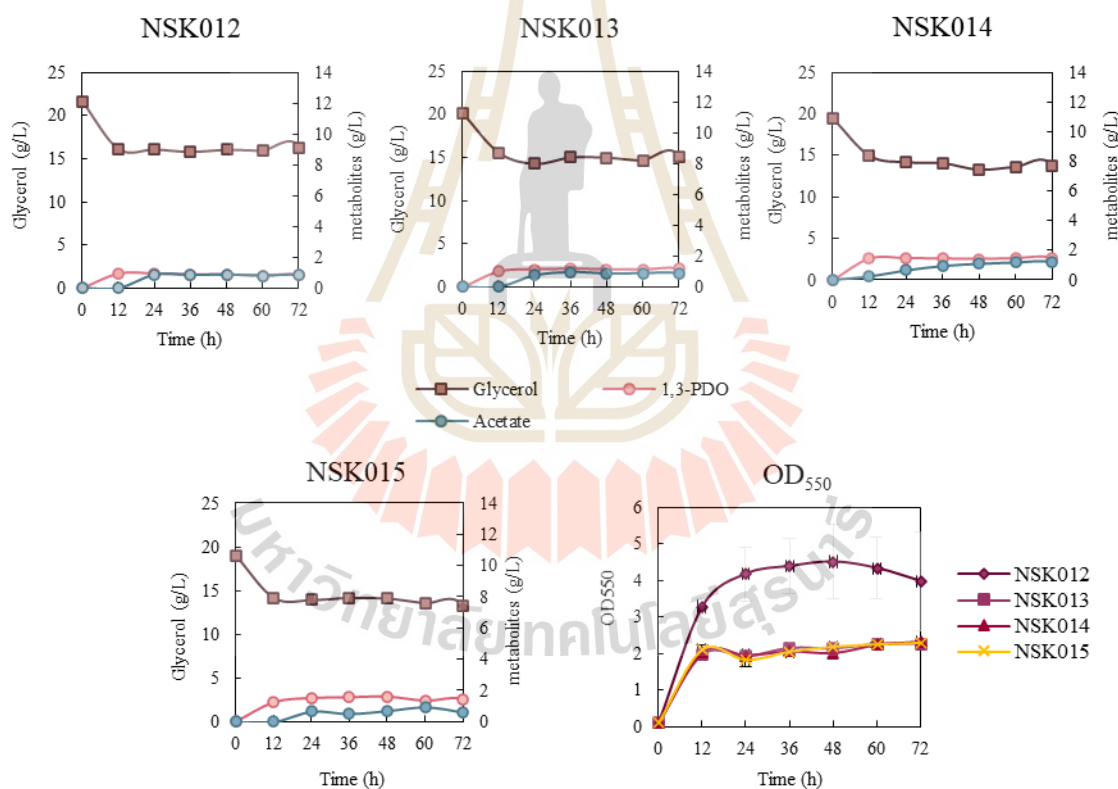


Figure 3.7 Fermentation profiles of 1,3-propanediol production by developed *E. coli* NSK strains from 20 g/L glycerol in AM1 medium without 100 mM KHCO₃ in 500 mL shaking flasks .

3.3.4 Improved 1,3-propanediol yield by the supplementation of glucose but not yeast extract

The yield of 1,3-PDO production reached 0.43 mol/mol by *E. coli* NSK015. However, the yield did not yet approach the theoretical maximum. Tong and Cameron (1992) suggested that the maximum theoretical yield of 1,3-PDO varied in the range of 0.67-1.0 mol/mol depending on the substrate used. This also depended on the availability of external sources of reducing powers (derived from glucose, xylose, or H₂) and nutritional constraints during fermentation (Stephanopoulos et al. 1998; Tong et al, 1991). This study at first hypothesized that yeast extract serving as building blocks and additional reducing equivalents may be required by the developed strains during 1,3-PDO production. An addition of yeast extract (5 g/L) into AM1 medium resulted in a two folds increase of biomass up to 3 g/L (OD₅₅₀ ≈ 9.0) in both *E. coli* NSK014 and NSK015 strains compared to those without yeast extract (Fig. 3.6A). However, the 1,3-PDO yields and concentrations by both strains were not improved (Fig. 3.8A and B) when compared to those without yeast extract (Fig. 3.6B and C). Further investigation was done by the addition of both yeast extract and glucose (20 g/L) into AM1 medium containing glycerol. The 1,3-PDO concentrations and yields (Fig. 4.8C and D) were dramatically improved up to 0.94 mol/mol for both strains, accounting for two folds increases (Fig. 3.6B). This clearly indicated that glucose had much more affected the 1,3-PDO production over yeast extract. Further, yeast extract was removed from the medium to observe the sole effect of glucose on 1,3-PDO biosynthesis. The yields from

both strains (0.90-0.92 mol/mol) in the medium containing both glucose and glycerol as co-substrate were also comparable to those with the supplementation of yeast extract (Fig. 3.6B and Fig. 3.8E and F) while no production of 1,3-PDO was observed in the medium containing only glucose (data not shown). An enhanced 1,3-PDO yield by glucose may be explained by two possibilities. First, glucose may serve as a source of carbon intermediates during glycolysis thus generating ATP and NADH for biosynthesis. This may result in a reduced carbon partitioning from glycerol through the central metabolism for biosynthesis and may elevate the direct conversion of glycerol through 1,3-PDO pathway. Second, glucose may be partially utilized by hexose monophosphate (HMP) shunt to generate NADPH as a preferred reducing equivalent coupled in the reduction of 3-HPA to 1,3-PDO by the activity of YqhD (Fig. 3.1). The additional reducing equivalents derived from glucose in both glycolysis and HMP pathways contributed to the high yield of 1,3-PDO closed to the theoretical maximum, 1.0 mol/mol glycerol used. Lee et al. (2010) discovered that YqhD had an alternative activity of an NADPH-dependent aldehyde reductase that involves in glyoxal and aldehyde detoxification and was a part of a glutathione-independent response to a lipid peroxidation. Additionally, Alkim et al. (2015) suggested that YqhD appeared to be the major glycolaldehyde reductase in *E. coli* that is required NADPH for an optimal activity. Both activities may also attribute to the reduction reaction of 3-HPA to 1,3-PDO.

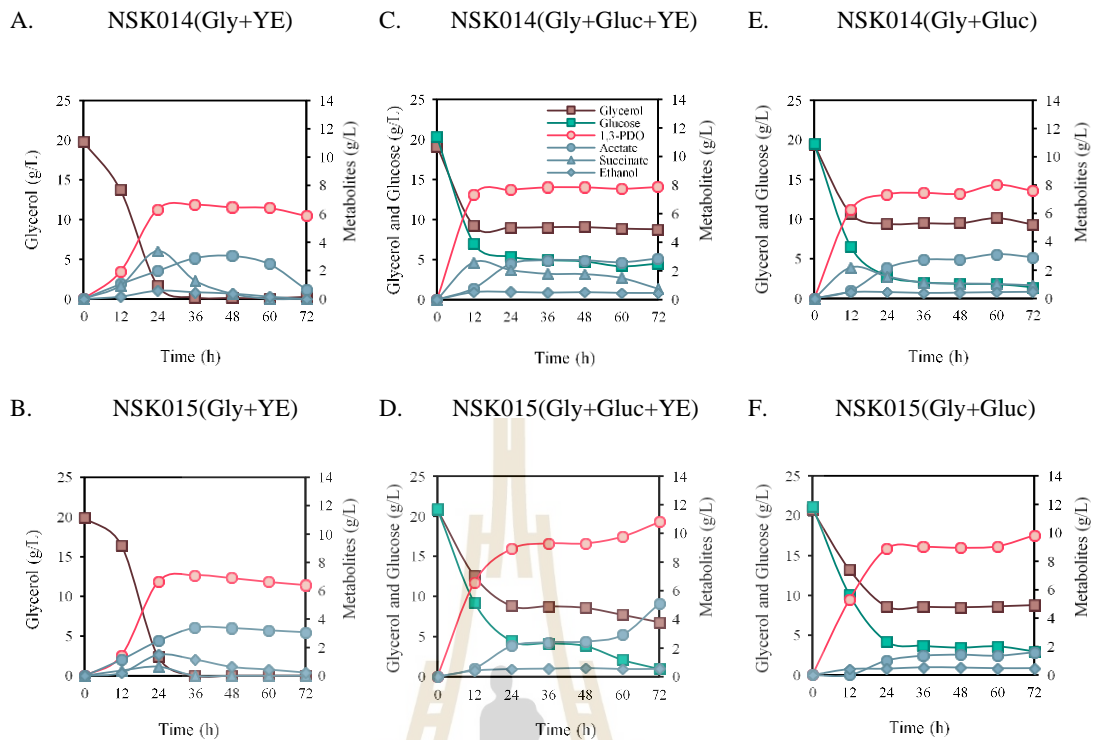


Figure 3.8 Fermentation profiles of developed *E. coli* NSK strains in AM1 medium containing only 20 g/L glycerol and 100 mM KHCO_3 in 500 mL shaking flasks)A-F (and in AM1 containing 50 g/L co-substrate of glycerol and glucose)G (or cassava starch)H (in 2 L fermenter .Gly; glycerol, Gluc; glucose and YE; yeast extract.

G. NSK015 (Gly+Gluc) in 2L scale

H. NSK015 (Gly+Cassava starch) in 2L scale

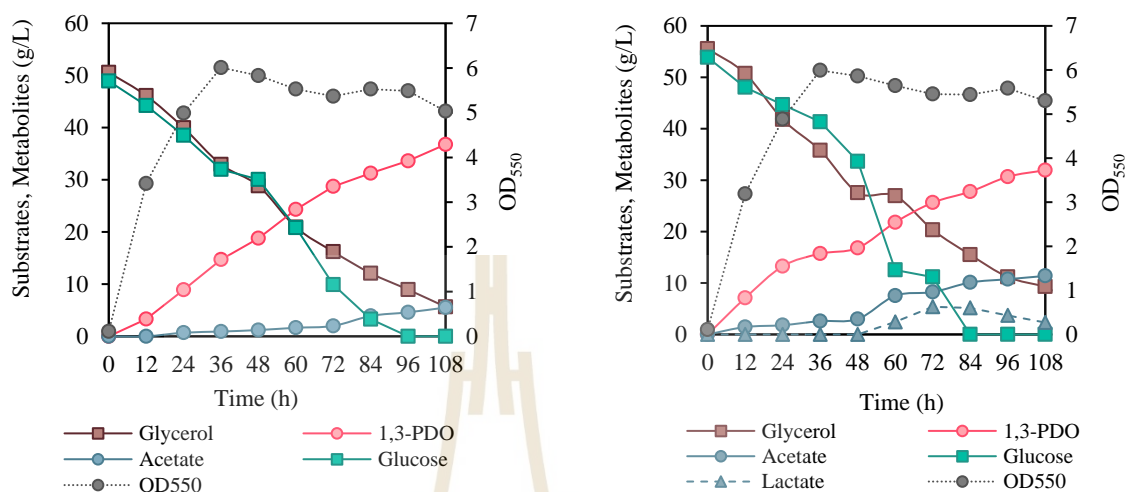


Figure 3.8 (Continued).

3.3.5 1,3-propanediol production from co-substrate of glycerol and glucose or cassava starch in a 2 L fermenter by *E. coli* NSK015

The production of 1,3-PDO was evaluated in AM1 medium containing 5% (w/v) co-substrate of pure glucose and glycerol at the equimolar ratio by *E. coli* NSK015 in a 2L scale. Glucose was exhausted after 96 h incubation while glycerol remained (Fig. 3.8G). The level and yield of 1,3-PDO at 36.8 g/L and 0.99 mol/mol glycerol utilized respectively, were produced with acetate as a sole by-product of 5.0 g/L. This 1,3-PDO yield was reached the theoretical maximum (1.0 mol/mol) defined by the proposed equation of $2\text{Glycerol} + \text{glucose} \rightarrow 2(1,3\text{-PDO}) + 2 \text{acetate} + \text{formate}$ by Tong and Cameron (1992). Comparison to previous works that utilized the mixture of

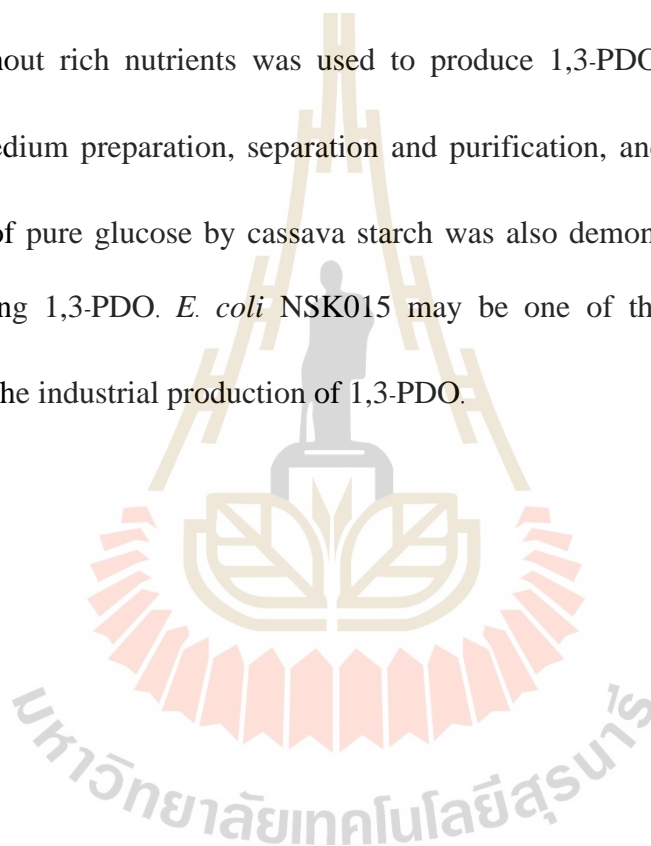
glycerol and glucose for 1,3-PDO, Skraly et al. (1998) reported that 1,3-PDO was produced at 6.3 g/L with the yield of 0.82 mol/mol by *E. coli* over-expressing *K. pneumoniae dha* operon harbouring on pTC53 plasmid. Yang et al. (2018) produced 1,3-PDO at the level of 13.5 g/L with the yield of 0.64 mol/mol by *E. coli* carrying two inducible plasmids harbouring *dhaB-gdrAB-yqhD* and *gapN-galP-glk* operons. Yun et al. (2021) demonstrated the co-culture of *E. coli* Rosetta-*dhaB12* and *E. coli* BL21 overexpressing *dhaT* in the medium containing glucose/glycerol mixture. The yield of 1,3-PDO at 0.67 mol/mol was only achieved. Tang et al. (2009) reported the yield of 1,3-PDO yield at 1.09 mol/mol when overexpressing *C. butyricum dhaB12* operon and *E. coli yqhD* harbouring on an inducible plasmid. However, they reported the yield was over the theoretical maximum due to the use of yeast extract that may provide an additional source of reducing powers during fermentation. Additionally, on the contrary to our work in this study, all previously developed strains required plasmid-dependent systems to overexpress heterologous genes required for 1,3-PDO production pathway. Antibiotics and IPTG, and even yeast extract were mandatory for enhancing growth, preventing the plasmid instability, and maintaining enzymatic activities essentially for 1,3-PDO production. To this end, the production cost may be increased.

Cassava starch is a cheap agricultural product containing glucose sub-units. It has been used as a carbon substrate for sustainable productions of biochemicals including succinate, lactate and 2,3-butanediol (Khor et al., 2016; In et al., 2020; Khunnonkwao et al., 2020). Therefore, *E. coli* NSK015 was elucidated an ability to co-

metabolize glycerol and cassava starch as a source of glucose for the of biosynthesis 1,3-PDO to reduce production cost related to the use of a pure glucose. The result revealed that the use of hydrolysed cassava starch with glycerol did not affect the microbial growth. The cell growth was similar to that observed when a pure glucose was used in which the maximum biomass was reached 2 g/L after 36 h. Glucose was exhausted within 84 h while about 10 g/L of glycerol remained. However, 1,3-PDO concentration was reduced to 31.9 g/L with the yield of 0.84 mol/mol. Acetate was produced with a two-fold increase as a main by-product (11.4 g/L) compared to that of a pure glucose (5.5 g/L) (Fig. 3.8G and H). The glucose consumption rate by the strain in the condition of cassava starch was significantly higher than that of glycerol. This may be the effect of nitrogen sources in the cassava starch thus accelerating glucose consumption. The rapid consumption of glucose derived from cassava starch caused a high glycolytic flux from glycolysis through the acetate-producing pathway to prevent the redox imbalance (high NADH/NAD ratio) and resulted in the carbon wasting to an acetate excretion rather than the biosynthesis of 1,3-PDO. It also affected the generation of NAD(P)H via HMP pathway thus depleting 1,3-PDO production. With our results, *E. coli* NSK015 possessed heterologous enzymes over-expressed on its genome essentially for the biosynthesis of 1,3-PDO and offered the highest yield and concentration in the mineral salts medium containing glucose or cassava starch and glycerol without rich nutrients (yeast extract and peptone) compared to those of strains published in previous literature (Table 2.1).

3.4. Conclusions

This is a pioneer work reported the 1,3-PDO yield at 99% of the theoretical maximum by a metabolically *E. coli* NSK015 over-expressing heterologous genes devoid of strong and inducible plasmids-expression systems. Antibiotics and IPTG were not required for plasmid maintenance and gene induction. A mineral salts AM1 medium without rich nutrients was used to produce 1,3-PDO thus reducing costs related to medium preparation, separation and purification, and waste disposal. The substitution of pure glucose by cassava starch was also demonstrated for efficiently biosynthesizing 1,3-PDO. *E. coli* NSK015 may be one of the potential microbial factories for the industrial production of 1,3-PDO.



CHAPTER IV

OPTIMIZATION OF METABOLICALLY ENGINEERED *Escherichia coli* NSK015 FOR PROGRESSIVE IMPROVEMENT OF 1,3-PROPANEDIOL PRODUCTION

4.1 Introduction

The productivity of 1,3-Propanediol or 1,3-PDO from previous study was still not impressive (0.34 g/L/h). To improve 1,3-PDO productivity and concentration, optimization process was then applied in this study. Various parameters including co-substrate utilization, yeast extract, aerations, inoculum size, pH and fed-batch mode were adjusted for improving 1,3-PDO production by *E. coli* NK015 strain. Different forms of the cofactor, including vitaminB12 and coenzymB12 were also evaluated thus affecting 1,3-PDO production. The difference of space between two Rushton impellers was observed upon the effect of productivity. Additionally, different agitation speeds with increasing k_La values were employed to find the best conditions. Mode of fed-batch fermentation was finally designed to avoid the substrate inhibition and achieved the high 1,3-PDO production. These optimized conditions would be further applied and being the start point in the production of 1,3-PDO by metabolically engineering *E. coli* in larger scale.

4.2 Methods and materials

4.2.1 Microorganism

E. coli NSK015 was mainly used for 1,3-PDO production in this study. Briefly, *E. coli* C was metabolically engineered by replacing *gdrAB-dhaB123* operon in the region of *ldhA*. The major by-product genes, including *ackA* (acetate kinase), *frdABCD* (fumarate reductase), *pflB* (pyruvate-formate lyase) were removed for eliminating by-products formation.

4.2.2 Medium and culture conditions

A few colonies of *E. coli* NSK015 was re-streaked on LB agar containing 20 µg/mL chloramphenicol and incubated at 37°C for 16 h. To prepare inoculum for fermentation in the fermenter, one full loop of *E. coli* NSK015 was then cultured in 250 mL Erlenmeyer flask containing 100 mL LB broth and 20 µg/mL chloramphenicol. The inoculum was agitated at 200 rpm, 37°C. After 16 h, the inoculum was following provided in the fermenter with total final working volume 1100 mL of AM1 medium by setting the initial OD₅₅₀ of 0.1 in fermenter. Aeration was provided by air flowing through sterilized filters and constantly provided at 1.0 vvm. pH was monitored at 7.0 by adjusting with 3M KOH automatically. The percentage of dissolved oxygen (DO) was determined by DO probe detector connecting to monitor of fermenter and must be calibrated before performing fermentation. The initial DO before adding microorganism was therefore 100%.

Luria-Bertani (LB) agar and broth containing 5 g/L yeast extract, 5 g/L NaCl, and 10 g/L tryptone was routinely used for culturing *E. coli* NSK015. AM1 medium containing 19.92 mM $(\text{NH}_4)_2\text{HPO}_4$, 7.56 mM $\text{NH}_4\text{H}_2\text{PO}_4$, 2.0 mM KCl, 1.50 mM $\text{MgSO}_4 \cdot 7\text{H}_2\text{O}$, 1.0 mM Betaine-KCl, 1X Trace metal (Martinez et al., 2007), and CoenzymeB12 (7.5-30 μM depending on experiment) was routinely used as a medium for fermentation and optimization. To reduce foam forming in the fermentation, 10%(v/v) antifoam (Antifoam Y-30 Emulsion, A5758, Sigma) was prepared. The 1-2 mL of the diluted antifoam was added directly to the fermenter when the presence of foam.

4.2.3 Batch fermentation

To find the suitable conditions for enhancement of 1,3-PDO concentration and productivity, different parameters were verified by performing batch fermentation. The optimization was divided into 2 phases according to the number of Rushton turbine used for agitation. The first phase depended on using only one Rushton turbine for agitation (Fig. 4.1A). Vitamin B12 was initially replaced to coenzyme B12 for reducing the cost and examining the possibility to use vitamin B12 instead of coenzyme B12. In the second phase of optimization, two Rushton turbines were adjusted and used for agitation. The effect of speed levels and k_{LA} were varied at 200, 300, and 400 rpm. To further reduce the cost of coenzyme B12, the varied amounts of coenzyme B12 at 7.5 and 15 μM were then observed the effect upon 1,3-PDO production at the optimized speed. All batch fermentations were performed in duplicate. Fermentation was carried out in 2 L fermenter (BIOFLO 110, New Brunswick Scientific, USA)

containing 1100 mL of working volume. In optimization step, pH, temperature, and aeration were constantly set at 7.0, 37°C, and 1.0 vvm, respectively, throughout experiments.

4.2.4 Fed-batch fermentation

Fed-batch fermentation was performed in 2 L fermenter (BIOFLO 110, New Brunswick Scientific, USA) with 1 L of working volume. The inoculum was fed into the fermenter with the final OD₅₅₀ of 0.1. The agitation speed of 300 rpm and the use of 2 impellers for agitation (Fig. 4.1B) were used as the controlled parameters in the fed-batch fermentation. Different modes of co-substrate feeding were designed as shown in Table 4.3 and investigated the suitable condition. Substrate stock was prepared with two different ratios. The first substrate stock was prepared by using the same ratio of glycerol and glucose at 50 g: 50 g in a total volume of 180 mL (mild continuous mode). The second substrate stock used for mode 2 to mode 4 (low continuous, high continuous, and 2 continuous-pulsed modes) was prepared by using the ratio of glycerol/glucose at 1.2:1.5 according to the substrate uptake rates in the optimized batch fermentation. All component of AM1 were also combined in the substrate stock with a half of concentrations that was usually used in the batch fermentation. Coenzyme B12 was provided additionally in the substrate stock by the ratio of 50 g/L glycerol:7.5 µM coenzyme B12. To provide substrates during fermentation, time at 24 h was selected as the initial feeding.

4.2.5 Determination of k_{La}

In order to optimize the production of 1,3-PDO, k_{La} or volumetric mass transfer coefficient was evaluated as an important parameter to improve concentration and productivity of 1,3-PDO by using the equation expression as following;

$$k_{La} = \text{ABS}(\ln(1-(C/C^*)))$$

where C^* is the saturation concentration of the oxygen and C is the actual concentration of the oxygen. The k_{La} at 1.0 L working volume of AM1 medium with 50% (w/v) glycerol and glucose was determined under different agitation speed of 200, 300 and 400 rpm.

4.2.6 Analytical method

Sample was taken twice per day to determine metabolites and cell growth. One mL of sample was divided and centrifuged at 12,500 rpm for 4 min. Cell pellet was then resuspended with 1 mL of DI water and measured OD_{550} by spectrophotometer (Spekol@1500). Whereas, the supernatant used for further analysis of metabolites by HPLC. Biomass was finally estimated from an equation derived from the graph of OD_{550} plotting against dry mass. Approximately, 2.68 OD_{550} equals to one gram of biomass.

To measure the metabolites, 200 microliters of sample supernatant derived from centrifugation were diluted with 800 μL of 20 mM H_2SO_4 and passed through the 0.2 μm filter membrane before analysis. The Rezex ROA organic acid H^+ (8%), 250 \times 4.6 mm phase-reverse column (Phenomenex, France), connecting to a

Refractive Index detector was used with HPLC for separation of metabolites. The temperature of column was kept constantly at 30°C and used with 10 mM H₂SO₄ as a mobile phase at a flow rate of 170 µL per min.

4.2.7 Statistic analysis

The batch fermentations were carried out in duplicate. The data values were reported with standard deviations and their significant differences were determined by SPSS. Duncan's algorithm was selected to compare the significant differences between mean values of individual groups under different conditions.

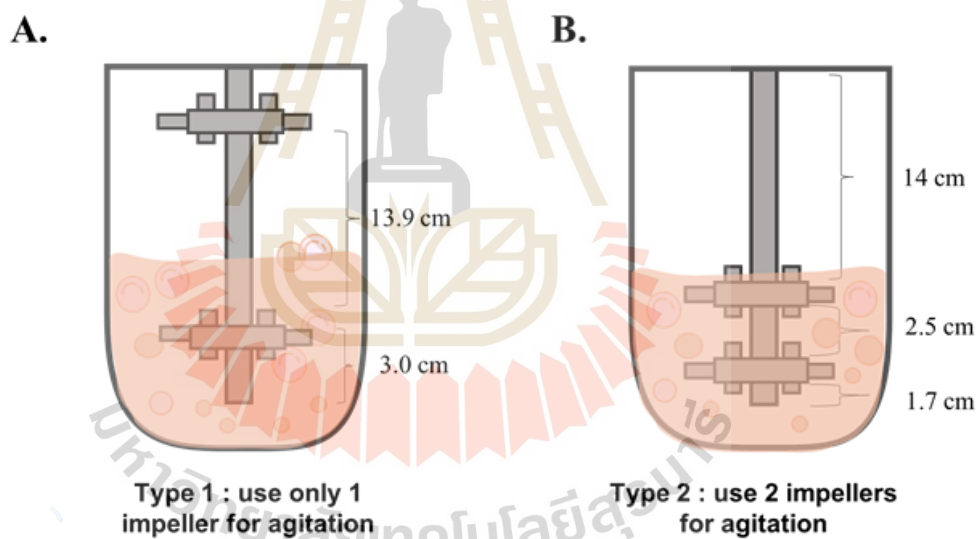


Figure 4.1 Schematics of different impeller localizations in 2 L fermenters. A: Type 1 model using one impeller for agitation and B: Type 2 model using two impellers for agitation (performed at INP, France).

4.3 Results and discussion

4.3.1 Effect of vitamin B12 and coenzymeB12 on 1,3-propanediol production

In our previous study, coenzyme B12-dependent glycerol dehydratase genes were overexpressed under *ldhA* promoter to produce 1,3-PDO in the recombinant *E. coli* NSK015. This strain requires coenzyme B12 serving as a cofactor of the enzyme for converting glycerol to 3-HPA. However, *E. coli* cannot synthesize vitamin B12 or coenzyme B12 by itself. Out of around 30 genes in native coenzyme B12 producers like *Samonella typhimurium*, only two-third of certain genes involving in the cobalamin synthesis are found in *E. coli* (Roth et al., 1993). As a result, cobalamin or coenzymeB12 is generated only the presence of the complex intermediate, cobinamide (Lawrence and Roth, 1995). Both vitamin B12 and coenzyme B12 have the same core structure with corrin ring. Only the upper part of the structure, especially, adenosyl group, is different and plays a key role for catalysis of glycerol to 3-HPA. Though, the use of coenzyme B12 may thus not be worthy to an economical production of 1,3-PDO as the price for coenzyme B12 was more expensive than vitamin B12 about 3 folds. DuPont used vitamin B12 for supplementing the medium for 1,3-PDO production instead.

To observe the possibility to use vitamin B12 as a cofactor, this study was conducted to prove whether *btuR* (adenosyltransferase gene), one of cobalamin-utilizing genes in *E. coli* functions in converting vitamin B12 to be an active

adenosylated form of vitamin B12 (Rosnow et al., 2018). It thus could further activate the glycerol dehydratase activity. The same fermentative condition of 200 rpm agitation, 1 vvm aeration with 15 μ M vitamin B12 was carried out to evaluate the efficiency of vitamin B12 as a cofactor for coenzyme B12-dependent glycerol dehydratase genes (Fig. 4.2A). The result showed that 1,3-PDO was produced up to 19.3 g/L (yield=0.85 mol/mol, Table 4.1). At the end of fermentation (168 h), 1,3-PDO concentration was not increased and lower than that of the coenzyme B12 (around 30 g/L) (Fig.4.2B). This implied that *btuR* was capable of catalyzing the adenylation of vitamin B12. However, its activity may still not strongly enough to efficiently generate the adenylation of vitamin B12 reaching the suitable level for supporting the full activity of glycerol dehydratase compared to those of directly utilizing coenzyme B12 thus delaying 1,3-PDO production. To further improve 1,3-PDO production in the future study, *btuR* may be overexpressed to enhance its enzymatic level and activities.

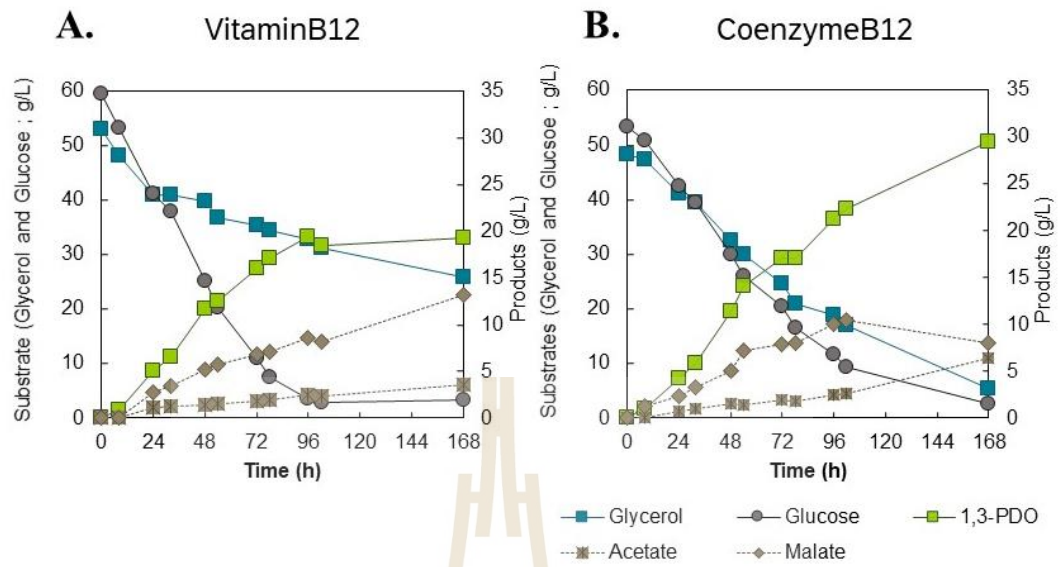


Figure 4.2 Effect of vitamin B12 and coenzyme B12 as a cofactor in the fermenter with type 1 of impeller localization for 1,3-propanediol production with 200 rpm agitation and 1.0 vvm aeration. A. vitamin B12. B. coenzyme B12.

Table 4.1 Comparison of fermentation profile in type 1 of impeller localization with 200 rpm agitation and 1.0 vvm aeration.

Conditions	k_{La} (h^{-1})	Max Biomass (OD_{550})	Time for observation	1,3-PDO (g/L)	Malate (g/L)	Acetate (g/L)	Glycerol residue (g/L)	Glucose residue (g/L)	Yield (mol/mol)	Productivity (g/L/h)
Coenzyme B12 ^a	ND	6.01±0.03	108	36.8±0.8	ND	5.5±0.3	5.7±0.8	-	0.99±0.04	0.34±0.01
Type 1 of impeller, Vitamin B12	19.61±3.17	5.91±0.72	102	19.3±1.3	10.3±3.1	3.0±0.9	23.9±10.4	5.2±3.4	0.85±0.25	0.19±0.01
Type 1 of impeller, Coenzyme B12	22.01±6.61	5.92±2.0	168	29.5±1.3	8.00±1.3	6.4±2.7	5.5±5.3	2.7±1.1	0.84±0.09	0.18±0.01

^a Data obtained in the previous chapter (SUT, Thailand) with different fermenter geometry. ND= Not determined

Table 4.2 Comparison of fermentation profile in type 2 of impeller localization with different coenzyme B12

Condition	k_{La} (h ⁻¹)	Maximum Biomass (OD ₅₅₀)	Time	1,3-PDO (g/L)	Malate (g/L)	Acetate (g/L)	Glycerol residue (g/L)	Glucose residue (g/L)	Yield	Productivity (g/L/h)
200 rpm, 15 μ M	14.48 \pm 1.72	4.20 \pm 0.13 ^a	102	25.8 \pm 3.8 ^a	13.6 \pm 2.7 ^a	2.4 \pm 0.8 ^a	6.9 \pm 7.1 ^a	5.3 \pm 5.5 ^{a,b}	0.70 \pm 0.12 ^a	0.25 \pm 0.04 ^a
300 rpm, 7.5 μ M	33.62 \pm 4.53	11.64 \pm 0.05 ^b	48	38.1 \pm 4.4 ^b	5.2 \pm 3.7 ^b	5.78 \pm 0.1 ^{a,b}	3.1 \pm 1.1 ^a	2.2 \pm 2.0 ^{a,b}	0.93 \pm 0.08 ^a	0.79 \pm 0.09 ^c
300 rpm, 15 μ M	33.62 \pm 4.53	9.65 \pm 0.14 ^b	48	35.9 \pm 0.8 ^b	11.1 \pm 0.8 ^c	4.4 \pm 0.5 ^{a,b}	7.7 \pm 0.1 ^a	1.1 \pm 1.6 ^a	0.88 \pm 0.18 ^a	0.75 \pm 0.02 ^c
400 rpm, 15 μ M	59.33 \pm 3.51	21.65 \pm 3.13 ^c	48	22.7 \pm 0.8 ^a	0.70 \pm 1.0 ^d	8.3 \pm 4.0 ^b	23.0 \pm 0.8 ^b	11.3 \pm 1.1 ^b	0.80 \pm 0.09 ^a	0.47 \pm 0.02 ^b

^(a-c)The superscript represents the significant difference of individual average ($p < 0.05$) in different conditions.



4.3.2 Effect of k_{LA} and localization of impeller

k_{LA} , one of important parameters, was used for an optimization in this study. It represents how much oxygen is being transmitted into the medium and diffusing into the microbial cell in that specific system. The presence of oxygen is known as the importance for cell metabolism and viability (Rao et al., 2009). Based on a previous study, 1,3-PDO concentration of 36.8 g/L was obtained within 108 h with productivity of 0.34 g/L/h and yield of 0.99 mol/mol. To improve productivity and concentration, *E. coli* NSK015 was carried out to observe 1,3-PDO production at the same speed and aeration (200 rpm, 1 vvm, 37°C, k_{LA} of 22.01 h⁻¹) in Type 1 fermenter (INP, France) as previously performed in the previous chapter in the different geometry fermenter performed at SUT, Thailand (unknown k_{LA}). The results confirmed that both concentration and productivity did not seem satisfactory. The 1,3-PDO at the concentration of 29.5 g/L (Fig.4.2B) were lower than that (36.8 g/L) of the previous study (Fig.3.8A). Furthermore, the total fermentation time was longer (168 h), leading the decrease in productivity about 50% (0.18 g/L/h) than that of previous experiments (Chapter 3).

To make the controlled condition similar to the previous study, number of impellers were adjusted in which two impellers of Rushton turbines (Type 1) were used instead of one impeller as a Type 2 fermenter (Fig.4.1). The concentration of 1,3-PDO reached 25.8 g/L within 102 h, (Fig. 4.3). The productivity was improved about 39 % from 0.18 g/L/h to 0.25 g/L/h. (Table 4.1 and 4.2). Though, k_{LA} at 14.48 h⁻¹ in type 2 of

impeller fermenter seemed lower than type 1 fermenter. However, productivity was not the same to previous study at 0.34 g/L/h. The possible reasons may be the geometry of fermenters and baffles were not the same, leading to the difference of vortex flow and influencing 1,3-PDO production (Rao et al., 2009; Echaroj et al., 2020).

Further, k_{LA} optimization by increasing agitation speeds to 300 and 400 rpm, by maintaining aeration of 1 vvm and temperature of 37°C as shown in Fig.4.4 was performed. By increasing speed from 200 to 300 rpm (33.62 h^{-1}), 1,3-PDO concentration (35.9 g/L) was produced within the short time at 48 h, resulting in the improvement of almost 4 folds of productivity (0.75 g/L/h) and a 50% increase of biomass compared to those of 200 rpm (0.25 g/L/h) (Table 4.2). An increasing k_{LA} of 59.33 h^{-1} at 400 rpm was further studied. In contrast, 1,3-PDO concentration (22.7 g/L) and productivity were not high as expected, compared to those of 200 and 300 rpm, respectively. Only cell density was risen dramatically to 21.65 of OD_{550} within 16 h and then dropped to 13.65. Acetate was produced around 10 g/L which was higher than that of 300 rpm. At the same time, the DO value of 400 rpm (Fig.4.5E) was increased up to 100% rapidly from 16 to 86 h. This may reflect that carbon substrates were overflowed to glycolysis with the high metabolic rate and built up only biomass, making the rapid reduction of DO (dissolve oxygen) within 16 h. After that, the metabolic rate was then slow down reflected by the lower requirement of oxygen than that supplemented to the fermenter. As a reduced metabolic rate, the production of 1,3-PDO was low. These results demonstrated that products are not always obtained with high concentration along with the increasing

agitating speed. Either the higher speed or the increasing level of DO may result in the shear force, leading to the degradation of microbial cell and less formation of product thus impacting upon yield and productivity (Audet et al., 1996; Rao et al., 2009)

At 300 rpm, the condition seemed to be suitable. Even this result was different to several previous reports in which they indicated that anaerobic or microaerobic conditions were the most suitable conditions for 1,3-PDO in either *K. pneumoniae* or *L. reuteri* (Chen et al., 2003; Huang et al., 2002; Ju et al., 2020). This was likely due to that glycerol dehydratase has ever understood that it functions effectively under anaerobic conditions (Forage and Foster, 1982). In contrast, Lama et al. (2020) recently reported that *K. pneumoniae* could efficiently produce 1,3-PDO under aerobic conditions from glucose. This study also used a similar condition at 300 rpm and confirmed that 1,3-PDO can be produced under aerobic conditions. As a result, the condition of 300 rpm, was selected and determined the glycerol and glucose uptake rates for further conducting the fed-batch fermentation.

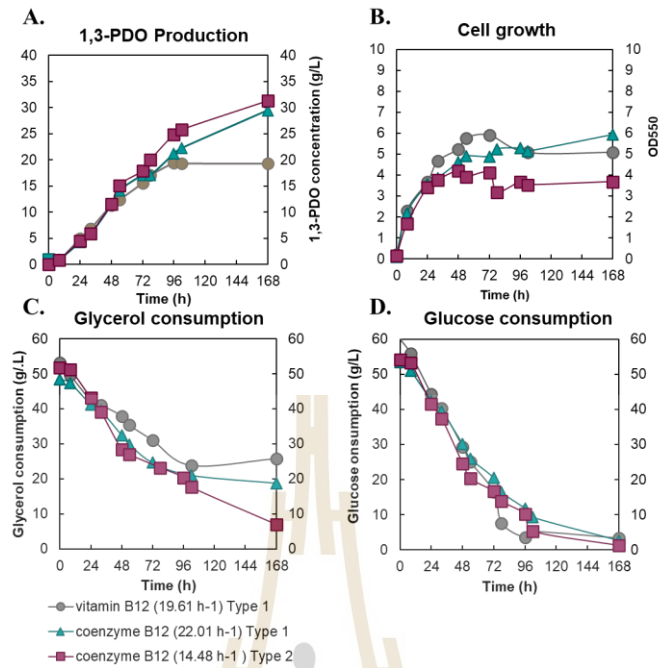


Figure 4.3 Comparison of 1,3-propanediol production at different k_{La} in type 1 and type 2 of impeller localization at 200 rpm, 1 vvm. A: 1,3-propanediol production, B: cell growth, C: glycerol consumption, and D: glucose consumption.

Figure 4.4 1,3-PDO profiles under different k_{La} in type 2 of impeller localization (A-C);

A. 14.48 h^{-1} or 200 rpm, B. 33.62 h^{-1} or 300 rpm, and C. 59.93 h^{-1} or 400 rpm.

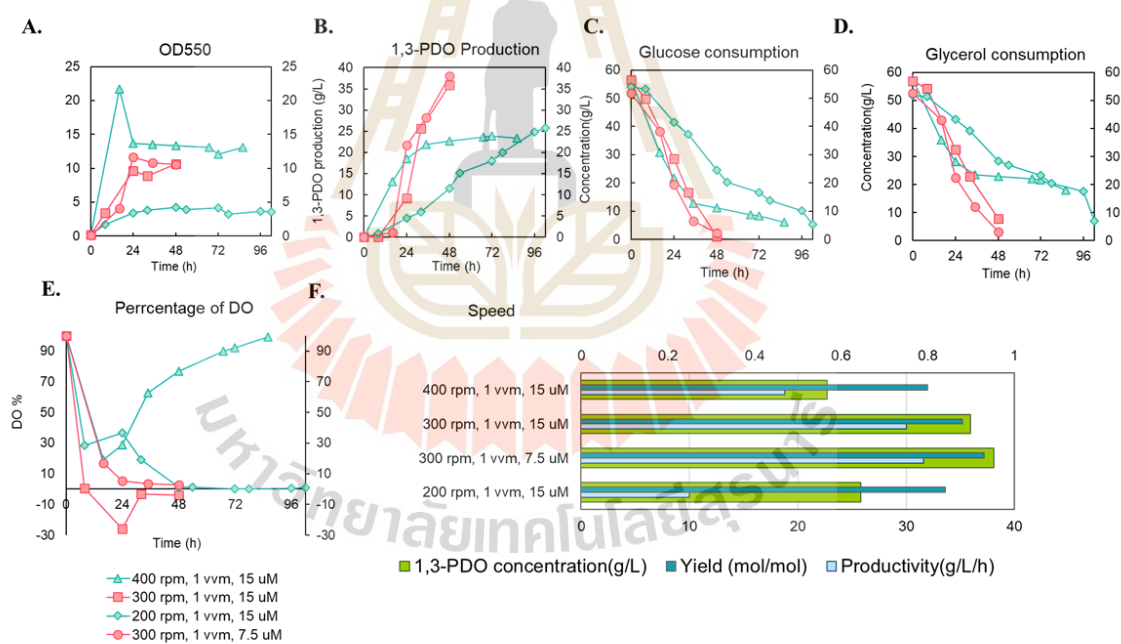


Figure 4.5 Comparison of 1,3-PDO production under different k_{La} . (A) cell growth (B)

1,3-PDO production (C) glucose consumption (D) glycerol consumption (E)

%DO (F) yield, concentration, and productivity.

4.3.3 Effect of concentration of coenzyme B12 with optimal k_{La}

Figure. 4.6 Comparison of different coenzyme B12 concentrations with optimal k_{La} .

A. 15 μM coenzyme B12 in 300 rpm, B. 7.5 μM coenzyme B12 in 300 rpm.

As mentioned, coenzyme B12 is required to produce 1,3-PDO when non-native producer like *E. coli* was used as a host. It is necessarily provided coenzyme B12 into the fermentation broth. This eventually results in the increment of cost in the industry production. Several publications reported about 1,3-PDO or 3-hydroxypropionic acid (3-HP) production using the different coenzyme B12 concentration in range of 1.5-50 μM (Chu et al., 2015; Huang et al., 2017; Kim et al., 2014; Kwak et al., 2013; Wang et al., 2007; Yang et al., 2018). However, these works supplied yeast extract into the medium that may contain vitamin B12 thus partially supporting the function of glycerol dehydratase. Based on the determination of glycerol dehydratase *in situ* studied by Honda et al. (1980), the concentration of 15 μM coenzyme

B12 was brought maximum to verify the activity in this study. To reduce the cost in the industrial scale, concentrations of coenzyme B12 at 7.5 and 15 μM were verified during the production of 1,3-PDO by the strain in the optimized agitating speed of 300 rpm and the aeration of 1.0 vvm. The results showed that the reduction of coenzyme B12 amount from 15 to 7.5 μM did not affect the production of 1,3-PDO, even though yeast extract did not provide in the fermentation. The concentration of 1,3-PDO and productivity derived from 7.5 μM coenzyme B12 (38 g/L) was not different significantly from 15 μM (36 g/L) (Fig. 4.6). This result seemed that coenzyme B12 was used with smaller amount in comparison to the work of Zhang et al. (2006) that 1,3-PDO could be achieved up to 43.9 g/L in the presence of 61.8 mg/L glycerol, 6.2 g/L yeast extract, and 49 mg/L vitamin B12. As a result, our study demonstrated that it can probably reduce the cost of 1,3-PDO production by reducing the concentration of coenzyme B12 in addition the absence of yeast extract.

Table 4.3 Detail of different modes of co-substrate feeding.

Mode	Feeding time)	Feeding type	Stock of glycerol (g)/glucose(g)	Fed volume (mL)	Glycerol feeding rate (g/h)	Glucose feeding rate (g/h)
1	24-88 = 64 h	Mild continuous (MC)	50/50	180	0.78	0.78
2	24-144 = 120 h	Low continuous (LC)	60/70	150	0.5	0.58
3	24-144 = 120 h	High continuous (HC)	130/160	315	1.08	1.33
4	24-56 = 32 h/ 80-112 = 32 h	2 continuous - pulsed (2CF)	70/96	190	1.10	1.50

4.3.4 Improvement of 1,3-PDO concentration by fed-batch fermentation

To improve the concentration of 1,3-PDO, a high concentration of substrate should be provided into the fermentation. However, *E. coli* cannot typically tolerate the high concentrations of substrates. Fed-batch fermentation, one of effective approach to reduce the osmotic pressure from high concentrations of substrates was then adopted by gradually feeding substrates. Different modes of co-substrate feeding as shown in Table 4.3 were designed to observe the effect upon the productivity, the concentration of 1,3-PDO, and the remained glycerol in the fermenter.

At the time of 24 h, the beginning time point of stationary phase in the optimized batch fermentation (Fig. 4.7) was used as the initial time for feeding. Glycerol and glucose feeding rates were determined based on glycerol and glucose uptake rates in batch fermentation between 1.2 g/h and 1.5 g/h, respectively. Co-substrate feeding was then divided into two main modes including a constantly continuous feeding and the two continuously pulsed feeding (Fig. 4.7). The mode of constantly continuous feeding was further divided into 3 different modes including mild, low, and high feeding rates. For the pulsed feeding, substrates were fed at a continuously high rate but paused in the certain periods.

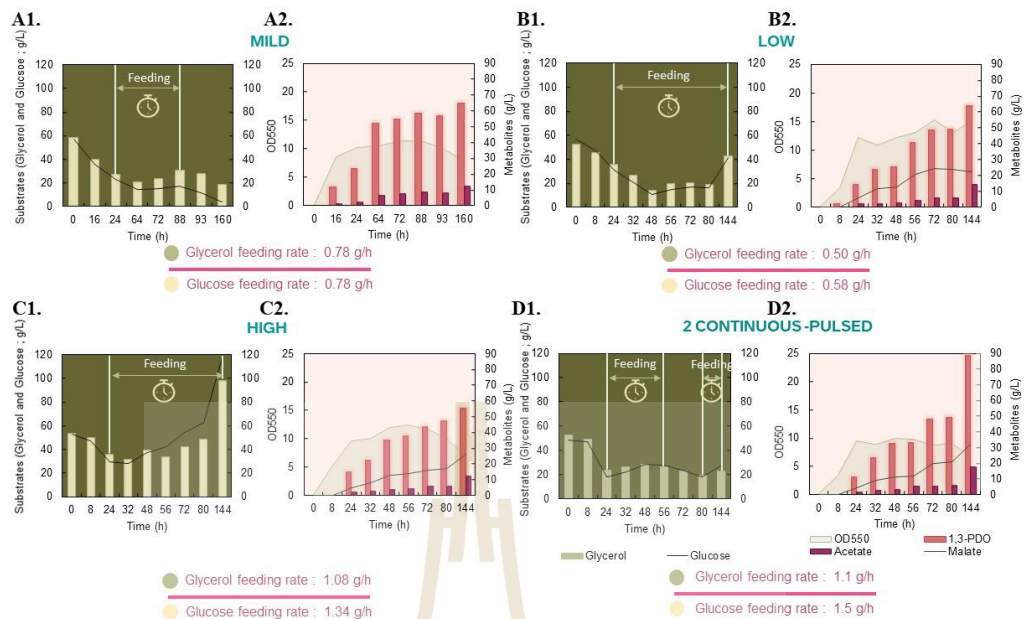


Figure 4.7 Fed-batch fermentation with the different co-substrate feedings. (A) mild (B) low and (C) high rates of co-substrate feedings. (D) 2 continuous-pulsed feeding (1) glycerol and glucose concentrations during cultivation. (2) metabolites and cell growth.

In the mild feeding as shown in Fig.4.7A., glycerol and glucose were designed and limited to the same ratio of 50 g and 50 g in 180 mL of stock solution, identical to the initial concentration of co-substrates in the fermenter. Then, the stock solution of glycerol and glucose was fed at the rate of 0.78 g/h, respectively from 24 h till to 88 h. At the end of fermentation of 160 h, 1,3-PDO concentration was reached to 64.8 g/L (Fig.4.7A), accounting for about 70% increment, while the productivity (0.41 g/L/h) was not improved but was lower than that of the batch conditions at 0.75 g/L/h.

Glycerol had remained at 18.6 g/L that was higher than the glucose concentration (Table 4.4). The possible reason may be explained that the glucose consumption rate in aerobic conditions was slightly higher than glycerol. This led the reducing power not sufficient and not efficiently re-oxidized, causing no further glycerol consumption.

Feeding rates were re-assessed by increasing the glucose concentration higher than the glycerol concentration and dividing it into different modes (LC, HC, and 2CF). The low feeding mode (LC) was tested with the feeding rate at an approximate half of co-substrate uptake rate in batch fermentation (Fig.4.7B). Not as expected, 1,3-PDO was obtained at 64.2 g/L within 144 h and not significantly different in comparison to the mild feeding mode (Table 4.4). Whereas glycerol (42.8 g/L) and glucose (41.4 g/L) were still presented at very high concentrations at 144 h (Table 4.4). Further, the high feeding mode (HC) was investigated at the same rate of co-substrate uptake rates (Fig. 4.7C) by feeding from 24 h to 144 h. Certainly, glycerol and glucose were accumulated at the rate of 0.53 and 0.73 g/h, respectively. This indicated that substrates were excessively supplied than those of the consumption rates. However, these results implied that continuous feeding throughout the process may not be appropriated to apply in the fed-batch fermentation.

Additionally, the substrate feeding was divided into 2 periods (2CF); the first period was started from 24 to 56 h and the second period was started from 80 to 112 h with the high continuous feeding rate closed to the glycerol and glucose uptake rates in the optimized batch mode. By using the alternate continuous feeding, the

maximum biomass was obtained at the lowest cell dry weight (3.7 g/L) compared to all other modes. But 1,3-PDO was increased with the impressive concentration of 88.6 g/L with productivity of 0.62 g/L/h (Fig.4.7D, Table 4.4).

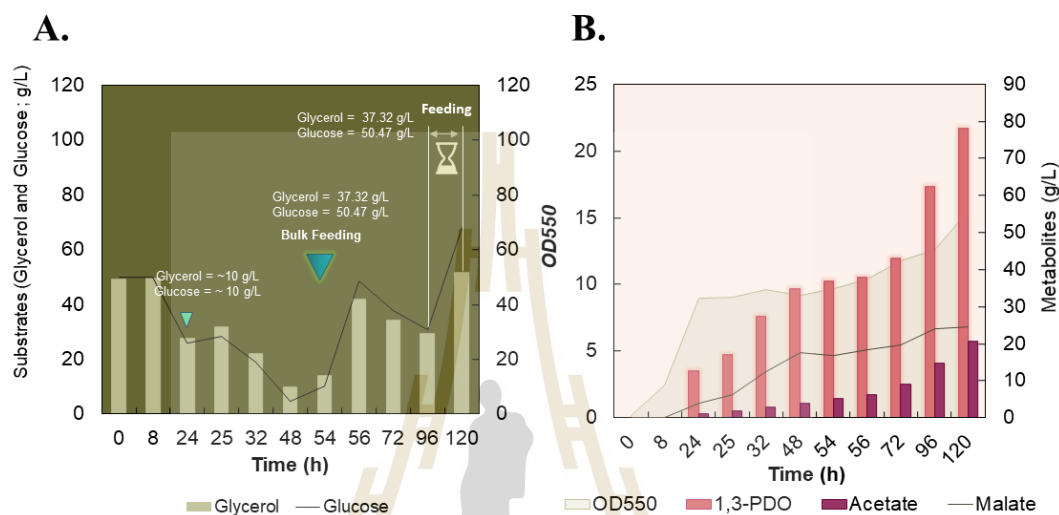


Figure. 4.8 Fermentation profiles in the informal condition. A. represents substrates profile and feeding approach. B. represent the metabolites profile and cell growth.

With another attempt, glycerol and glucose were allowed to almost exhausting and then the co-substrate was fed at a single time (Fig.4.8). This may eliminate the problem of the insufficient essential mineral, nitrogen source and glycerol accumulation during fermentation. By feeding with a single time, the microbial cell might utilize substrates and nutrition sufficiently. 1,3-PDO was obtained in the relatively short time with the concentration of 77.6 g/L within 120 h (0.65 g/L/h).

However, this mode should be further investigated in depth since compositions of the nutrients and substrates could not be easily determined.

4.4 Conclusions

This study demonstrated the optimization process for the metabolically engineered *E. coli* NSK015 to improve 1,3-PDO production. The aerobic conditions at 300 rpm, 1 vvm with the reduced coenzymeB12 of 7.5 μM were identified as the best condition and applied in fed-batch fermentation. Under the fed-batch fermentation, *E. coli* NSK015 could produce 1,3-PDO up to 88.6 g/L with the productivity of 0.62 g/L/h.

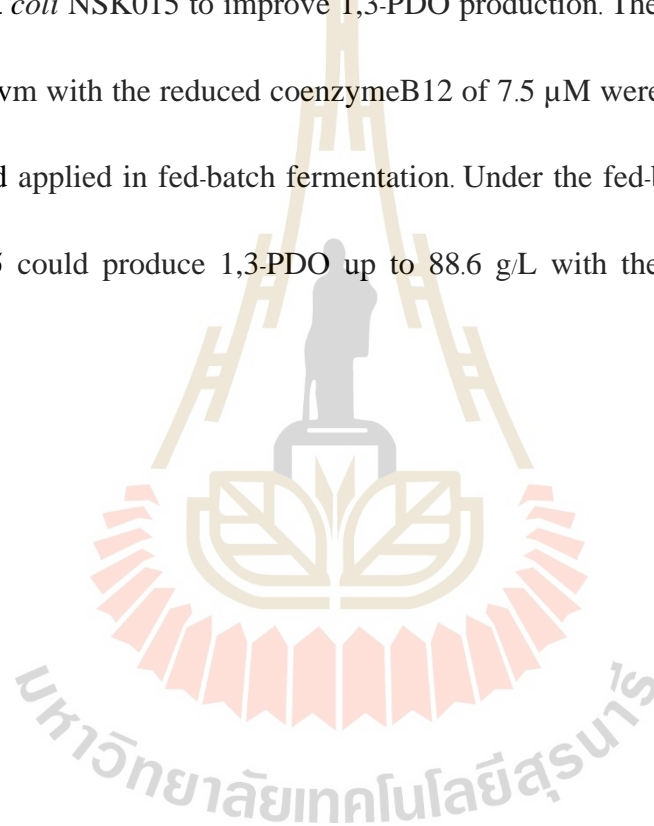


Table 4.4 Comparison of fermentation profiles at different feeding modes in type 2 fermenter.

Conditions	Feeding type	Maximum CDW	1,3-PDO (g/L)	Total added glycerol/glucose (g)	Residual glycerol (g/L)	Residual glucose (g/L)	Consumed glycerol and glucose (g/L)	Yield	Productivity (g/L/h)
1	MC	4.35	64.8	107.9/104.7	18.6	3.8	89.3/102.3	0.88	0.41
2	LC	5.72	64.2	108.3/127.9	42.8	41.4	65.4/86.5	1.19	0.45
3	HC	4.62	55.0	180.3/214.4	98.3	117.3	82.0/97.7	0.82	0.39
4	2CF	3.66	88.6	123.9/144.3	22.7	27.6	101.2/116.8	1.0	0.62

CHAPTER V

GENERAL CONCLUSION AND RECOMMENDATIONS

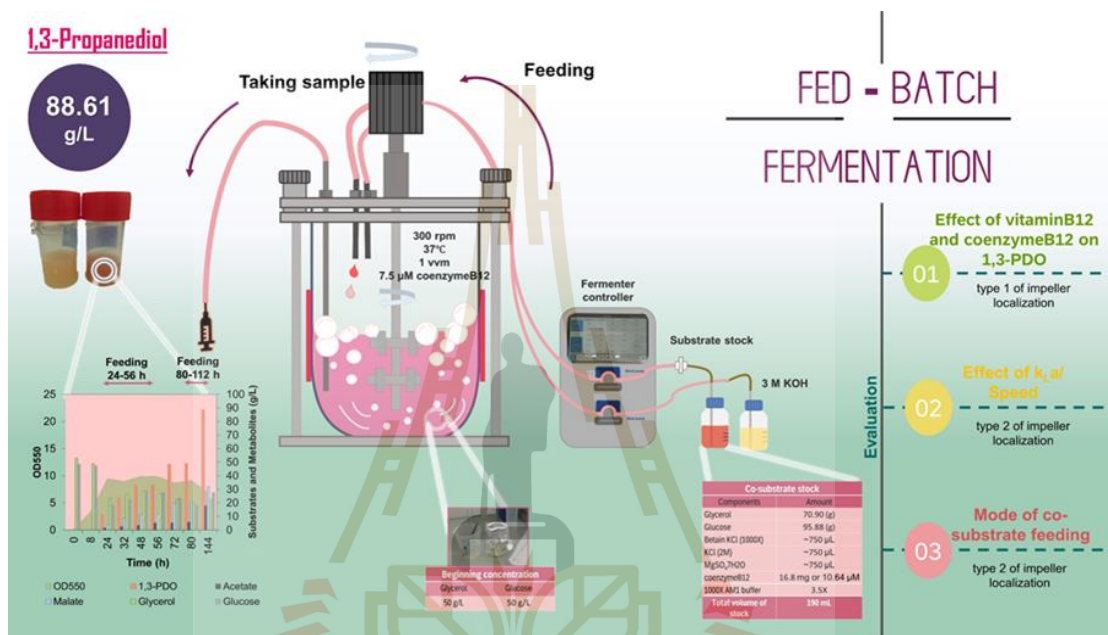


Figure 5.1 Summary of optimized process for 1,3-PDO production by *E. coli* NSK015.

In this dissertation, we reported the production of 1,3-PDO by using the novel metabolically engineered *Escherichia coli* NSK015 in mineral AM1 medium. The efficient production of 1,3-PDO was determined and divided into two main parts including the development of the metabolically engineered *E. coli* NSK015 and the optimization of 1,3-PDO in the fermenter. This study can solve problems on 1,3-PDO production when *E. coli* is employed as a microbial host while overexpression of heterologous genes has been done on genomic DNA using the native host promoter.

In the first part of this study, *E. coli* C was used as parental strain for engineering to efficiently produce 1,3-PDO. 1,3-PDO pathway containing 2 simple reactions by conversion of glycerol to 3-hydroxypropionaldehyde (3-HPA) and further catalyzation of 3-HPA to 1,3-PDO, respectively, were adopted and designed in *E. coli*. Genes involving glycerol dehydratase with reactivating factors derived from *K. pneumoniae* were rearranged to further transcribed in the one direction. The *gdrAB-dhaB123* operon was exchanged with the structural *ldhA* gene for its overexpression under *ldhA* promoter of *E. coli*. By this means, *ldhA* was simultaneously removed and substituted with the new heterologous genes. To evaluate the expression of heterologous gene, the clones capable of producing 1,3-PDO were initially verified on the modified aldehyde indicator plates. The clones could change the pale pink color to the dark red color on the modified aldehyde indicator plate. This ability indicated that the heterologous gene could function and the clones were further selected to evaluate 1,3-PDO production in the shaking flask. In addition, the removal of *ackA* and *pflB* genes from the clone were also deleted to minimize acetate and formate formation.

To reduce the possibility of the toxic 3-HPA intermediate accumulation, *yqhD* gene encoding 1,3-PDO oxidoreductase was integrated in frame with the *pflB* promoter in the same way of *ldhA*. The *frdABCD* was finally interrupted for removing succinate production. The final strain, *E. coli* NSK015, was constructed and used as a biocatalyst for 1,3-PDO production throughout this study. The yield of 1,3-PDO was achieved at 0.43 mol/mol glycerol when glycerol was used as a sole substrate. In the presence of

glucose, the yield was improved almost two folds to 0.90 mol/mol in the shaking flask. In 2 L fermenter, the metabolically engineered *E. coli* NSK015 was tested for 1,3-PDO production in AM1 medium without supplementing yeast extract at 200 rpm agitation and 1 vvm aeration using 50 g/L of each substrate of glycerol and glucose. 1,3-PDO concentration was achieved at 36.8 g/L in 108 h with the yield of 99% theoretical yield (0.99 mol/mol). When cassava starch was used instead of glucose, 1,3-PDO concentration was reduced to 31.9 g/L with yield of 0.84 mol/mol. All of results indicated that the heterologous genes were capable of overexpressing under native promoters regardless of the use of IPTG for inducing gene expression in which the plasmid instability was neglectable.

The improvement of 1,3-PDO productivity was further accomplished by the conventional optimization process. Vitamin B12, k_{LA} , impeller positions, coenzyme B12 concentration, and agitation speed were verified in batch fermentation to select the best condition, leading to increase the productivity of 1,3-PDO production. As a result, the most suitable condition for applying the fed-batch fermentation was identified using optimized parameters from batch fermentation in which two impellers for agitation were used for agitation at 300 rpm. The reduced concentration of coenzyme B12 of 7.5 μ M was done without affecting 1,3-PDO production. By discovery of this condition, the productivity was improved from 0.34 to 0.75 g/L/h. The glycerol and glucose uptake rates were taken to calculate the feeding rate to employ in fed-batch fermentation.

To observe the possible maximum concentration of 1,3-PDO from *E. coli* NSK015, the fed-batch fermentation was carried out with the different modes of co-substrate feeding. By using the continuously pulsed feeding mode, glycerol and glucose were prepared in the ratio of 1.2:1.5 with the final concentration in the stock of 370 g/L and 505 g/L. Feeding was implemented intermittently for two periods from 24-56 h and 80-112 h, respectively, with the rate of feeding glycerol and glucose at 1.1 and 1.5 g/h, respectively. Under this condition, *E. coli* NSK015 could produce 1,3-PDO with impressive concentration up to 88.6 g/L within 144 h. The yield of 1 mol/mol was achieved. However, glycerol and glucose at about 22-28 g/L were still accumulated at the end of fermentation (Fig. 5.1).

This work can solve problems and support other works in research field of 1,3-PDO and even 3-hydroxypropionic acid (3-HP) productions. Because both products are linked together with the first same reaction of the pathway. This work demonstrated the overexpression of heterologous genes that efficiently function under native host promoters while some previously published works showed that expression levels of enzymes involving in 1,3-PDO pathway on inducible plasmids did not efficient enough to drive 1,3-PDO production at high concentration. Consequently, our success can reduce the concern of instability of plasmid and reduce the cost of 1,3-PDO production in the industrial scale. For making 1,3-PDO production better and more interested, the future work can be further done as followings.

1. Since aldehyde-dependent pathway is one of the routes to produce both 1,3-PDO and 3-HP. Therefore, 3-HP can be further produced by removing *yqhD* from this strain and other aldehyde dehydrogenases should be introduced and overexpressed. Based on this study, the fermentation conditions could be applied directly to produce 3-HP.

2. Since glycerol dehydratase genes derived from *K. pneumoniae* depend on coenzyme B12, this seemed to kind of expensive and uneconomical for the industry. In contrast, the glycerol dehydratase derived from *Clostridium* is independent on coenzyme B12. Then coenzyme B12 independent-glycerol dehydratase of *Clostridium* *dhaB1* and *dhaB2* genes can be substituted *dhaB123* derived from *K. pneumoniae* to test the possibility to produce 1,3-PDO without coenzymB12.

3. Conversion of glucose to glycerol and then finally to 1,3-PDO might be better alternative choices in *E. coli*. Genes involving in conversion of glucose to glycerol may be further introduced into *E. coli* NSK015 and should be overexpressed under one of some native host promoters.

REFERENCES

- Alkim, C., Cam, Y., Trichez, D., Auriol, C., Spina, L., Vax, A., Bartolo, F., Besse, P., François, J.M., Walther, T., 2015. Optimization of ethylene glycol production from (D)-xylose via a synthetic pathway implemented in *Escherichia coli*. **Microb. Cell Fact.** 14, 1-12. <https://doi.org/10.1186/s12934-015-0312-7>
- Arntz, D., Haas, T., Schäfer-Sindlinger, A., 1994. Process for the Preparation of 1,3-Propanediol by the Hydrogenation of Hydroxypropionaldehyde. 5364984.
- Audet, J., Lounes, M., Thibault, J., 1996. Pullulan fermentation in a reciprocating plate bioreactor. **Bioprocess Eng.** 15, 209-214. <https://doi.org/10.1007/BF00369484>
- Bradford, M.M., 1976. A rapid and sensitive method for the quantitation of microgram quantities of protein utilizing the principle of protein-dye binding. **Anal. Biochem.** 72, 248-254. <https://doi.org/10.1006/abio.1976.9999>
- Braak, H. R. 1928 Onderzoekingen over Vergisting van Glycerine. Thesis, Delft.
- Brown, H.S., Casey, P.K., Donahue, J.M., 2000. Poly(Trimethylene Terephthalate) Polymer for Fibers. **NF New Fibres**. <http://www.technica.net/NF/NF1/eptt.htm>. (accessed 15 December 2020)

- Bunch, P., Mat-jan, F., Lee, N., Clark, D.P., 1997. The *ldhA* gene encoding the fermentative lactate dehydrogenase of *Escherichia coli*. **Microbiology** 147, 2437-46.
- Chen, X., Zhang, D.J., Qi, W.T., Gao, S.J., Xiu, Z.L., Xu, P., 2003. Microbial fed-batch production of 1,3-propanediol by *Klebsiella pneumoniae* under micro-aerobic conditions. **Appl. Microbiol. Biotechnol.** 63, 143-146.
<https://doi.org/10.1007/s00253-003-1369-5>
- Chen, Z., Liu, H., Liu, D., 2011. Metabolic pathway analysis of 1,3-propanediol production with a genetically modified *Klebsiella pneumoniae* by overexpressing an endogenous NADPH-dependent alcohol dehydrogenase. **Biochem. Eng. J.** 54, 151-157.
<https://doi.org/https://doi.org/10.1016/j.bej.2011.02.005>
- Cheng, K.K., Liu, D.H., Sun, Y., Liu, W. Bin, 2004. 1,3-Propanediol production by *Klebsiella pneumoniae* under different aeration strategies. **Biotechnol. Lett.** 26, 911-915. <https://doi.org/10.1023/B:bile.0000025902.44458.f4>
- Chu, H.S., Kim, Y.S., Lee, C.M., Lee, J.H., Jung, W.S., Ahn, J.H., Song, S.H., Choi, I.S., Cho, K.M., 2015. Metabolic engineering of 3-hydroxypropionic acid biosynthesis in *Escherichia coli*. **Biotechnol. Bioeng.** 112, 356-364.
<https://doi.org/10.1002/bit.25444>

Cintolesi, A., Clomburg, J.M., Rigou, V., Zygorakis, K., Gonzalez, R., 2012.

Quantitative analysis of the fermentative metabolism of glycerol in *Escherichia coli*. **Biotechnol. Bioeng.** 109, 187-198.

<https://doi.org/10.1002/bit.23309>

Claisse, O., Lonvaud-Funel, A., 2001. Primers and a specific *dna* probe for detecting

lactic acid bacteria producing 3-hydroxypropionaldehyde from glycerol in

spoiled ciders. **J. Food Prot.** 64, 833-837. [https://doi.org/10.4315/0362-028X-](https://doi.org/10.4315/0362-028X-64.6.833)

[64.6.833](https://doi.org/10.4315/0362-028X-64.6.833)

da Silva, G.P., Mack, M., Contiero, J., 2009. Glycerol: A promising and abundant

carbon source for industrial microbiology. **Biotechnol. Adv.** 27, 30-39.

<https://doi.org/10.1016/j.biotechadv.2008.07.006>

Daniel, R., Bobik, T.A., Gottschalk, G., 1998. Biochemistry of coenzyme B12-

dependent glycerol and diol dehydratases and organization of the encoding

genes. **FEMS Microbiol. Rev.** 22, 553-566. [https://doi.org/10.1016/S0168-](https://doi.org/10.1016/S0168-6445(98)00021-7)

[6445\(98\)00021-7](https://doi.org/10.1016/S0168-6445(98)00021-7)

Datsenko, K.A., Wanner, B.L., 2000. One-step inactivation of chromosomal genes in

Escherichia coli K-12 using PCR products. **Proc. Natl. Acad. Sci. U. S. A.** 97,

6640-6645. <https://doi.org/10.1073/pnas.120163297>

Della Pina, C., Falletta, E., Rossi, M., 2011. A green approach to chemical building

blocks. The case of 3-hydroxypropanoic acid. **Green Chem.** 13, 1624-1632.

<https://doi.org/10.1039/c1gc15052a>

Department of Alternatives Energy Development and Efficiency, M.O.E., 2019.

Thailand Energy Efficiency Situation.

Dharmadi, Y., Murarka, A., Gonzalez, R., 2006. Anaerobic fermentation of glycerol

by *Escherichia coli*: A new platform for metabolic engineering. **Biotechnol.**

Bioeng. 94, 821–829. <https://doi.org/10.1002/bit.21025>

Dolejš, I., Líšková, M., Krasňan, V., Markošová, K., Rosenberg, M., Lorenzini, F.,

Marr, A.C., Rebroš, M., 2019. Production of 1,3-propanediol from pure and

crude glycerol using immobilized *Clostridium butyricum*. **Catalysts.** 9, 1–13.

<https://doi.org/10.3390/catal9040317>

Echaroj, S., Ong, H.C., Chen, X., 2020. Simulation of mixing intensity profile for

bioethanol production via two-step fermentation in an unbaffled agitator

reactor. **Energies.** 13. <https://doi.org/10.3390/en13205457>

Emptage, M., Haynie, S.L., Laffend, L.A., Pucci, J.P., Whited, G., 2003. Process for

the biological production of 1,3-propanediol with high titer. **United States**

Patent. US6514733B1.

Engels, C., Schwab, C., Zhang, J., Stevens, M.J.A., Bieri, C., Ebert, M.O., McNeill,

K., Sturla, S.J., Lacroix, C., 2016. Acrolein contributes strongly to

antimicrobial and heterocyclic amine transformation activities of reuterin. **Sci.**

Rep. 6, 1–13. <https://doi.org/10.1038/srep36246>

Eurostat, 2018. Energy, transport and environment indicators. 2018 edition, **Eurostat –**

Statistica Books.

- Forage, R.G., Foster, M.A., 1982. Glycerol fermentation in *Klebsiella pneumoniae*: Functions of the coenzyme B12-dependent glycerol and diol dehydratases. **J. Bacteriol.** 149, 413-419. <https://doi.org/10.1128/jb.149.2.413-419.1982>
- Forsberg, C.W., 1987. Production of 1,3-propanediol from glycerol by *Clostridium acetobutylicum* and other *Clostridium* species. **Appl. Environ. Microbiol.** 53, 639-643. <https://doi.org/10.1128/aem.53.4.639-643.1987>
- Friebs, K., 2004. Plasmid copy number and plasmid stability. **Adv. Biochem. Eng. Biotechnol.** 86, 47-82. <https://doi.org/10.1007/b12440>
- González-Pajuelo, M., Meynial-Salles, I., Mendes, F., Soucaille, P., Vasconcelos, I., 2006. Microbial conversion of glycerol to 1,3-propanediol: Physiological comparison of a natural producer, *Clostridium butyricum* VPI 3266, and an engineered strain, *Clostridium acetobutylicum* DG1(pSPD5). **Appl. Environ. Microbiol.** 72, 96-101. <https://doi.org/10.1128/AEM.72.1.96-101.2006>
- Gonzalez, Y.D.A.M.R., 2006. Anaerobic fermentation of glycerol by *Escherichia coli*: A new platform for metabolic engineering. **Biotechnol. Bioeng.** 94, 821-829. <https://doi.org/10.1002/bit>
- Hájek, M., Skopal, F., 2010. Treatment of glycerol phase formed by biodiesel production. **Bioresour. Technol.** 101, 3242-3245. <https://doi.org/10.1016/j.biortech.2009.12.094>

- Hasona, A., Kim, Y., Healy, F.G., Ingram, L.O., Shanmugam, K.T., 2004. Pyruvate formate lyase and acetate kinase are essential for anaerobic growth of *Escherichia coli* on xylose. **J. Bacteriol.** 186, 7593-7600.
<https://doi.org/10.1128/JB.186.22.7593-7600.2004>
- Heckman, K.L., Pease, L.R., 2007. Gene splicing and mutagenesis by PCR-driven overlap extension. **Nat. Protoc.** 2, 924-932. <https://doi.org/10.1038/nprot.2007.132>
- Homann, T., Tag, C., Biebl, H., Deckwer, W.D., Schink, B., 1990. Fermentation of glycerol to 1,3-propanediol by *Klebsiella* and *Citrobacter* strains. **Appl. Microbiol. Biotechnol.** 33, 121-126. <https://doi.org/10.1007/BF00176511>
- Honda, Susumu, Toraya, Tetsuo, Fukui, S., 1980. In Situ Reactivation of Glycerol-Inactivated Coenzyme B12-Dependent Enzymes , **Glycerol Dehydratase and Diol Dehydratase** 143, 1458-1465.
- Hong, E., Kim, J., Ha, S. jin, Ryu, Y., 2015. Improved 1,3-propanediol production by *Escherichia coli* from glycerol due to Co-expression of glycerol dehydratase reactivation factors and succinate addition. **Biotechnol. Bioprocess Eng.** 20, 849-855. <https://doi.org/10.1007/s12257-015-0293-8>
- Houck, M.M., Menold, R.E., Huff, R.A., 2001. Poly(trimethylene terephthalate): A “new” type of polyester fibre. **Z Zagadnien Nauk Sadowych.** 46, 217-221.
- Huang, H., Gong, C., Tsao, G.T., 2002. Production of 1,3-Propanediol by *Klebsiella pneumoniae*. **Appl. Biochem. Biotechnol.** 98-100, 687-698.

Huang, J., Wu, Y., Wu, W., Zhang, Y., Liu, D., Chen, Z., 2017. Cofactor recycling for co-production of 1,3-propanediol and glutamate by metabolically engineered *Corynebacterium glutamicum*. **Sci. Rep.** 7, 1–10.

<https://doi.org/10.1038/srep42246>

In, S., Khunnonkwao, P., Wong, N., Phosiran, C., Jantama, S.S., Jantama, K., 2020.

Combining metabolic engineering and evolutionary adaptation in *Klebsiella oxytoca* KMS004 to significantly improve optically pure D-(–)-lactic acid yield and specific productivity in low nutrient medium. **Appl. Microbiol. Biotechnol.** 104, 9565–9579.

<https://doi.org/10.1007/s00253-020-10933-0>

Jantama, K., Polyiam, P., Khunnonkwao, P., Chan, S., Sangproo, M., Khor, K.,

Jantama, S.S., Kanchanatawee, S., 2015. Efficient reduction of the formation of by-products and improvement of production yield of 2,3-butanediol by a combined deletion of alcohol dehydrogenase, acetate kinase-phosphotransacetylase, and lactate dehydrogenase genes in metabolically engineered *Klebsiella oxytoca* in mineral salts medium. **Metab. Eng.** 30, 16–26.

<https://doi.org/10.1016/j.ymben.2015.04.004>

Jantama, K., Zhang, X., Moore, J.C., Shanmugam, K.T., Svoronos, S.A., Ingram,

L.O., 2008. Eliminating side products and increasing succinate yields in engineered strains of *Escherichia coli* C. **Biotechnol. Bioeng.** 101, 881–893.

<https://doi.org/10.1002/bit.22005>

- Ji, X.J., Huang, H., Zhu, J.G., Hu, N., Li, S., 2009. Efficient 1,3-propanediol production by fed-batch culture of *Klebsiella pneumoniae*: The role of pH fluctuation. **Appl. Biochem. Biotechnol.** 159, 605-613.
<https://doi.org/10.1007/s12010-008-8492-9>
- Jiang, W., Zhuang, Y., Wang, S., Fang, B., 2015. Directed evolution and resolution mechanism of 1, 3-propanediol oxidoreductase from *Klebsiella pneumoniae* toward higher activity by error-prone PCR and bioinformatics. **PLoS One.** 10, 1-10. <https://doi.org/10.1371/journal.pone.0141837>
- Ju, J.H., Wang, D., Heo, S.Y., Kim, M.S., Seo, J.W., Kim, Y.M., Kim, D.H., Kang, S.A., Kim, C.H., Oh, B.R., 2020. Enhancement of 1,3-propanediol production from industrial by-product by *Lactobacillus reuteri* CH53. **Microb. Cell Fact.** 19, 1-10. <https://doi.org/10.1186/s12934-019-1275-x>
- Kaur, G., Srivastava, A.K., Chand, S., 2012. Advances in biotechnological production of 1,3-propanediol. **Biochem. Eng. J.** 64, 106-118.
<https://doi.org/10.1016/j.bej.2012.03.002>
- Khor, K., Sawisit, A., Chan, S., Kanchanatawee, S., Jantama, S.S., Jantama, K., 2016. High production yield and specific productivity of succinate from cassava starch by metabolically-engineered *Escherichia coli* KJ122. **J. Chem. Technol. Biotechnol.** 91, 2834-2841. <https://doi.org/10.1002/jctb.4893>

- Khunnonkwao, P., Jantama, S.S., Jantama, K., Joannis-Cassan, C., Taillandier, P., 2020. Sequential coupling of enzymatic hydrolysis and fermentation platform for high yield and economical production of 2,3-butanediol from cassava by metabolically engineered *Klebsiella oxytoca*. **J. Chem. Technol. Biotechnol.** <https://doi.org/10.1002/jctb.6643>
- Khunnonkwao, P., Jantama, S.S., Kanchanatawee, S., Jantama, K., 2018. Re-engineering *Escherichia coli* KJ122 to enhance the utilization of xylose and xylose/glucose mixture for efficient succinate production in mineral salt medium. **Appl. Microbiol. Biotechnol.** 102, 127–141. <https://doi.org/10.1007/s00253-017-8580-2>
- Kim, K., Kim, S.K., Park, Y.C., Seo, J.H., 2014. Enhanced production of 3-hydroxypropionic acid from glycerol by modulation of glycerol metabolism in recombinant *Escherichia coli*. **Bioresour. Technol.** 156, 170–175. <https://doi.org/10.1016/j.biortech.2014.01.009>
- Knietsch, A., Bowien, S., Whited, G., Gottschalk, G., Daniell, R., 2003. Identification and characterization of coenzyme B12-dependent glycerol dehydratase- and diol dehydratase-encoding genes from metagenomic DNA libraries derived from enrichment cultures. **Appl. Environ. Microbiol.** 69, 3048–3060. <https://doi.org/10.1128/AEM.69.6.3048-3060.2003>

- Kwak, S., Park, Y.C., Seo, J.H., 2013. Biosynthesis of 3-hydroxypropionic acid from glycerol in recombinant *Escherichia coli* expressing *Lactobacillus brevis dhaB* and *dhaR* gene clusters and *E. coli* K-12 *aldH*. **Bioresour. Technol.** 135, 432–439. <https://doi.org/10.1016/j.biortech.2012.11.063>
- Lacoursiere, A., Thompson, B.G., Kole, M.M., Ward, D., Gerson, D.F., 1986. Effects of carbon dioxide concentration on anaerobic fermentations of *Escherichia coli*. **Appl. Microbiol. Biotechnol.** 23, 404–406. <https://doi.org/10.1007/BF00257042>
- Lama, S., Seol, E., Park, S., 2020. Development of *Klebsiella pneumoniae* J2B as microbial cell factory for the production of 1,3-propanediol from glucose. **Metab. Eng.** 62, 116–125. <https://doi.org/10.1016/j.ymben.2020.09.001>
- Laura, M., Monica, T., Dan-Cristian, V., 2020. The effect of crude glycerol impurities on 1,3-propanediol biosynthesis by *Klebsiella pneumoniae* DSMZ 2026. **Renew. Energy.** 153, 1418–1427. <https://doi.org/10.1016/j.renene.2020.02.108>
- Lawrence, F.R., Sullivan, R.H., 1972. Process for Making a Dioxane. United States Patent, US3687981A.
- Lawrence, J.G., Roth, J.R., 1995. The cobalamin (coenzyme B12) biosynthetic genes of *Escherichia coli*. **J. Bacteriol.** 177, 6371–6380. <https://doi.org/10.1128/jb.177.22.6371-6380.1995>

- Lee, C., Kim, I., Lee, J., Lee, K.L., Min, B., Park, C., 2010. Transcriptional activation of the aldehyde reductase YqhD by YqhC and its implication in glyoxal metabolism of *Escherichia coli* K-12. **J. Bacteriol.** 192, 4205-4214.
<https://doi.org/10.1128/JB.01127-09>
- Lee, Jung Hun, Jung, M.Y., Oh, M.K., 2018. High-yield production of 1,3-propanediol from glycerol by metabolically engineered *Klebsiella pneumoniae*. **Biotechnol. Biofuels.** 11, 1-13. <https://doi.org/10.1186/s13068-018-1100-5>
- Lee, Jae Hyeon, Lama, S., Kim, J.R., Park, S.H., 2018. Production of 1,3-Propanediol from Glucose by Recombinant *Escherichia coli* BL21(DE3). **Biotechnol. Bioprocess Eng.** 23, 250-258. <https://doi.org/10.1007/s12257-018-0017-y>
- Liang, Q., Zhang, H., Li, S., Qi, Q., 2011. Construction of stress-induced metabolic pathway from glucose to 1,3-propanediol in *Escherichia coli*. **Appl. Microbiol. Biotechnol.** 89, 57-62. <https://doi.org/10.1007/s00253-010-2853-3>
- Lim, H.G., Noh, M.H., Jeong, J.H., Park, S., Jung, G.Y., 2016. Optimum Rebalancing of the 3-Hydroxypropionic Acid Production Pathway from Glycerol in *Escherichia coli*. **ACS Synth. Biol.** 5, 1247-1255.
<https://doi.org/10.1021/acssynbio.5b00303>
- Lin, J., Zhang, Y., Xu, D., Xiang, G., Jia, Z., Fu, S., Gong, H., 2016. Deletion of *poxB*, *pta*, and *ackA* improves 1,3-propanediol production by *Klebsiella pneumoniae*. **Appl. Microbiol. Biotechnol.** 100, 2775-2784.
<https://doi.org/10.1007/s00253-015-7237-2>

- Liu, H., Xu, Y., Zheng, Z., Liu, D., 2010. 1,3-Propanediol and its copolymers: Research, development and industrialization. *Biotechnol. J.* 5, 1137-1148.
<https://doi.org/10.1002/biot.201000140>
- Liu, H.J., Zhang, D.J., Xu, Y.H., Mu, Y., Sun, Y.Q., Xiu, Z.L., 2007. Microbial production of 1,3-propanediol from glycerol by *Klebsiella pneumoniae* under micro-aerobic conditions up to a pilot scale. *Biotechnol. Lett.* 29, 1281-1285.
<https://doi.org/10.1007/s10529-007-9398-2>
- Luers, F., Seyfried, M., Daniel, R., Gottschalk, G., 1997. Glycerol conversion to 1,3-propanediol by *Clostridium pasteurianum*: Cloning and expression of the gene encoding 1,3-propanediol dehydrogenase. *FEMS Microbiol. Lett.* 154, 337-345. [https://doi.org/10.1016/S0378-1097\(97\)00351-0](https://doi.org/10.1016/S0378-1097(97)00351-0)
- Ma, Z., Rao, Z., Xu, L., Liao, X., Fang, H., Zhuge, B., Zhuge, J., 2009. Production of 1,3-propanediol from glycerol by engineered *Escherichia coli* using a novel co-expression vector. *African J. Biotechnol.* 8, 5489-5494.
<https://doi.org/10.5897/AJB2009.000-9463>
- Maervoet, V.E.T., De Maeseneire, S.L., Avci, F.G., Beauprez, J., Soetaert, W.K., De Mey, M., 2016. High yield 1,3-propanediol production by rational engineering of the 3-hydroxypropionaldehyde bottleneck in *Citrobacter werkmanii*. *Microb. Cell Fact.* 15, 1-11. <https://doi.org/10.1186/s12934-016-0421-y>

- Magdouli, S., Rouissi, T., Brar, K., 2016. Propylene Glycol: An Industrially Important C3 **Platform Chemical**. <https://doi.org/10.1016/B978-0-12-802980-0.00005-5>
- Martinez, A., Grabar, T.B., Shanmugam, K.T., Yomano, L.P., York, S.W., Ingram, L.O., 2007. Low salt medium for lactate and ethanol production by recombinant *Escherichia coli* **B. Biotechnol. Lett.** 29, 397-404. <https://doi.org/10.1007/s10529-006-9252-y>
- McCloskey, D., Xu, J., Schrübbers, L., Christensen, H.B., Herrgård, M.J., 2018. RapidRIP quantifies the intracellular metabolome of 7 industrial strains of *E. coli*. **Metab. Eng.** 47, 383-392. <https://doi.org/10.1016/j.ymben.2018.04.009>
- Mu, Y., Teng, H., Zhang, D.J., Wang, W., Xiu, Z.L., 2006. Microbial production of 1,3-propanediol by *Klebsiella pneumoniae* using crude glycerol from biodiesel preparations. **Biotechnol. Lett.** 28, 1755-1759. <https://doi.org/10.1007/s10529-006-9154-z>
- Nakamura, C.E., Whited, G.M., 2003. Metabolic engineering for the microbial production of 1,3-propanediol. **Curr. Opin. Biotechnol.** 14, 454-459. <https://doi.org/10.1016/j.copbio.2003.08.005>
- Ogunkunle, O., Ahmed, N.A., 2019. A review of global current scenario of biodiesel adoption and combustion in vehicular diesel engines. **Energy Reports.** 5, 1560-1579. <https://doi.org/10.1016/j.egyr.2019.10.028>

- Oh, B.R., Lee, S.M., Heo, S.Y., Seo, J.W., Kim, C.H., 2018. Efficient production of 1,3-propanediol from crude glycerol by repeated fed-batch fermentation strategy of a lactate and 2,3-butanediol deficient mutant of *Klebsiella pneumoniae*. **Microb. Cell Fact.** 17, 1-9. <https://doi.org/10.1186/s12934-018-0921-z>
- Oh, B.R., Seo, J.W., Heo, S.Y., Hong, W.K., Luo, L.H., Kim, S., Park, D.H., Kim, C.H., 2012. Optimization of culture conditions for 1,3-propanediol production from glycerol using a mutant strain of *Klebsiella pneumoniae*. **Appl. Biochem. Biotechnol.** 166, 127-137. <https://doi.org/10.1007/s12010-011-9409-6>
- Pasteur L (1866). Etudes sur le vin, ses maladies; causes qui les provoquent, procédées nouveaux pour le conserver et pour le vieillir. vieillir. **Masson, Paris**
- Przystałowska, H., Lipiński, D., Słomski, R., 2015a. Biotechnological conversion of glycerol from biofuels to 1,3-propanediol using *Escherichia coli*. **Acta Biochim. Pol.** 62, 23-34. https://doi.org/10.18388/abp.2014_885
- Przystałowska, H., Zeyland, J., Szymanowska-Powałowska, D., Szalata, M., Słomski, R., Lipiński, D., 2015b. 1,3-Propanediol production by new recombinant *Escherichia coli* containing genes from pathogenic bacteria. **Microbiol. Res.** 171, 1-7. <https://doi.org/10.1016/j.micres.2014.12.007>
- Rao, A.R., Kumar, B., Patel, A.K., 2009. Vortex behaviour of an unbaffled surface aerator. **Science Asia.** 35, 183-188. <https://doi.org/10.2306/scienceasia1513-1874.2009.35.183>

Rathnasingh, C., Raj, S.M., Jo, J.-E., Park, S., 2009. Development and evaluation of efficient recombinant *Escherichia coli* strains for the production of 3-hydroxypropionic acid from glycerol. **Biotechnol. Bioeng.** 104, 729-739.
<https://doi.org/10.1002/bit.22429>

Raynaud, C., Sarçabal, P., Meynial-Salles, I., Croux, C., Soucaille, P., 2003. Molecular characterization of the 1,3-propanediol (1,3-PD) operon of *Clostridium butyricum*. **Proc. Natl. Acad. Sci. U. S. A.** 100, 5010-5015.
<https://doi.org/10.1073/pnas.0734105100>

Rentschler, H., and Tanner, H. 1951 Formation of bitterness in red wines. Acrolein in beverages and the relation to the formation of bitterness in wines. **Mitt. Gebiete Lebensm. Hyg.**, 42, 463-475.

REN21, 2016. Renewables 2016 Global Status Report, Renewables 2016 Global Status Report. [https://doi.org/ISBN 978-3-9818107-0-7](https://doi.org/ISBN%20978-3-9818107-0-7)

Repaske, R., Clayton, M.A., 1978. Control of *Escherichia coli* growth by CO₂. **J. Bacteriol.** 135, 1162-1164. <https://doi.org/10.1128/jb.135.3.1162-1164.1978>

Rosnow, J.J., Hwang, S., Killinger, B.J., Kim, Y.M., Moore, R.J., Lindemann, S.R., Maupin-Furrow, J.A., Wright, A.T., 2018. A cobalamin activity-based probe enables microbial cell growth and finds new cobalamin-protein interactions across domains. **Appl. Environ. Microbiol.** 84, 1-14.
<https://doi.org/10.1128/AEM.00955-18>

Roth, J.R., Lawrence, J.G., Rubenfield, M., Kieffer-Higgins, S., Church, G.M., 1993.

Characterization of the cobalamin (vitamin B12) biosynthetic genes of *Salmonella typhimurium*. **J. Bacteriol.** 175, 3303-3316.

<https://doi.org/10.1128/jb.175.11.3303-3316.1993>

Sattayasamitsathit, S., Methacanon, P., Prasertsan, P., 2011. Enhance 1,3-propanediol

production from crude glycerol in batch and fed-batch fermentation with two-phase pH controlled strategy. **Electron. J. Biotechnol.** 14, 1-12.

<https://doi.org/10.2225/vol14-issue6-fulltext-6>

Sauvageot, N., Muller, C., Hartke, A., Auffray, Y., Laplace, J.M., 2002.

Characterisation of the diol dehydratase pdu operon of *Lactobacillus collinoides*. **FEMS Microbiol. Lett.** 209, 69-74. <https://doi.org/10.1111/j.1574-6968.2002.tb11111.x>

Saxena, R.K., Anand, P., Saran, S., Isar, J., 2009. Microbial production of 1,3-

propanediol: Recent developments and emerging opportunities. **Biotechnol. Adv.** 27, 895-913. <https://doi.org/10.1016/j.biotechadv.2009.07.003>

Scanes, K.T., Hohmann, S., Prior, B., 1998. Glycerol production by the yeast

Saccharomyces and its relevance to wine. *South African J. Enol. Vitic.*

Serjak, W.C., Day, W.H., Vanlanen, J.M., Boruff, C.S., 1954. Acrolein production by

bacteria found in distillery grain mashes. **Appl. Microbiol.** 2, 14-20.

<https://doi.org/10.1128/aem.2.1.14-20.1954>

Shibata, N., Mori, K., Hieda, N., Higuchi, Y., Yamanishi, M., Toraya, T., 2005.

Release of a damaged cofactor from a coenzyme B12-dependent enzyme: X-ray structures of diol dehydratase-reactivating factor. **Structure**. 13, 1745-1754. <https://doi.org/10.1016/j.str.2005.08.011>

Skraly, F.A., Lytle, B.L., Cameron, D.C., 1998. Construction and characterization of a 1,3-propanediol operon. **Appl. Environ. Microbiol.** 64, 98-105.

<https://doi.org/10.1128/aem.64.1.98-105.1998>

Stephanopoulos, G.N., Aristidou, A.A., Nielsen, J., 1998. Examples of Pathway

Manipulations: Metabolic Engineering in Practice, in: Gregory N.

Stephanopoulos, Aristos A. Aristidou, Nielsen, J. (Ed.), **Metabolic**

Engineering. Academic Press, San Diego, CA, pp.203-283.

<https://doi.org/10.1016/B978-012666260-3/50007-8>

Sun, Y.Q., Shen, J.T., Yan, L., Zhou, J.J., Jiang, L.L., Chen, Y., Yuan, J.L., Feng,

E.M., Xiu, Z.L., 2018. Advances in bioconversion of glycerol to 1,3-

propanediol: Prospects and challenges. **Process Biochem.** 71, 134-146.

<https://doi.org/10.1016/j.procbio.2018.05.009>

Szymanowska-Powałowska, D., Białas, W., 2014. Scale-up of anaerobic 1,3-

propanediol production by *Clostridium butyricum* DSP1 from crude glycerol.

BMC Microbiol. 14, 1-10. <https://doi.org/10.1186/1471-2180-14-45>

- Tang, X., Tan, Y., Zhu, H., Zhao, K., Shen, W., 2009. Microbial conversion of glycerol to 1,3-propanediol by an engineered strain of *Escherichia coli*. **Appl. Environ. Microbiol.** 75, 1628–1634. <https://doi.org/10.1128/AEM.02376-08>
- Tong, I.T., Cameron, D.C., 1992. Enhancement of 1,3-Propanediol production by cofermentation in *Escherichia coli* expressing *Klebsiella pneumoniae dha* regulon genes. **Appl. Biochem. Biotechnol.** 34–35, 149–159. <https://doi.org/10.1007/BF02920542>
- Tong, I.T., Liao, H.H., Cameron, D.C., 1991. 1,3-Propanediol production by *Escherichia coli* expressing genes from the *Klebsiella pneumoniae dha* regulon. **Appl. Environ. Microbiol.** 57, 3541–3546. <https://doi.org/10.1128/aem.57.12.3541-3546.1991>
- Toraya, T., 2000. Radical catalysis of B12 enzymes: Structure, mechanism, inactivation, and reactivation of diol and glycerol dehydratases. **Cell. Mol. Life Sci.** 57, 106–127. <https://doi.org/10.1007/s000180050502>
- Toraya, T., Mori, K., 1999. A reactivating factor for coenzyme B12-dependent diol dehydratase. **J. Biol. Chem.** 274, 3372–3377. <https://doi.org/10.1074/jbc.274.6.3372>
- Toraya, T., Tanokuchi, A., Yamasaki, A., Nakamura, T., Ogura, K., Tobimatsu, T., 2016. Diol Dehydratase-Reactivase Is Essential for Recycling of Coenzyme B12 in Diol Dehydratase. **Biochemistry.** 55, 69–78. <https://doi.org/10.1021/acs.biochem.5b01023>

- Vivek, N., Pandey, A., Binod, P., 2016. Biological valorization of pure and crude glycerol into 1,3-propanediol using a novel isolate *Lactobacillus brevis* N1E9.3.3. **Bioresour. Technol.** 213, 222-230.
<https://doi.org/10.1016/j.biortech.2016.02.020>
- Vollenweider, S., Lacroix, C., 2004. 3-Hydroxypropionaldehyde: Applications and perspectives of biotechnological production. **Appl. Microbiol. Biotechnol.** 64, 16-27. <https://doi.org/10.1007/s00253-003-1497-y>
- Warcollier, G., and Le Moal, A. 1932 The accidental presence of acrolein in the distilled liquor from cider. **Compt. rend. (Acad. Sci.)**, 194, 1394-1396.
- Warcollier, G., Le Moal, A., and Tavernier, J. 1934 The accidental presence of acrolein in cider, brandy and pear juice. Its formation from glycerol. **Comp. rend. (Acad. Sci.)**, 198, 1546-1548.
- Wagner, A.F.V., Schultz, S., Bomke, J., Pils, T., Knappe, J., Lehmann, W.D., 2001. YfiD of *Escherichia coli* and Y061 of bacteriophage T4 as autonomous glycol radical cofactors reconstituting the catalytic center of oxygen-fragmented pyruvate formate-lyase. **Biochem. Biophys. Res. Commun.** 285, 456-462.
<https://doi.org/10.1006/bbrc.2001.5186>
- Wang, F., Qu, H., Zhang, D., Tian, P., Tan, T., 2007. Production of 1,3-propanediol from glycerol by recombinant *E. coli* using incompatible plasmids system. **Mol. Biotechnol.** 37, 112-119. <https://doi.org/10.1007/s12033-007-0041-1>

Werkman, C.H., Gillen, G.F., 1932. Bacteria Producing Trimethylene Glycol 1. **J.**

Bacteriol. 23, 167-182. <https://doi.org/10.1128/jb.23.2.167-182.1932>

Werpy, T., Petersen, G., 2004. Top Value Added Chemicals from Biomass Volume I.

US Nrel Medium: ED; Size: 76 pp. pages. <https://doi.org/10.2172/15008859>

Wilkens, E., Ringel, A.K., Hortig, D., Willke, T., Vorlop, K.D., 2012. High-level

production of 1,3-propanediol from crude glycerol by *Clostridium butyricum*

AKR102a. **Appl. Microbiol. Biotechnol.** 93, 1057-1063.

<https://doi.org/10.1007/s00253-011-3595-6>

Wischrall, D., Zhang, J., Cheng, C., Lin, M., De Souza, L.M.G., Pessoa, F.L.P.,

Pereira, N., Yang, S.T., 2016. Production of 1,3-propanediol by *Clostridium*

beijerinckii DSM 791 from crude glycerol and corn steep liquor: Process optimization and metabolic engineering. **Bioresour. Technol.** 212, 100-110.

<https://doi.org/10.1016/j.biortech.2016.04.020>

Wood, B.E., Yomano, L.P., York, S.W., Ingram, L.O., 2005. Development of

Industrial-Medium-Required Elimination of the 2,3-Butanediol Fermentation

Pathway to Maintain Ethanol Yield in an Ethanologenic Strain of *Klebsiella oxytoca*. **Biotechnol. Prog.** 21, 1366-1372.

<https://doi.org/https://doi.org/10.1021/bp050100e>

- Xin, B., Tao, F., Wang, Y., Liu, H., Ma, C., Xu, P., 2017. Coordination of metabolic pathways: Enhanced carbon conservation in 1,3-propanediol production by coupling with optically pure lactate biosynthesis. **Metab. Eng.** 41, 102–114. <https://doi.org/10.1016/j.ymben.2017.03.009>
- Xin, B., Wang, Y., Tao, F., Li, L., Ma, C., Xu, P., 2016. Co-utilization of glycerol and lignocellulosic hydrolysates enhances anaerobic 1,3-propanediol production by *Clostridium diolis*. **Sci. Rep.** 6, 1–10. <https://doi.org/10.1038/srep19044>
- Yang, B., Liang, S., Liu, H., Liu, J., Cui, Z., Wen, J., 2018. Metabolic engineering of *Escherichia coli* for 1,3-propanediol biosynthesis from glycerol. **Bioresour. Technol.** 267, 599–607. <https://doi.org/10.1016/j.biortech.2018.07.082>
- Yang, G., Tian, J., Li, J., 2007. Fermentation of 1,3-propanediol by a lactate deficient mutant of *Klebsiella oxytoca* under microaerobic conditions. **Appl. Microbiol. Biotechnol.** 73, 1017–1024. <https://doi.org/10.1007/s00253-006-0563-7>
- Yun, J., Yang, M., Magocha, T.A., Zhang, H., Xue, Y., Zhang, G., Qi, X., Sun, W., 2018. Production of 1,3-propanediol using a novel 1,3-propanediol dehydrogenase from isolated *Clostridium butyricum* and co-biotransformation of whole cells. **Bioresour. Technol.** 247, 838–843. <https://doi.org/10.1016/j.biortech.2017.09.180>

- Yun, J., Zayed, H.M., Zhang, Y., Parvez, A., Zhang, G., Qi, X., 2021. Co-fermentation of glycerol and glucose by a co-culture system of engineered *Escherichia coli* strains for 1,3-propanediol production without vitamin B12 supplementation. **Bioresour. Technol.** 319, 124218.
<https://doi.org/10.1016/j.biortech.2020.124218>
- Zhang, X., Jantama, K., Moore, J.C., Shanmugam, K.T., Ingram, L.O., 2007. Production of L-alanine by metabolically engineered *Escherichia coli*. **Appl. Microbiol. Biotechnol.** 77, 355–366. <https://doi.org/10.1007/s00253-007-1170-y>
- Zhang, X., Li, Y., Zhuge, B., Tang, X., Shen, W., Rao, Z., Fang, H., Zhuge, J., 2006. Construction of a novel recombinant *Escherichia coli* strain capable of producing 1,3-propanediol and optimization of fermentation parameters by statistical design. **World J. Microbiol. Biotechnol.** 22, 945–952.
<https://doi.org/10.1007/s11274-006-9139-z>
- Zheng, P., Wereath, K., Sun, J., van den Heuvel, J., Zeng, A.P., 2006. Overexpression of genes of the *dha* regulon and its effects on cell growth, glycerol fermentation to 1,3-propanediol and plasmid stability in *Klebsiella pneumoniae*. **Process Biochem.** 41, 2160–2169.
<https://doi.org/10.1016/j.procbio.2006.06.012>
- Zhu, J., Shalel-Levanon, S., Bennett, G., San, K.-Y., 2007. The YfiD protein contributes to the pyruvate formate-lyase flux in an *Escherichia coli* *arcA* mutant strain. **Biotechnol. Bioeng.** 97, 138–143.
<https://doi.org/https://doi.org/10.1002/bit.21219>

Eurostat statistics Explained, (2020). Oil and petroleum products - a statistical

overview. <https://ec.europa.eu/eurostat/statistics-explained>.

(accessed 20 June 2020)

MECRK, (2021). VitaminB12.

<https://www.sigmaaldrich.com/catalog/search?term=Vitamin+B12&interface=All>

&N=0&mode=partialmax&lang=fr®ion=FR&focus=product (accessed 12

March 2021

1,3-Propanediol (PDO) Market, (2020). **Market research report.**

<https://www.marketsandmarkets.com/PressReleases/1-3-propanediol-pdo.asp>.

(accessed 15 December 2020)



APPENDIX

1. Determination of k_{LA}

To optimize the production of 1,3-PDO, k_{LA} is used as an important parameter to verify how to improve concentration and productivity of 1,3-PDO. k_{LA} is thus determined from equation 1. The equation 1 is then integrated, becoming to Eq. 2. A slope of Eq.2 is then used as k_{LA} .

$$dC/dt = k_L a (C^* - C_L) \quad \text{Eq. 1}$$

To measure k_{LA} , water or AM1 medium without our microorganism was added into fermenter with the same working volume used in this study. DO probe was connected to controller for at least 6 h before taking the data for calculating k_{LA} . After 6 h, DO probe was initially calibrated to prepare for measurement of oxygen dissolved in the medium. Fermenter was flushed with nitrogen and waited until value became zero or stable. DO was set zero. Oxygen or air was then flushed in the fermenter until DO value reached 100 and set span as 100. Nitrogen was finally flushed and set to be zero again after DO value decreased to zero.

After DO probe was calibrated. Oxygen was flushed into fermenter. DO value was recorded every second until the value was around 100 or stable. The final DO at the stable point was taken account to C^* or saturation concentration of oxygen in Eq 2. For every DO value, they were then taken account to C in Equation 2. Finally, graph was plotted for $ABS(\ln(1-(C/C_s)))$ against time in the unit of minute. The slope was calculated as k_{La} . The unit of k_{La} derived from Eq.2 is expressed as the unit per minute.

$$k_{La} = \text{ABS}(\ln(1-(C/C^*))) \quad \text{Eq. 2}$$

2. Determination of cell dry weight

In order to evaluate cell dry weight directly from optical density, OD_{550} was plotted against cell dry mass for obtaining the slope value from equation. Twelve mL of individual sample was taken from cultivation to measure OD_{550} and cell dry mass. One mL of sample was divided for centrifugation at 12,500 rpm for 4 min and resuspended with 1 mL DI water before determining optical density by spectrophotometer at wavelength of 550 nm.

For measurement of cell dry mass, two mL of Eppendorf tube was dried at 105°C for 2 days before pre-weighing. Ten mL of sample was then centrifuged for collecting 1 mL cell suspension and aliquoted to the 2 mL pre-weight Eppendorf tube. The cell suspension was centrifuged again to remove water before drying at 105°C for 3 days and weighed. Biomass was finally calculated by determination of the difference between the pre-dried weight and post-dried weight of Eppendorf tube. The different value was

divided by total volume of sample (10 mL). Finally, the value was multiplied by working volume. All data from individual batch of fermentation were rearranged from low to high values and plot between OD and biomass. Equation was derived from this graph and determined biomass directly from OD with $2.68OD_{550} = 1\text{g/L CDW}$ (Fig. A.1).

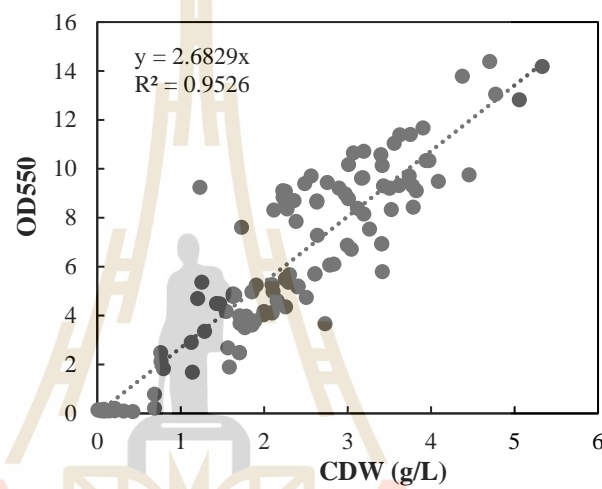


Figure A.1 Graph plotting between OD₅₀₀ against cell dry weight.

มหาวิทยาลัยเทคโนโลยีสุรนารี

BIOGRAPHY

Miss Nonthaporn Wong was born on March 25, 1991, Nauru. She graduated with a Bachelor's degree in Biology and Biotechnology from Nakhon Sawan Rajabhat University in 2014. In 2014, she was selected from Her Royal Highness Princess Maha Chakri Sirindhorn to be Thai Representative to participate in DESY summer student camp, Hamburg, Germany. She received the Royal Golden Jubilee Ph.D. (RGJ-PHD) Program (Grant no. PHD/0125/2556) under supervision of Assoc. Prof. Dr. Kaemwich Jantama. RGJ-PHD program that supports all expenses to study and performs research at School of Biotechnology, Institute of Agricultural Technology, Suranaree University of Technology and Institute National Polytechnique de Toulouse, France.

มหาวิทยาลัยเทคโนโลยีสุรนารี